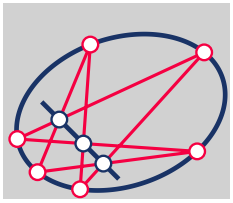

Hexagonal meshes as discrete minimal surfaces

Dissertation

zur Verleihung des akademischen Grades

Doktor der Technischen Wissenschaften

an der Technischen Universität Graz

vorgelegt von

Mag. Christian Müller

Institut für Geometrie

betreut von

Univ.-Prof. Dipl.-Ing. Mag. Dr. Johannes Wallner

Graz, am 26.2.2010

Contents

Abstract

In the present thesis we consider discrete minimal surfaces as a subject of discrete differental geometry. The main interest in discrete differential geometry is not just sampling objects like curves and surfaces of smooth differential geometry and studying them with numerical methods, but discretizing the whole theory. The aim is to retrieve as many properties from the smooth setting as possible.

We consider two of the many different characterizations of minimal surfaces and study them in the discrete setting. First there is a discrete curvature theory for polyhedral surfaces due to A.I. Bobenko, H. Pottmann and J. Wallner. Minimal surfaces are defined as meshes, where the discrete mean curvature vanishes throughout the mesh. This condition immediately yields the notion of oriented mixed area of a pair of parallel polygons. We develop a recursion formula for the mixed area and interpret it in terms of incidence geometry. Our main interest is hexagonal meshes as discrete minimal surfaces.

In the second part of the thesis we develop a discrete version of the smooth Christoffel dual construction which applies to hexagonal meshes. A limit consideration motivates the definition of conformal hexagons for which we discuss a discrete dual construction. We show that this construction is a sensible discrete analogue of smooth Christoffel duality. From an isothermic parametrization of the sphere, which in our case is a hexagonal mesh where each face is a conformal hexagon, we obtain a minimal surface by applying this dual construction.

Kurzfassung

Die vorliegende Arbeit befasst sich mit diskreten Minimalflächen und ist daher im Gebiet der diskreten Differentialgeometrie angesiedelt. Diese studiert nicht, wie man auf den ersten Blick vermuten würde, diskret abgetastete Objekte der „üblichen“, also kontinuierlichen Differentialgeometrie, sondern diskrete Analoga der Theorie, die möglichst viele Eigenschaften der ursprünglichen Theorie behält.

Zwei der zahlreichen Charakterisierungen der glatten Minimalflächen werden in dieser Arbeit im diskreten Kontext untersucht. Zum einen gibt es eine von A.I. Bobenko, H. Pottmann and J. Wallner entwickelte diskrete Krümmungstheorie für polyedrische Flächen. Eine solche Fläche ist dann eine Minimalfäche, wenn die diskrete mittlere Krümmung überall gleich Null ist. Das führt zur Fragestellung, der elementargeometrischen Kennzeichnung der Situation zweier paralleler Polygone mit verschwindendem gemischten Flächeninhalt. Dieses Problem wird im ersten Teil dieser Arbeit gelöst, indem eine Rekursionsformel hergeleitet und geometrisch interpretiert wird. Dabei wird Sechsecksnetzen erhöhte Aufmerksamkeit geschenkt.

Der zweite Teil der Arbeit diskretisiert die Konstruktion von dualen Flächen nach Christoffel. Dabei werden wieder Sechsecksnetze verwendet. Limesbetrachtungen motivieren die Definition von konformen Sechsecken, die einer diskreten Variante der Christoffel-Dualität unterworfen werden können. Mit Hilfe dieser Überlegungen werden diskrete Minimalflächen aus Sechsecksnetzen gewonnen, die einer Kugel einbeschrieben sind und deren Facetten konforme Sechsecke sind.

EIDESSTATTLICHE ERKLÄRUNG

Ich erkläre an Eides statt, dass ich die vorliegende Arbeit selbstständig verfasst, andere als die angegebenen Quellen/Hilfsmittel nicht benutzt, und die den benutzten Quellen wörtlich und inhaltlich entnommene Stellen als solche kenntlich gemacht habe.

Graz, am ....
(Unterschrift)

Englische Fassung:

STATUTORY DECLARATION

I declare that I have authored this thesis independently, that I have not used other than the declared sources / resources, and that I have explicitly marked all material which has been quoted either literally or by content from the used sources.

....
date (signature)

Acknowledgements

First I want to thank my PhD advisor Prof. Johannes Wallner for providing me with the topic of this thesis and for always supporting me.

Further I wish to thank my colleagues at the Institute of Geometry for the nice working atmoshpere.

Many thanks to my family who always supported me in many various ways.

This research was supported in part by the Austrian Science Fund, FWF, within the framework of project S92-09 (National Research Network 'Industrial Geometry').

Introduction

The present thesis considers hexagonal meshes from the viewpoint of *discrete differential geometry*. Discrete differential geometry is a wide field which considers objects like polygons, meshes, and polytopes with the aim of finding discrete analogues of classical (i.e., smooth) differential geometry. In this sense not only objects but also properties and notions of the smooth setting are carried over to the discrete theory. Also the other way round is of great interest, which means that one explores attributes assigned to discrete objects which survive a refinement process to a continuous limit. A first treatise of discrete differential geometry can be found in the monograph *Differenzengeometrie* by R. Sauer [23] whereas a modern approach is contained in *Discrete Differential Geometry: Integrable Structure* by A.I. Bobenko and Yu.B. Suris [6]. Discrete differential geometry is not only interesting within pure mathematics (see e.g. [2, 3, 4, 5, 6]) but also in Computer Graphics and geometry processing (see e.g. [26]) and architectural design (see e.g. [20]). The general idea here is to get notions like curvature, offset surface, and conformal equivalence for discrete objects which are of great importance in applications.

Minimal surfaces represent a prominent topic which has attracted great interest for a long time and which several times has been the object of significant new developments. They combine differential geometry with other fields, notably complex analysis. Also the recent field of *discrete differential geometry* has not neglected them. Before entering into details we want to say a few general words on the analogies and differences between the smooth and discrete categories.

The appeal of smooth minimal surface theory is to a large extent due to the fact that the same class of surfaces is characterized by different properties which are unrelated a priori, such as vanishing mean curvature, local surface minimization, or analyticity of conformal parametrizations. Accord-

ingly there is a variety of constructions of minimal surfaces: as solutions of Plateau's problem, as real part of Lie's sum of curves surfaces, or by Christoffel duality.

Transferring all these properties to the discrete category at the same time is not easy. Obviously we can pick a class of discrete surfaces (for instance, triangle meshes) and consider those discrete surfaces which enjoy a certain property analogous to one of the known properties of smooth minimal surfaces. However it is not guaranteed that these discrete minimal surfaces have any of the other properties which make their smooth counterparts such an interesting object of study. Nevertheless, for *some* appropriate discretizations this is exactly what happens, and it is a major aim in discrete differential geometry to find them.

The following constructions stand out: U. Pinkall and K. Polthier [19] considered the class of triangle meshes and defined minimality by surface minimization. The resulting discrete minimal surfaces are, among others, minimizers of Dirichlet energy, capable of discrete conjugate surfaces, and allow for the solution of a discrete Plateau's problem. A.I. Bobenko and U. Pinkall [4] studied discrete isothermic surface parametrizations (this means quadrilateral meshes with planar faces and a cross ratio condition for the vertices). This approach led to a discrete Christoffel duality for isothermic parametrizations, where minimal surfaces and spheres correspond to each other, just as in the smooth case. This viewpoint is assumed by several papers based on [4], e.g. [27]. A.I. Bobenko, T. Hoffmann, and B. Springborn [2] took the idea of Christoffel duality further and applied it to Koebe polyhedra. They constructed a circle-based class of discrete minimal surfaces which exhibits convergence to the smooth case and makes it possible to find minimal surfaces from the combinatorics of the network of principal curvature lines.

It turned out that the discrete curvature theory for polyhedral surfaces introduced by H. Pottmann et al. [5, 20], which is based on the variation of surface area in offset surfaces, contains both [4] and [2] as special cases. Minimality of a polyhedral surface with respect to an edgewise parallel Gauss image is in that context defined by vanishing mixed area of corresponding faces.

This brings us to the first topic of the present thesis, which systematically studies the vanishing mixed area property for polygons, having in mind as a main application the discrete minimal surfaces in the class of hexagonal meshes (see [17]). After setting up the necessary definitions, we continue with

a geometric recursion for the computation of oriented mixed areas in Section 2.2. In Section 2.3 this leads to ways of characterizing pairs of parallel polygons whose mixed area is zero. Section 2.4 considers hexagonal meshes which are minimal and uses the incidence-geometric characterizations of vanishing mixed area which were obtained earlier for the construction of equilibrium forces in the edges of a minimal mesh. Finally we discuss an incidence geometric property for the faces of a constant mean curvature surface.

The second topic of the present thesis establishes a discrete Christoffel dual construction for special hexagonal meshes, namely conformal ones (see [16]). We start with equivalent characterizations of vertex offset meshes in Section 3.1. In Section 3.2, we give a definition and a motivation for the notion of a *conformal hexagon*. Properties of this type of hexagons as well as a dual construction are discussed in Section 3.3. The smooth and discrete Christoffel dual constructions and some of their properties are discussed in Sections 3.4 and 3.5. An elementary geometry construction of planar conformal hexagons which turn out to be discrete holomorphic is shown in Section 3.6. In the final Section 3.8 we discuss the connection between the Weierstrass representation and the Christoffel duality and use this to classify some examples of discrete minimal surfaces.

Chapter 1

Preliminaries

1.1 Notions of classical differential geometry

1.1.1 Parametrization

In this section we collect some notions of classical differential geometry which means the study of smooth curves and surfaces. We are mainly interested in the three-dimensional space $\mathbb{R}^3$.

A differentiable map $f : U \to \mathbb{R}^3$, where U is an open subset of $\mathbb{R}^2$, is *regular in* U if the two partial derivatives $f_x(a)$ and $f_y(a)$ are linearely independent for all $a \in U$. Such a map f is called *parametrization of the surface* $f(U) \subseteq \mathbb{R}^3$. When it is clear form context we will call the map f a surface.

A parametrization f is *conformal* if the partial derivatives are orthogonal and have the same length i.e.

$$\langle f_x(a), f_y(a) \rangle = 0 \qquad \|f_x(a)\| = \|f_y(a)\|$$

for all $a \in U$. Each surface can be conformally parametrized locally (see e.g. [25, p. 314 - 346]).

For the pupose of measuring lengths, angles, areas, and curvatures one introduces the first and second fundamental forms (here in matrix notation with their respective coordinate functions)

$$I = \begin{pmatrix} E & F \\ F & G \end{pmatrix} \qquad II = \begin{pmatrix} L & M \\ M & N \end{pmatrix},$$

where $E = \langle f_x, f_x \rangle$, $F = \langle f_x, f_y \rangle$, $G = \langle f_y, f_y \rangle$, $L = \langle n, f_{xx} \rangle$, $M = \langle n, f_{xy} \rangle$, $N = \langle n, f_{yy} \rangle$ with $n = (f_x \times f_y)/\|f_x \times f_y\|$ as the unit normal vector (the *Gauss map*). The area of a surface $f(U)$ is defined as

$$\int_U \sqrt{\det(I)}\, dxdy.$$

The *principal curvatures* κ_1 and κ_2 are defined as roots of the quadratic polynomial equation $\det(II - \kappa I) = 0$. It turns out that the principal curvatures always are real. The *mean curvature* H and the *Gaussian curvature* K are defined as

$$H = \frac{1}{2}(\kappa_1 + \kappa_2) \quad \text{and} \quad K = \kappa_1 \kappa_2.$$

For a vector v in the tangent plane, $v = af_x + bf_y$, the normal curvature in the direction of v is defined as

$$\kappa_n = \frac{Ma^2 + 2Nab + Lb^2}{Ea^2 + 2Fab + Gb^2}.$$

The maximum and the minimum of the normal curvatures are equal to the principal curvatures, and the associated vectors are called principal directions. They are orthogonal.

f is a *curvature line* parametrization if the parameter lines $f(x_0, \cdot)$ and $f(\cdot, y_0)$ are curvature lines, i.e., the tangent vectors f_x and f_y are principal directions. Each surface can be locally parametrized with curvature lines. A parametrization which is conformal and curvature line at the same time is called *isothermic*. It is not possible to obtain isothermic parametrizations for all surfaces. However, for minimal surfaces it is possible.

A *Koenigs net* is a map $f : U \to R^3$ which satisfies the differential equation

$$f_{xy} = \frac{\nu_y}{\nu} f_x + \frac{\nu_x}{\nu} f_y,$$

with some scalar function $\nu : U \to \mathbb{R} \setminus 0$ (see e.g. [7]).

1.2 The complex plane

1.2.1 Möbius transformations

A Möbius transformation is a map $M : \mathbb{C} \cup \{\infty\} \to \mathbb{C} \cup \{\infty\}$. Let $a, b, c, d \in \mathbb{C}$ such that $ad - cb \neq 0$. The Möbius transformation can be written in the form

$$M(z) = \begin{cases} \infty & \text{if } cz + d = 0, \\ a/c & \text{if } z = \infty, \\ \frac{az+b}{cz+d} & \text{otherwise.} \end{cases}$$

A Möbius transformation can be decomposed in translations, rotations, dilations, and maps of the form $z \mapsto 1/z$. The *cross-ratio* of four distinct points

$$\operatorname{cr}(z_0, z_1, z_2, z_3) := \frac{(z_0 - z_1)(z_2 - z_3)}{(z_1 - z_2)(z_3 - z_0)} \in \mathbb{C}, \tag{1.1}$$

is invariant under Möbius transformations. Considering lines as circles with infinite radius we can say that Möbius transformations map circles to circles. Möbius transformations and anti-Möbius transformations (i.e., $z \mapsto M(\overline{z})$) are conformal transformations wich means that they preserve the angle of two intersecting curves.

Another way to define Möbius transformations comes from incidence geometry where a Möbius transformation maps circles (including straight lines) on circles (see e.g. [1]). This implies to add the conjugation map $z \mapsto \overline{z}$ to the list of elementary transformations in which a Möbius transformation can be decomposed. We therefore see that from the incidence geometry the Möbius transformations include what previously was called an anti-Möbius transformation. If we do that, we have to accept the loss of the invariance of the cross-ratio under Möbius transformations. To fix this problem we have to consider the unordered pair $\{q, \overline{q}\}$ as cross-ratio of four points.

Möbius transformations in space (say in $\mathbb{R}^3$) can be defined as composition of translations, rotations, dilations, and inversions in the sphere. Unlike in the planar case, the spatial Möbius transformations are the only angle preserving transformations in space.

A Möbius transformation M maps a conformal parametrization f on a conformal parametrization $M \circ f$ again. In other words, conformal parametrizations are objects of Möbius geometry.

A *stereographic projection* from the plane to the sphere

$$\Phi(z) := \frac{1}{(|z^2|+1)}(2z, |z|^2 - 1) \in \mathbb{C} \times \mathbb{R} \cong \mathbb{R}^3$$

can be seen as the restriction of a Möbius transformation of $\mathbb{R}^3$ to a plane in $\mathbb{R}^3$.

1.2.2 Holomorphic functions

For complex analysis we refer to [22]. A complex function $f(z) = u(x,y) + iv(x,y)$, with $z = x + iy$ and real valued functions u, v, is *holomorphic* if the *Cauchy-Riemann differential equations* $u_x = v_y$ and $v_x = -u_y$ hold. Then $f'(z) = u_x(x,y) + iv_x(x,y)$. A holomorphic function is called *conformal* if $f'(z) \neq 0$ for all $z \in U$. A conformal parametrization of the plane in the sense of differential geometry is the same as a conformal map $f : \mathbb{C} \to \mathbb{C}$, where the parameter lines are $f(x + iy_0)$ and $f(x_0 + iy)$, for fixed x_0 and y_0, respectively. A complex function is called *meromorphic*, if it is holomorphic everywhere excapt in isolated points, which are poles.

A real valued function $u : U \to \mathbb{R}$, where U is simply connected, is called *harmonic* if the Laplacian

$$\Delta u = \frac{\partial^2 u}{\partial x^2} + \frac{\partial^2 u}{\partial y^2}$$

vanishes everywhere. The real and imaginary parts of a holomorphic function are harmonic. In this case u is said to be the *harmonic conjugate* to v. For each harmonic function u there exists a harmonic conjugate v such that $f = u + iv$ is holomorphic.

1.3 Minimal surfaces

We collect some characterizations of *minimal surfaces*:

Mean curvature. A surface is a minimal surface if the mean curvature H vanishes for all points.

Weierstrass representation. f is a conformal parametrization of a minimal surface if and only if it is of the form

$$f(x,y) = \operatorname{Re}\Big[\int h\cdot\left(\frac{1}{2}(\frac{1}{g}-g), -\frac{1}{2i}(\frac{1}{g}+g), 1\right) dz\Big]\Big|_{z=x+iy},$$

where $h : U \to \mathbb{C}$ is holomorphic and $g : U \to \mathbb{C}\cup\{\infty\}$ is meromorphic; g, h have no common root; and the components of the integrand have no pole (see e.g. [11]).

Christoffel duality. f is an isothermic parametrization of a minimal surface if and only if f^*, defined by the formulas

$$f_x^* = \frac{f_x}{\|f_x\|^2} \quad \text{and} \quad f_y^* = -\frac{f_y}{\|f_y\|^2},$$

exists and parametrizes a sphere (see [9] and Section 3.4).

Plateau problem. A surface which has the minimum of area of all surfaces with a given closed curve as boundary is a minimal surface (see e.g. [11]).

Björling problem. A surface of the form

$$f(x,y) = \operatorname{Re}\Big[c(z) - i\int_0^z n(\zeta)\times\dot{c}(\zeta)d\zeta\Big]\Big|_{z=x+iy},$$

is a minimal surface if $c, n : I \times iJ \to \mathbb{C}^3$ are holomorphic functions (I, J intervals with $0 \in I$) and if $c(I), n(I) \subset \mathbb{R}^3$. This minimal surface contains the curve $c(I)$ and has $n(I)$ as Gaussian image in the corresponding points (see e.g. [18]).

Lie sum. A surface is a minimal surface if and only if it can be represented as a translation surface $f(u,v) = \operatorname{Re}(g(u) + h(v))$, whose generators g, h are isotropic curves (which means curves $c : \mathbb{C} \to \mathbb{C}^3$ such that the (non-Hermitian) scalar product $\langle c', c'\rangle$ vaneshes. See e.g. [13]).

The Weierstrass representation provides each minimal surface $f(x,y)$ with an *associated family* f_θ ($\theta \in [0, 2\pi]$) of minimal surfaces. It is given by

$$f_\theta(x,y) = \operatorname{Re}\Big[e^{i\theta}\int h\cdot\left(\frac{1}{2}(\frac{1}{g}-g), -\frac{1}{2i}(\frac{1}{g}+g), 1\right) dz\Big]\Big|_{z=x+iy}.$$

Chapter 2

Oriented mixed area and discrete minimal surfaces

In the present chapter we systematically study the vanishing mixed area property for polygons, having in mind as a main application the discrete minimal surfaces in the class of hexagonal meshes. Most of this chapter can be found in [17].

2.1 Definitions

2.1.1 Convex polygons and parallelity

For two convex subsets $K, L \subseteq \mathbb{R}^2$, the area of nonnegative Minkowski combinations $\lambda K + \mu L$ obeys the law

$$\operatorname{area}(\lambda K + \mu L) = \lambda^2 \operatorname{area}(K) + 2\lambda\mu \operatorname{area}(K, L) + \mu^2 \operatorname{area}(L), \tag{2.1}$$

where the symbol $\operatorname{area}(K, L)$ means the *mixed area* of K and L (see for example [24]). If the boundary ∂K is a polygon P with vertices $p_0, \ldots, p_{N-1}$, then the oriented area of K is given by Leibniz' sector formula

$$\operatorname{area}(P) := \operatorname{area}(K) = \frac{1}{2} \sum\nolimits_{0 \le i < N} \det(p_i, p_{i+1}). \tag{2.2}$$

Here indices are taken modulo N. Obviously, there is a vector space of polygons with N vertices, and the area functional (2.2) is a quadratic form in this space. For us, the most interesting case is that K and L are bounded

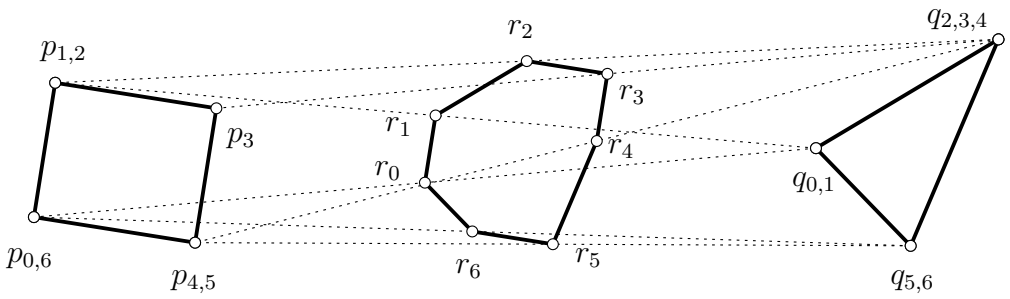

FIGURE 2.1: Labeling vertices of ∂K and ∂L with aid of $\partial(\frac{K+L}{2})$ such that they become parallel.

by *parallel polygons* P and Q, with vertices $p_0, \ldots, p_{N-1}$ and $q_0, \ldots, q_{N-1}$, respectively. This concept, which is not restricted to convex polygons, was introduced by [20] and means that

$$p_{i+1} - p_i,\ q_{i+1} - q_i \text{ are linearly dependent, for } i = 0, \ldots, N-1.$$

We assume for a moment that both P, Q have only nonzero edges (i.e., no coinciding vertices). Then the boundary $\partial(\lambda K + \mu L)$ has the vertices $(\lambda p_i + \mu q_i)_{0 \le i < N}$, whence $\operatorname{area}(\lambda K + \mu L) = \frac{1}{2} \sum_{0 \le i < N} \det(\lambda p_i + \mu q_i, \lambda p_{i+1} + \mu q_{i+1})$ and consequently

$$\operatorname{area}(P, Q) = \frac{1}{4} \sum\nolimits_{0 \le i < N} (\det(p_i, q_{i+1}) + \det(q_i, p_{i+1})). \tag{2.3}$$

This formula describes the symmetric bilinear form induced by the area functional in any vector space of polygons with N vertices.

If either P or Q has zero edges (i.e., multiple vertices), the vertices of $\partial(\lambda K + \mu L)$ need not equal $\lambda p_i + \mu q_i$, but if they do, (2.3) is valid.

Note that *arbitrary* polygons ∂K, ∂L can be seen as parallel polygons, as illustrated by Figure 2.1: We are labeling the vertices $r_0, \ldots, r_{N-1}$ of $\partial(K+L)$ consecutively, and subsequently give (possibly multiple) indices $p_0, \ldots, p_{N-1}$ and $q_0, \ldots, q_{N-1}$ to the vertices of ∂K and ∂L such that $p_i + q_i = r_i$. Then all three boundaries of K, L, $K + L$ and in fact $\lambda K + \mu L$ for $\lambda, \mu \ge 0$ are described by parallel polygons, and (2.3) can be used for computing the mixed area in the sense of (2.1).

2.1.2 The oriented mixed area

The polygons parallel to a given polygon $P = (p_0, \ldots, p_{N-1})$, not necessarily convex, constitute a vector space under vertex-wise addition and scalar mul-

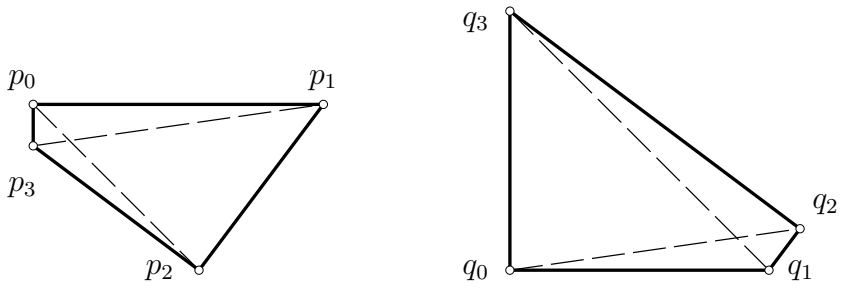

FIGURE 2.2: For nondegenerate parallel quads $p_0, \ldots, p_3$ and $q_0, \ldots, q_3$, parallel of one nonzero diagonal characterizes vanishing mixed area ($q_0q_2 \parallel q_1q_3$, or ($q_1q_3 \parallel q_0q_2$).

tiplication. Its dimension equals $N + \#\{i \mid p_i = p_{i+1}\}$. If there are no zero edges, we use the symbol

$$\mathcal{P}(P) = \{(q_0, \ldots, q_{N-1}) \mid q_{i+1} - q_i = \lambda_i(p_{i+1} - p_i), 0 \leq i < N\}/\mathbb{R}^2 \qquad (2.4)$$

for the vector space of polygons parallel to P, modulo parallel translations. Then $\dim \mathcal{P}(P) = N - 2$. If both P and Q have zero edges, still $P + Q$ might not have any, and consequently $P, Q, P + Q \in \mathcal{P}(P + Q)$. The expression defined by formula (2.3) is translation invariant. Following [20] we define:

Definition 2.1. *For parallel polygons $P = (p_0, \ldots, p_{N-1})$ and $Q = (q_0, \ldots, q_{N-1})$, the oriented mixed area is given by the bilinear form* (2.3).

Apparently the oriented mixed area, which extends the concept of mixed area for convex domains, is the bilinear form associated with the quadratic form measuring oriented area by Leibniz' sector formula.

2.1.3 Discrete minimal surfaces

The curvature theory presented in [20] deals with *parallel meshes*, which means a pair (Σ, Φ) of polyhedral surfaces having the same combinatorics, such that corresponding edges are parallel. Σ is viewed as Gauss image of Φ. The definition of parallelity of polygons extends to polygons which lie in parallel planes; in order to employ (2.3) for the computation of mixed area they have to be moved to a common plane by parallel translation. If P is a face and Q the corresponding face in the Gauss image, then P is assigned

the mean curvature

$$H_P = -\frac{\text{area}(P,Q)}{\text{area}(P)},$$

and Gaussian curvature

$$K_P = \frac{\text{area}(Q)}{\text{area}(P)}.$$

For this reason, *vanishing* mixed area of parallel polygons is characteristic for discrete minimal surfaces. The following result of [20], illustrated in Figure 2.2, is basic for the construction of minimal surfaces with regular quad mesh combinatorics:

Proposition 2.2. *Parallel quadrilaterals* $P = (p_0, p_1, p_2, p_3)$ *and* $Q = (q_0, q_1, q_2, q_3)$ *have vanishing mixed area if and only if diagonals* p_0p_2 *and* q_1q_3 *are parallel, which is equivalent to diagonals* p_1p_3 *and* q_0q_2 *being parallel.*

This condition actually discretizes the Christoffel duality between a minimal surface and its spherical Gauss image [20]. We therefore call a polyhedral surface and its parallel Gauss image where all mixed areas vanish, a *Christoffel dual pair*. It is an interesting fact that Proposition 2.2 applies to several constructions of discrete minimal surfaces based on quadrilaterals, namely the ones of [4, 2]. This chapter, which deals with vanishing mixed area in general, is focuses on *hexagonal* meshes.

2.2 Properties of the oriented mixed area

The main result of the present chapter is the recursion formula of Theorem 2.6 below, which for parallel polygons P, Q with an even number of vertices shows that $\text{area}(P,Q) = \text{area}(P^*,Q^*)$, where P^*, Q^* are derived polygons which have only the half number of vertices. It is used in Section 2.3 to derive geometric characterizations of parallel polygons with vanishing mixed area.

2.2.1 Formulas for the mixed area

There are equivalent formulae for the oriented mixed area of parallel polygons which take advantage of parallelity:

Lemma 2.3. *The bilinear form of Equation* (2.3) *is alternatively expressed as*

$$\begin{aligned}&\sum\nolimits_{i\in\{0,1,\dots,N-1\}}\Big(\det(p_i,q_{i+1})+\det(q_i,p_{i+1})\Big)\\ =&\sum\nolimits_{i\in\{0,1,\dots,N-1\}}\det(p_i,q_{i+1}-q_{i-1})\end{aligned}\tag{2.5}$$

(indices modulo N). For P,Q parallel and an even number of vertices,

$$\begin{aligned}2\,\mathrm{area}(P,Q)=&\sum\nolimits_{i\in\{0,2,\dots,N-2\}}\det(p_i,q_{i+1}-q_{i-1})\\ =&\sum\nolimits_{i\in\{1,3,\dots,N-1\}}\det(p_i,q_{i+1}-q_{i-1}).\end{aligned}\tag{2.6}$$

Proof. The first equality is found by rearranging indices:

$$\sum\nolimits_i\det(p_i,q_{i+1})+\sum\nolimits_i\det(q_i,p_{i+1})=\sum\nolimits_i\det(p_i,q_{i+1})+\sum\nolimits_i\det(q_{i-1},p_i).$$

In order to show the second equality, we observe that parallelity of P and Q implies $\det(p_{i+1}-p_i,q_{i+1}-q_i)=0$. Therefore,

$$\begin{aligned}&\sum\nolimits_{i\ \text{even}}\det(p_i,q_{i+1}-q_{i-1})\\ =&\sum\nolimits_{i\ \text{even}}(\det(p_i,q_{i+1}-q_i)+\det(p_i,q_i-q_{i-1}))\\ =&\sum\nolimits_{i\ \text{even}}(\det(p_i+(p_{i+1}-p_i),q_{i+1}-q_i)+\\ &\qquad+\det(p_i+(p_{i-1}-p_i),q_i-q_{i-1}))\\ =&\sum\nolimits_{i\ \text{even}}(\det(p_{i+1},q_{i+1}-q_i)+\det(p_{i-1},q_i-q_{i-1}))\\ =&\sum\nolimits_{i\ \text{even}}(\det(p_{i+1},q_{i+1}-q_i)+\det(p_{i+1},q_{i+2}-q_{i+1}))\\ =&\sum\nolimits_{i\ \text{even}}\det(p_{i+1},q_{i+2}-q_i)=\sum\nolimits_{i\ \text{odd}}\det(p_i,q_{i+1}-q_{i-1}).\end{aligned}$$

It follows that the expression for $4\,\mathrm{area}(P,Q)$ according to (2.3) reads

$$\Big(\sum_{i\ \text{even}}+\sum_{i\ \text{odd}}\Big)\det(p_i,q_{i+1}-q_{i-1})=\sum_{i\ \text{even}}2\det(p_i,q_{i+1}-q_{i-1}),$$

which is what we wanted to prove. □

We have now obtained an expression for the mixed area which makes use only of the vertices $p_0,p_2,\dots$ and $q_1,q_3,\dots$, which however does not have a direct relation to the areas associated with polygons $(p_0,p_2,\dots)$ and $(q_1,q_3,\dots)$.

2.2.2 Construction of a derived polygon

For the following construction of derived polygons, the polygons P, Q must have an even number N of vertices, and certain diagonals of P are forbidden to be parallel. We used the notation $[v]$ for the 1-dimensional subspace spanned by the vector v.

Definition 2.4. *Assume a pair of polygons $P = (p_0, \ldots, p_{N-1})$ and $Q = (q_0, \ldots, q_{N-1})$, where N is even, such that*

$$p_i - p_{i-2} \text{ and } p_{i+2} - p_i \text{ are linearly independent for } i = 0, 2, 4, \ldots \tag{2.7}$$

(indices are taken modulo N). Then a pair of derived polygons P^*, Q^* is constructed such that P^* consists of every other vertex of P, while the vertices of Q^* are found by parallel translating diagonals of P through points of Q:

$$\begin{aligned} p_i^* &= p_{2i}, \\ q_i^* &= (q_{2i+1} + [p_{2i+2} - p_{2i}]) \cap (q_{2i-1} + [p_{2i} - p_{2i-2}]). \end{aligned}$$

An index shift of 1 yields an analogous derived pair (P^{**}, Q^{**}) based on the odd vertices of P:

$$p_i^{**} = p_{2i+1}$$

and

$$q_i^{**} = (q_{2i+2} + [p_{2i+3} - p_{2i+1}]) \cap (q_{2i} + [p_{2i+1} - p_{2i-1}]),$$

provided the lines employed in this intersection are not parallel.

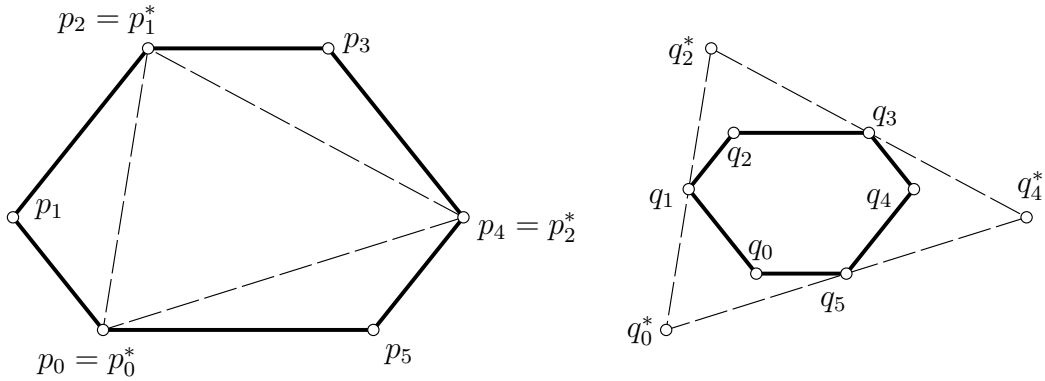

FIGURE 2.3: A pair of polygons P, Q and the derived polygons P^*, Q^*.

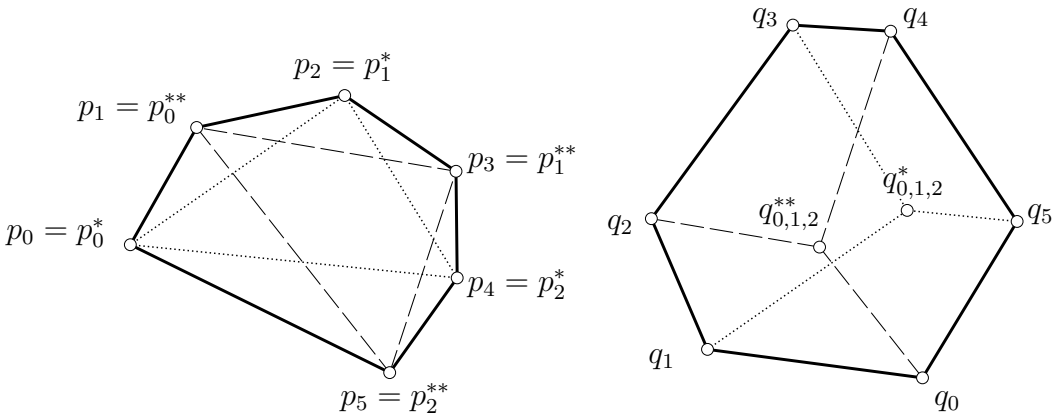

FIGURE 2.4: Illustration of Lemma 2.5. Polygons P^*, Q^* are orthogonal with respect to the bilinear form defined by the oriented are, if both derived polygons Q^* and Q^{**} degenerate into a point. The converse is not true.

This construction is illustrated by Figures 2.3 and 2.4. Note that if Q^* cannot be constructed because (2.7) is not fulfilled, still Q^{**} may be constructible. For quadrilaterals, (2.7) is never fulfilled, even after an index shift. We will be able to treat quadrilaterals as degenerate hexagons.

2.2.3 Non-parallel polygons

The bilinear function of Equation (2.3) which measures the oriented mixed area for parallel polygons can be evaluated for arbitrary pairs of polygons, without having a geometric meaning as mixed area in the classical sense. It still extends the quadratic functional which measures the oriented area by Leibniz' sector formula. The definition of derived polygons according to Definition 2.4 is not restricted to parallel polygons.

We here record a nice geometric property of this functional:

Lemma 2.5. *Polygons P, Q are orthogonal with respect to the bilinear function* (2.3)*, if both derived polygons Q^* and Q^{**} with respect to even and odd indices degenerate into points q^* and q^{**}, respectively.*

PROOF. By Lemma 2.3, we have to show that $\sum_{0 \le i < N} \det(p_i, q_{i+1} - q_{i-1}) = 0$. Our assumption on the degeneracy of derived polygons means that there are real numbers λ_i with

$$q^* = q_i + \lambda_i (p_{i-1} - p_{i+1}) \text{ for } i \text{ even},$$

$$q^{**} = q_i + \lambda_i(p_{i-1} - p_{i+1}) \text{ for } i \text{ odd.}$$
$$\implies \quad q_{i+1} - q_{i-1} = \lambda_{i-1}(p_{i-2} - p_i) - \lambda_{i+1}(p_i - p_{i+2}) \text{ for all } i.$$

We use this equality to evaluate (2.3):

$$\begin{aligned}
&\sum\nolimits_{0\le i<N} \det(p_i, q_{i+1} - q_{i-1}) \\
&= \sum\nolimits_{0\le i<N} \det(p_i, \lambda_{i-1}(p_{i-2} - p_i) - \lambda_{i+1}(p_i - p_{i+2})) \\
&= \sum\nolimits_{0\le i<N} \lambda_i \det(p_{i+1}, p_{i-1} - p_{i+1}) - \sum\nolimits_{0\le i<N} \lambda_i \det(p_{i-1}, p_{i-1} - p_{i+1}) \\
&= \sum\nolimits_{0\le i<N} \lambda_i \det(p_{i+1} - p_{i-1}, p_{i-1} - p_{i+1}) = 0
\end{aligned}$$

(indices are taken modulo N). This concludes the proof. □

2.2.4 Mixed area of derived polygons

The following theorem is the main technical contribution of the present chapter. It is the basis of geometric characterizations of polygons pairs with vanishing mixed area, and therefore the basis of constructions of discrete minimal surfaces.

Theorem 2.6. *For any pair of parallel polygons P, Q with an even number of vertices, the oriented mixed area is unaffected by the passage to derived polygons:*

$$\operatorname{area}(P, Q) = \operatorname{area}(P^*, Q^*) = \operatorname{area}(P^{**}, Q^{**}),$$

whenever the conditions of Definition 2.4, which allow construction of Q^* or Q^{**}, are fulfilled.

Proof. It is obviously sufficient to show the result for P^* and Q^*. An elementary computation yields the coordinates of Q^*'s vertices q_i^*:

$$\begin{aligned}
&q_i^* = \frac{1}{\gamma_i}\big(\alpha_i(p_{i+1}^* - p_i^*) + \beta_i(p_i^* - p_{i-1}^*)\big), \quad \text{where} \\
&\alpha_i = \det(q_{2i-1}, p_i^* - p_{i-1}^*), \quad \beta_i = \det(p_{i+1}^* - p_i^*, q_{2i+1}), \\
&\gamma_i = \det(p_{i+1}^* - p_i^*, p_i^* - p_{i-1}^*).
\end{aligned}$$

For the mixed area of P^* and Q^*, we consider the following sum, where indices i range from 0 to $N/2 - 1$, and indices j range from 0 to $N - 1$:

$$\begin{aligned}
&\sum\nolimits_i \det(q_i^*, p_{i+1}^* - p_{i-1}^*) = \\
&= \sum\nolimits_i \frac{1}{\gamma_i} \det\left(\alpha_i(p_{i+1}^* - p_i^*) + \beta_i(p_i^* - p_{i-1}^*), p_{i+1}^* - p_{i-1}^*\right) \\
&= \sum\nolimits_i \frac{1}{\gamma_i} \big(\alpha_i(-\det(p_{i+1}^*, p_{i-1}^*) - \det(p_i^*, p_{i+1}^*) + \det(p_i^*, p_{i-1}^*) \\
&\qquad +\beta_i(\det(p_i^*, p_{i+1}^*) - \det(p_i^*, p_{i-1}^*) - \det(p_{i-1}^*, p_{i+1}^*))\big) \\
&= \sum\nolimits_i \frac{1}{\gamma_i} \Big(\alpha_i\gamma_i - \beta_i\gamma_i\Big) \\
&= \sum\nolimits_i \Big(\det(q_{2i-1}, p_i^* - p_{i-1}^*) - \det(p_{i+1}^* - p_i^*, q_{2i+1})\Big) \\
&= \sum\nolimits_{j \text{ even}} \Big(\det(q_{j-1}, p_j - p_{j-2}) + \det(q_{j+1}, p_{j+2} - p_j)\Big).
\end{aligned}$$

An index shift shows that

$$\begin{aligned}
&\sum_{j \text{ even}} \det(q_{j-1}, p_j - p_{j-2}) = \sum_{j \text{ even}} \det(q_{j+1}, p_{j+2} - p_j) \\
&= \sum_{j \text{ odd}} \det(q_j, p_{j+1} - p_{j-1}),
\end{aligned}$$

so we conclude that

$$\begin{aligned}
&\text{area}(P^*, Q^*) = \frac{1}{4} \sum\nolimits_i \det(q_i^*, p_{i+1}^* - p_{i-1}^*) \\
&= \frac{1}{2} \sum\nolimits_{j \text{ odd}} \det(q_j, p_{j+1} - p_{j-1}).
\end{aligned}$$

By Lemma 2.3, this expression equals $\text{area}(P, Q)$, which concludes the proof. □

This result concerning the mixed area of parallel polygons is strong in reducing the number of vertices to deal with by a factor 2. However, if we apply it to two arbitrary polygons, which are made artificially parallel like those of Figure 2.1, we only obtain a fact which is obvious from the definition of mixed area anyway. As illustrated by Figure 2.5, Q^* then describes the boundary of the domain L^* constructed from K and L as the intersection of all supporting half-spaces of L whose boundary is parallel to an edge of K. Obviously, $\text{area}(K, L) = \text{area}(K, L^*)$.

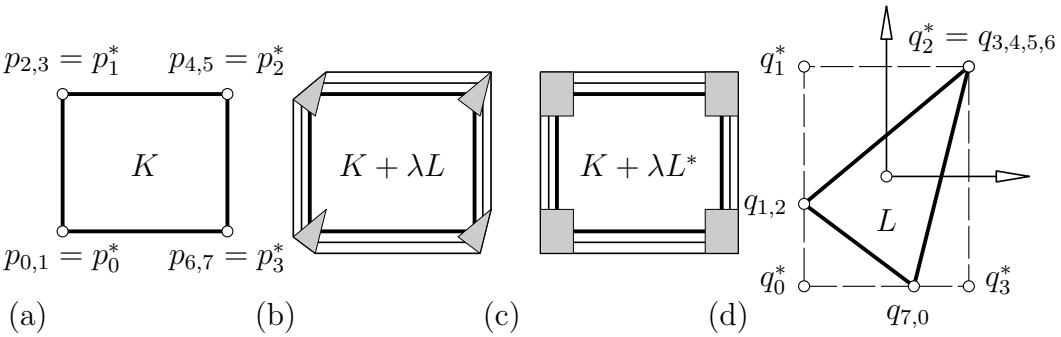

FIGURE 2.5: An explanation of the fact $\text{area}(P, Q) = \text{area}(P^*, Q^*)$ for artificially parallel polygons which occur as boundaries $P = \partial K$ and $Q = \partial L$. (a) Both polygons P and P^* describe the boundary ∂K. (b) Convex domains $K + \lambda L$, where λ equals 0.1 and 0.2. (c) The same for L^* instead of L, where the boundary ∂L^* is given by the polygon Q^*. (d) Polygons Q and Q^*. Obviously the linearly growing part of $\text{area}(K + \lambda L)$ along the edges of ∂K is not affected if we replace L by L^*.

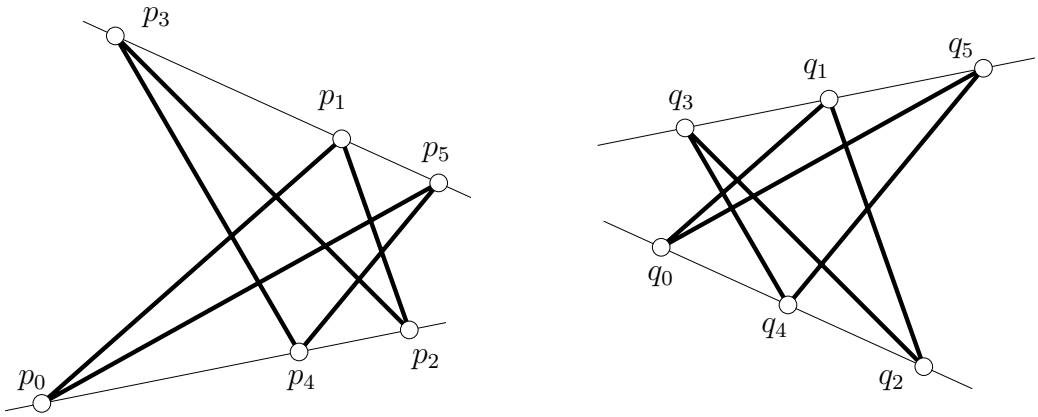

FIGURE 2.6: A Pappos hexagon does not fulfill the requirements of Definition 2.4, and so Theorem 2.7 is not applicable to this pair of parallel Pappos hexagons with $\text{area}(P, Q) = 0$ (we must apply Proposition 2.8 instead).

2.3 Vanishing mixed areas

This sections applies Theorem 2.6 to parallel polygons P, Q whose mixed area *vanishes*. As mentioned in § 2.1.3, such pairs of polygons are especially

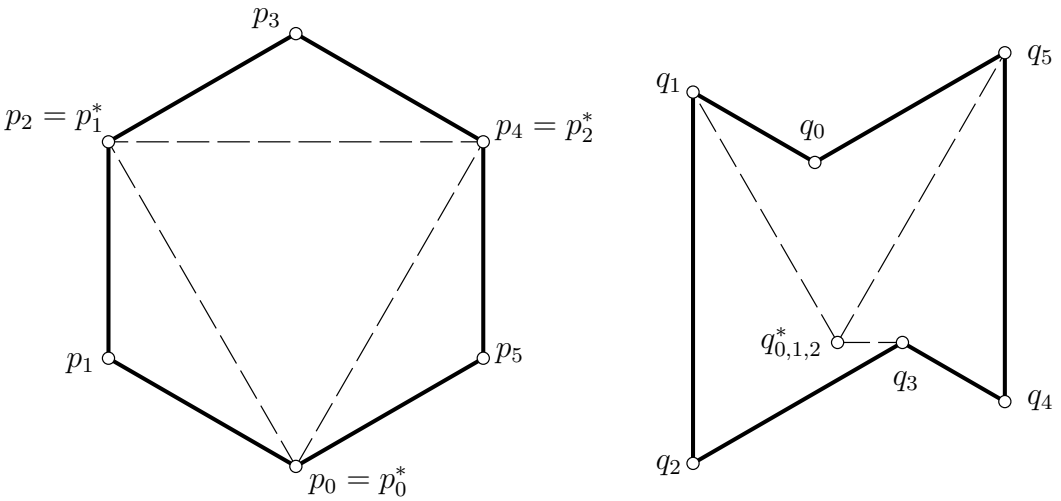

FIGURE 2.7: Parallel hexagons P, Q with vanishing mixed area (the derived triangle Q^* degenerates).

interesting for the construction of discrete minimal surfaces.

2.3.1 Vanishing mixed area for parallel hexagons

Here we treat both quadrilaterals and 5-gons as special hexagons. Before we derive a geometric criterion for the vanishing of mixed area for parallel hexagons, we discuss pairs P, Q of hexagons where Theorem 2.6 cannot be applied, because neither derived polygon Q^*, Q^{**} can be constructed. Obviously, this is the case if and only both p_0, p_2, p_4 and p_1, p_3, p_5 are collinear, i.e., P is a Pappos hexagon (see Figure 2.6). Exchanging the role of P and Q helps, except for the case that both q_0, q_2, q_4 and q_1, q_3, q_5 are collinear.

Theorem 2.7. *For parallel hexagons P, Q where one, say P, is not a Pappos hexagon, there is a labeling of vertices such that the derived polygons P^*, Q^* can be constructed. Then* $\operatorname{area}(P, Q) = 0$ *if and only if all vertices of the triangle Q^* coincide, i.e., if the lines*

$$q_1 + [p_2 - p_0], \quad q_3 + [p_4 - p_2], \quad q_5 + [p_0 - p_4]$$

intersect in a common point.

PROOF. The derived polygons P^*, Q^* are parallel triangles, with $Q^* = \lambda P^* + a$. It follows that $\operatorname{area}(P^*, Q^*) = \lambda \operatorname{area}(P^*)$. By non-collinearity of P^*, this area vanishes if and only if $\lambda = 0$. □

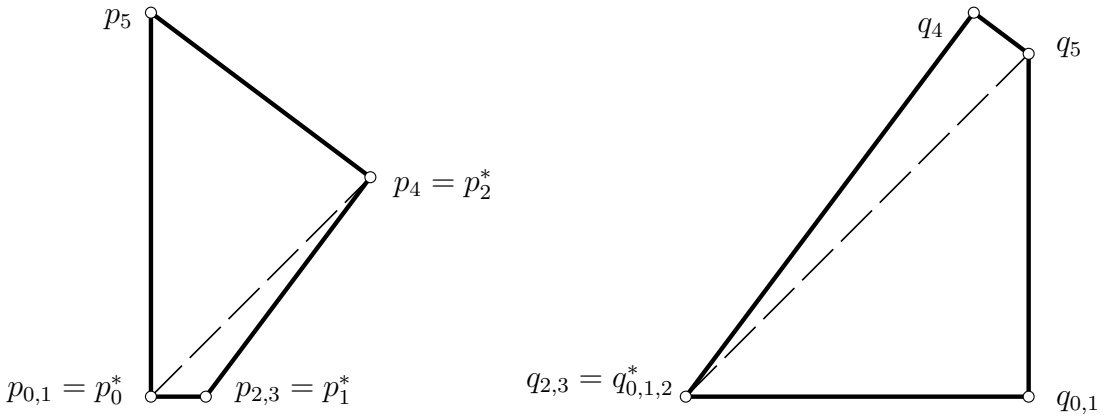

FIGURE 2.8: Quadrilaterals with antiparallel diagonals are degenerate hexagons P, Q, where the triangle Q^* degenerates into a point.

The case of two Pappos hexagons has to be treated separately:

Proposition 2.8. *Suppose that P, Q are two parallel hexagons such that p_1, p_3, p_5 as well as q_0, q_2, q_4 are collinear (this includes the case of parallel Pappos hexagons). Then* $\operatorname{area}(P, Q) = 0$ *in exactly the following cases:*

(i) $p_1 = p_3 = p_5$ *or* $q_0 = q_2 = q_4$.

(ii) The triples (p_1, p_3, p_5) and (q_4, q_0, q_2) are affinely equivalent.

(iii) The lines which carry p_1, p_3, p_5 and q_0, q_2, q_4 are parallel.

PROOF. By parallel translation we can achieve that the straight lines pass through the origin of the coordinate system, so there are $v, w \in \mathbb{R}^2 \setminus 0$ with $p_i = \lambda_i v$ for $i = 1, 3, 5$ and $q_j = \mu_j w$ for $j = 0, 2, 4$. By Equation (2.5),

$$\begin{aligned} 2\operatorname{area}(P, Q) &= \sum\nolimits_{i=1,3,5} \det(\lambda_i v, (\mu_{i+1} - \mu_{i-1})w) \\ &= \det(v, w)(\lambda_1(\mu_2 - \mu_0) + \lambda_3(\mu_4 - \mu_2) + \lambda_5(\mu_0 - \mu_4)) \\ &= \det(v, w)((\lambda_1 - \lambda_3)(\mu_2 - \mu_4) - (\lambda_1 - \lambda_5)(\mu_0 - \mu_4)). \end{aligned}$$

In case (iii) we have $\det(v, w) = 0$, so $\operatorname{area}(P, Q) = 0$. In case (i) we have

$$\lambda_1 = \lambda_3 = \lambda_5, \quad \text{or} \quad \mu_0 = \mu_2 = \mu_4,$$

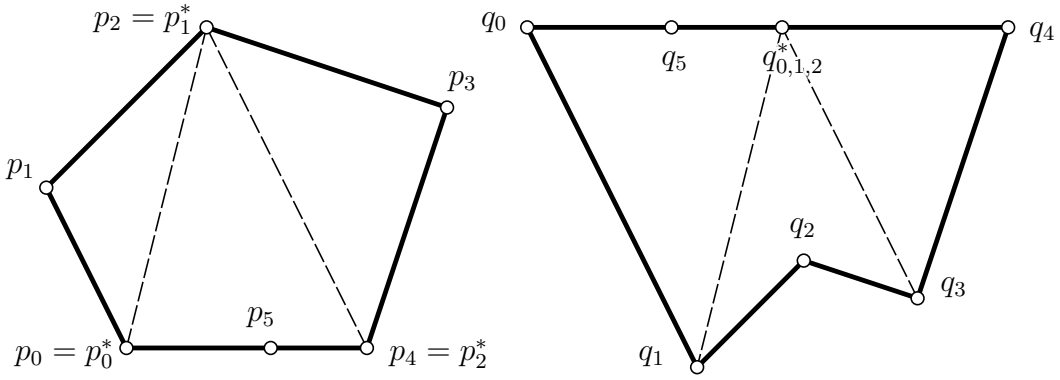

FIGURE 2.9: A pair of parallel 5-gons P, Q seen as hexagons, and a geometric characterization of vanishing mixed area which follows from this interpretation. Index shifts produce equivalent configurations.

which likewise implies vanishing mixed area. We now assume that we have neither case (i) nor case (iii). Then

$$\text{area}(P, Q) = 0 \iff (\lambda_1 - \lambda_3) : (\lambda_1 - \lambda_5) = (\mu_4 - \mu_0) : (\mu_4 - \mu_2),$$

i.e., if and only if the ratio of collinear points p_1, p_3, p_5 equals the ratio of collinear points q_4, q_0, q_2. This is equivalent to (ii). □

We refrain from an exhaustive discussion of cases. An example of two parallel Pappos hexagons with vanishing mixed area is shown by Figure 2.6.

2.3.2 Vanishing mixed area for 4- and 5-gons as degenerate 6-gons

Two parallel *quadrilaterals* are converted to parallel hexagons if we count two pairs of corresponding vertices twice. This operation does not change the mixed area, and Theorem 2.7 immediately gives the known result of Proposition 2.2 that vanishing mixed area is characterized by anti-parallelity of diagonals (see Figures 2.2 and 2.8). Anyway Proposition 2.2 follows directly from Lemma 2.3, because for parallel quads, (2.6) expands to

$$\text{area}(P, Q) = \det(p_0 - p_2, q_1 - q_3).$$

For 5-gons, we have the following result:

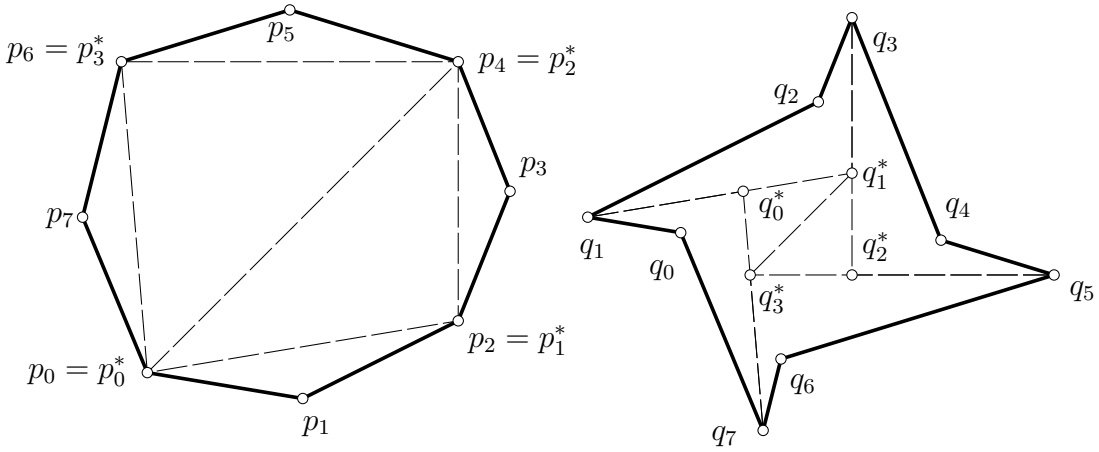

FIGURE 2.10: Parallel 8-gons P, Q with vanishing mixed area. The derived polygons P^*, Q^* are parallel quads with $\operatorname{area}(P^*, Q^*) = 0$ and consequently antiparallel diagonals.

Corollary 2.9. *The oriented mixed area of two parallel 5-gons*

$$P = (p_0, \dots, p_4) \quad \textit{and} \quad Q = (q_0, \dots, q_4)$$

vanishes if both of them are contained in a straight line. If this is not the case, $\operatorname{area}(P, Q) = 0$ *is characterized by the following geometric condition for one index i (and equivalently for all indices i): The lines*

$$q_{i+1} + [p_{i+2} - p_i] \quad \textit{and} \quad q_{i+3} + [p_{i+4} - p_{i+2}]$$

meet on the edge $q_{i+4}q_i$, where indices are taken modulo 5.

PROOF. It is sufficient to assume that p_0, p_1, p_4 are not collinear and show the result for the case $i = 0$ illustrated by Figure 2.9. By introducing vertices p_5, q_5 in the edges p_4p_0 and q_4q_0, resp., we convert both P and Q into parallel hexagons, and Theorem 2.7 is applicable. The statement that Q^* degenerates to a point translates to the statement we want to show. □

2.3.3 Vanishing mixed area for 8-, 7- and 6-gons (again)

Theorem 2.6 is recursively applicable, but the number of cases to be distinguished because diagonals are parallel and derived polygons cannot be constructed becomes greater. The following result for generic 8-gons follows directly from Theorem 2.6 and Proposition 2.2 (see Figure 2.10).

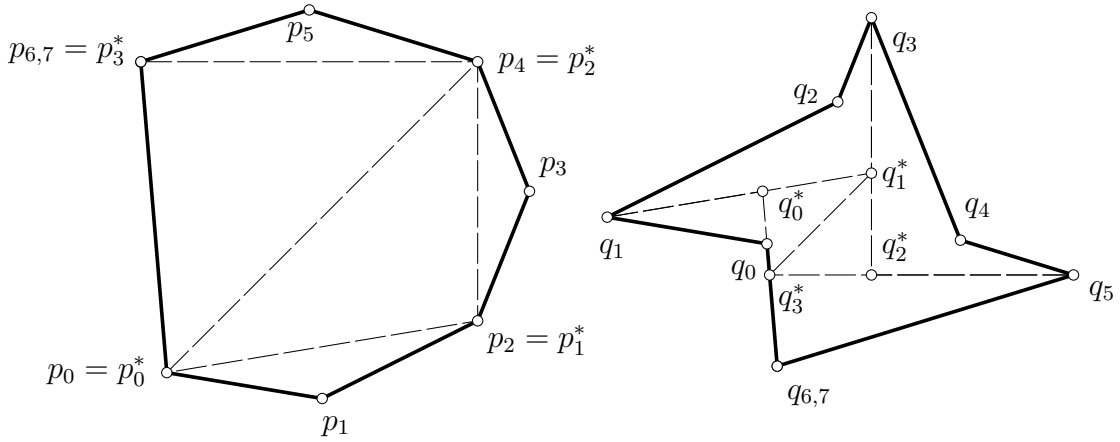

FIGURE 2.11: Parallel 7-gons P, Q with vanishing mixed area, which are interpreted as 8-gons with $p_6 = p_7$ and $q_6 = q_7$, respectively. The derived polygons P^*, Q^* are parallel quads with $\text{area}(P^*, Q^*) = 0$ and consequently antiparallel diagonals.

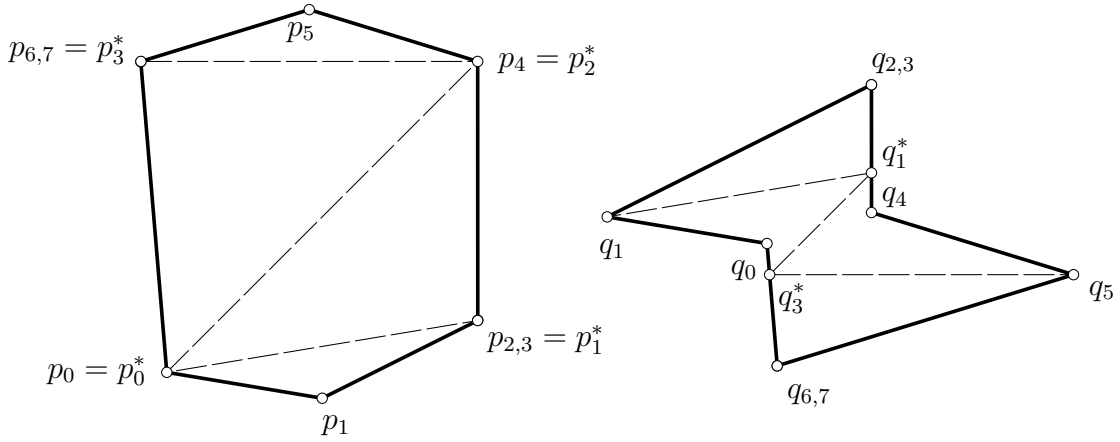

FIGURE 2.12: Parallel hexagons P, Q with vanishing mixed area, which are interpreted as 8-gons with $p_6 = p_7, p_2 = p_3$ and $q_6 = q_7, q_2 = q_3$ respectively. The derived polygons P^*, Q^* are parallel quads with $\text{area}(P^*, Q^*) = 0$ and consequently antiparallel diagonals. For a geometric characterization, only one half of Q^* is needed.

Corollary 2.10. *Parallel 8-gons P, Q where the derived polygons P^*, Q^* can be constructed have vanishing mixed area exactly in the following three cases:*

(i) both sets $\{p_0, p_2, p_4, p_6\}$ *and* $\{q_0^*, q_1^*, q_2^*, q_3^*\}$ *are contained in a straight line;*

(ii) $p_0 \neq p_4$ *and* p_0p_4 *is parallel to* $q_1^*p_3^*$,

(iii) $p_2 \neq p_6$ *and* p_2p_6 *is parallel to* $q_0^*p_2^*$.

The obvious way to treat parallel 7-gons is as 8-gons with two coincident vertices: We simply add an 8th vertex $p_7 = p_6$ and $q_7 = q_6$ to each an apply Corollary 2.10. This is illustrated by Figure 2.11. It is interesting to observe that also for hexagons we get again an easy geometric condition if we treat them as 8-gons with 2 coincident vertices (see Figure 2.12). Disregarding special cases, we have:

Corollary 2.11. *The parallel hexagons* $(p_0, p_1, p_2, p_4, p_5, p_6)$ *and* $(q_0, q_1, q_2, q_4, q_5, q_6)$ *generically have zero oriented mixed area if and only if* $p_0 \vee p_4 \parallel q_1^* \vee q_3^*$, *where*

$$q_1^* = (q_1 + [p_2 - p_0]) \cap (q_2 \vee q_4), \quad q_3^* = (q_5 + [p_4 - p_6]) \cap (q_6 \vee q_0).$$

Proof. The polygons are extended to 8-gons P, Q with the same mixed area by letting $p_3 := p_2$, $p_7 := p_6$, $q_3 := q_2$, and $q_7 := q_6$. The derived quadrilateral Q^* according to Corollary 2.10 has the two vertices q_1^*, q_3^*, so the result follows. □

2.3.4 Polygons with vanishing mixed area as a result of a closing theorem

The following proposition, which is some kind of a closing theorem, generates parallel pairs of polygons with vanishing mixed area.

Proposition 2.12. *Let* k *be an even number and* $P = (p_0, \ldots, p_{k-1})$ *a planar polygon. Moreover, let* d_0 *and* d_1 *be arbitrary points in* $\mathbb{R}^2$ *and* $q_0 \in d_0 + [p_1 - p_{k-1}]$. *Then there exists a unique polygon* $Q = (q_0, \ldots, q_{k-1})$ *such that* $q_i - q_{i+1} \parallel p_i - p_{i+1}$, *the lines*

$$\{q_i + [p_{i-1} - p_{i+1}] \mid i \text{ even})\}$$

intersect in d_0 *and*

$$\{q_i + [p_{i-1} - p_{i+1}] \mid i \text{ odd})\}$$

intersect in d_1 *(see Figure 2.13).*

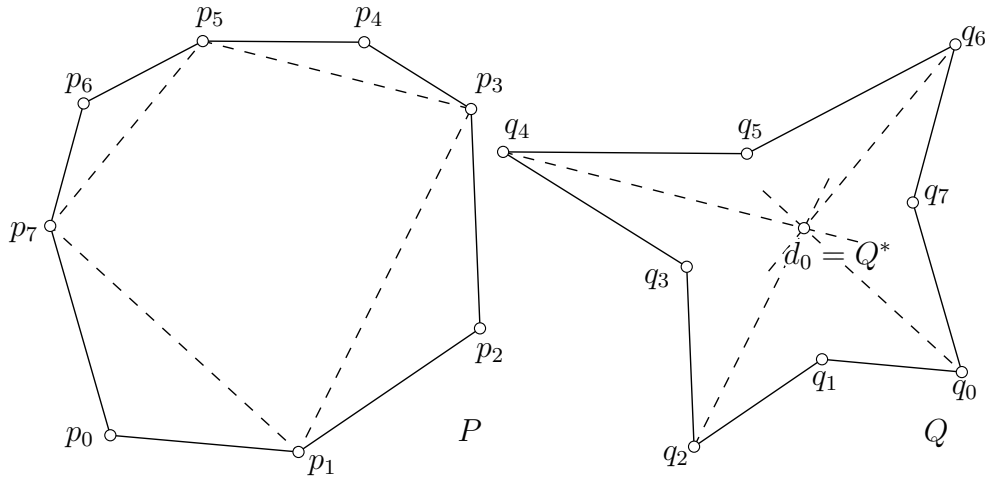

FIGURE 2.13: Illustration of the closing theorem stated in Proposition 2.12. Since Q^* degenerates to a single point d_0, the mixed area of P and Q vaneshes.

PROOF. Uniqueness follows from the construction. To prove the existence of the polygon Q, we construct the 2-periodic sequence $(d_i)_{i\in\mathbb{Z}}$ with $d_{i+2} = d_i$ from the given points d_0, d_1.

The polygon Q with the desired properties exists if and only if Q is parallel to P and if the concurrence of

$$q_i + [p_i - p_{i+1}], \quad d_{i+1} + [p_i - p_{i+2}] \quad \text{and} \quad q_{i+1} + [p_{i+1} - p_{i+2}]$$

for all $i \in \{0 \dots k-2\}$ implies that

$$q_{k-1} + [p_{k-1} - p_0], \quad d_0 + [p_{k-1} - p_1] \quad \text{and} \quad q_0 + [p_0 - p_1]$$

are concurrent.

The lines

$$q_i + [p_i - p_{i+1}], \quad d_{i+1} + [p_i - p_{i+2}] \quad \text{and} \quad q_{i+1} + [p_{i+1} - p_{i+2}]$$

are concurrent for all $i \in \{0 \dots k-1\}$ if and only if

$$\det\left[\begin{pmatrix} q_i \\ 1 \end{pmatrix} \times \begin{pmatrix} p_i - p_{i+1} \\ 0 \end{pmatrix}, \begin{pmatrix} d_{i+1} \\ 1 \end{pmatrix} \times \begin{pmatrix} p_i - p_{i+2} \\ 0 \end{pmatrix}, \begin{pmatrix} q_{i+1} \\ 1 \end{pmatrix} \times \begin{pmatrix} p_{i+1} - p_{i+2} \\ 0 \end{pmatrix}\right] = 0.$$

This determinant has the form

$$\det\begin{pmatrix} -p_i^2+p_{i+1}^2 & -p_i^2+p_{i+2}^2 & -p_{i+1}^2+p_{i+2}^2 \\ p_i^1-p_{i+1}^1 & p_i^1-p_{i+2}^1 & p_{i+1}^1-p_{i+2}^1 \\ \det(q_i,p_i-p_{i+1}) & \det(d_{i+1},p_i-p_{i+2}) & \det(q_{i+1},p_{i+1}-p_{i+2}) \end{pmatrix} =$$
$$= \det(q_i,p_i-p_{i+1})\cdot\det(p_i-p_{i+2},p_{i+1}-p_{i+2}) -$$
$$-\det(d_{i+1},p_i-p_{i+2})\cdot\det(p_i-p_{i+1},p_{i+1}-p_{i+2}) +$$
$$+\det(q_{i+1},p_{i+1}-p_{i+2})\cdot\det(p_i-p_{i+1},p_i-p_{i+2}).$$

Because of the equations

$$\det(p_i-p_{i+1},p_i-p_{i+2}) = \det(p_i-p_{i+1},p_{i+1}-p_{i+2})$$
$$=\det(p_i-p_{i+2},p_{i+1}-p_{i+2}),$$

this determinant equals zero if and only if

$$s_i := \det(q_i,p_i-p_{i+1})-\det(d_{i+1},p_i-p_{i+2})+\det(q_{i+1},p_{i+1}-p_{i+2}) = 0. \quad (2.8)$$

Assuming that Equation (2.8) holds for all $i \in \{0\dots k-2\}$ we have to show (2.8) for $i = k-1$.

$$0 = \sum_{i=0}^{k-2}(-1)^i s_i = \det(q_0,p_0-p_1) - \sum_{i=0}^{k-2}(-1)^i\det(d_{i+1},p_i-p_{i+2}) +$$
$$+\underbrace{(-1)^{k-2}}_{=1}\det(q_{k-1},p_{k-1}-p_k)$$

because k is even. The sum $\sum_{i=0}^{k-2}(-1)^i\det(d_{i+1},p_i-p_{i+2})$ can be written as

$$\sum_{\substack{i=0\\ i \text{ even}}}^{k-2}\det(d_1,p_i-p_{i+2}) - \sum_{\substack{i=1\\ i \text{ odd}}}^{k-3}\det(d_0,p_i-p_{i+2}) =$$
$$= \det(d_1,p_0-p_2+p_2-p_4+\ldots+p_{k-2}-p_k) -$$
$$-\det(d_0,p_1-p_3+p_3-p_5+\ldots p_{k-3}-p_{k-1}) = 0+\det(d_0,p_1-p_{k-1})$$

because $k \equiv 0 \mod (k)$. So we get

$$\det(q_0,p_0-p_1)-\det(d_0,p_1-p_{k-1})+\det(q_{k-1},p_{k-1}-p_k) = 0$$

which is Equation (2.8) for $i = k-1$ (with indices modulo k). □

The property that this closing theorem generates pairs of parallel polygons with vanishing mixed area is based on Lemma 2.5.

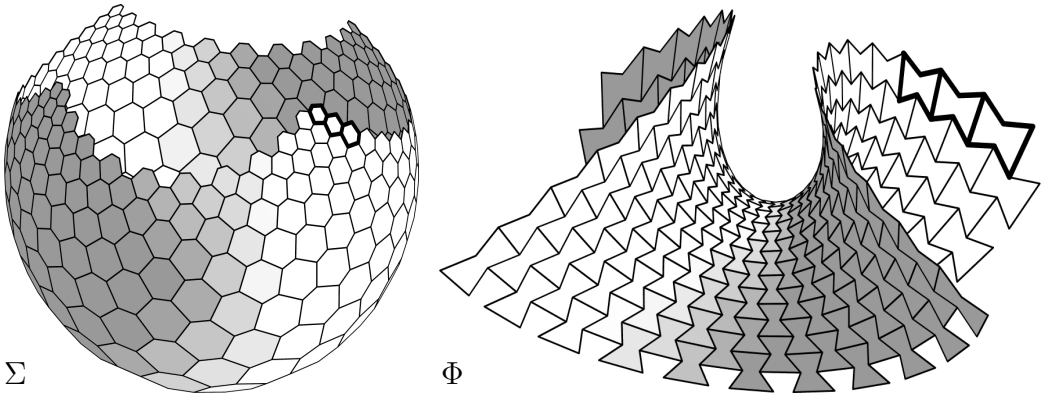

FIGURE 2.14: A discrete Enneper's surface Φ in the shape of a hexagonal mesh, which corresponds to a spherical mesh Σ by a discrete Christoffel duality. The marked hexagons correspond to each other.

2.4 Discrete minimal surfaces

Section 2.1.3 already introduced in general terms the definitions of curvature according to [5, 20]. Recall that a polyhedral surface Φ is a discrete minimal surface with respect to a Gauss image Σ, if Φ, Σ are parallel meshes such that corresponding faces have vanishing mixed area. We view Φ as a discrete Christoffel dual of Σ, and vice versa.

Not every quadrilateral mesh Σ with planar faces (i.e., not every a polyhedral surface with regular grid combinatorics) has a Christoffel dual Φ: It turns out that exactly the discrete Koenigs nets (see [6, 7]) have this property. A quadrilateral mesh $\mathcal{M}$ with regular grid combinatorics is called *discrete Koenigs net* (see [7]) if there exists a *dual* mesh $\mathcal{M}^*$, which is parallel to $\mathcal{M}$, such that the non-corresponding diogonals are parallel (see Figure 2.8). A remarkable charakterization of discrete Koenigs nets in terms of the Desargues configuration can be found in [7]. The property of being a smooth or discrete Koenigs net is invariant under projective transformations.

2.4.1 Construction of hexagonal minimal surfaces

Figure 2.14 illustrates a parallel pair (Σ, Φ) of meshes (for more details, see the example below). The faces of Σ are tangent to the unit sphere, so it makes sense to consider Σ as a discrete Gauss image of Φ. As Φ has been constructed such that the mixed area of corresponding faces vanishes, Φ

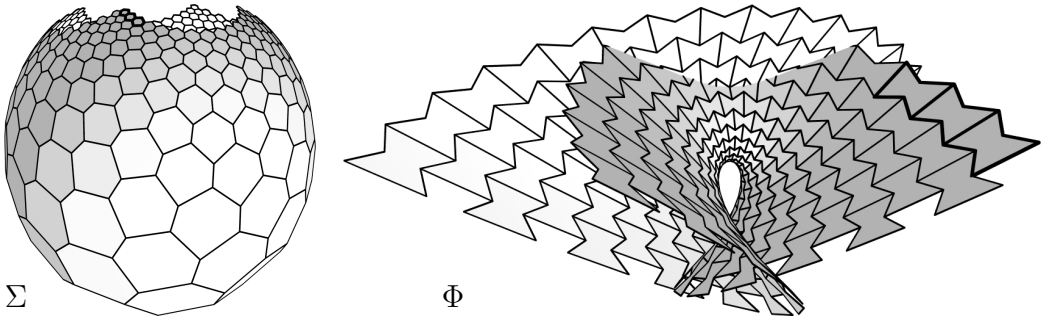

FIGURE 2.15: A discrete Enneper's surface created in the same way as Figure 2.14, but with a different size of the spherical mesh Σ. Here Φ has self-intersections. The viewpoint is different from that of Figure 2.14.

is discrete minimal. It should be mentioned in this place that the exact relation between the discrete Gauss image Σ and the unit sphere S^2 can be of a different nature: We could also require that vertices of Σ lie in S^2, or its edges are tangent to S^2. The three cases of vertices, edges, and faces having an exact tangency relation with S^2 correspond to the mesh Φ having offset meshes $\Phi + d\Sigma$ at constant vertex-vertex distance d, or edge-edge distance d, or face-face distance d [21, 20]. Note that the property of vanishing mixed area does not only occur between minimal surface and Gauss image, but also between a surface Φ of constant mean curvature H with respect to a Gauss image Σ, and its offset $\Phi + \frac{1}{H}\Sigma$.

The construction of a discrete Christoffel dual (i.e., Φ from Σ) for hexagonal meshes is easy, as there are enough degrees of freedom. The fact that $\dim \mathcal{P}(P) = 4$ leads to a three-dimensional space of parallel polygons Q with $\text{area}(P, Q) = 0$. Consequently adding a new hexagon of Φ to already constructed ones is an operation which has $3 - k$ degrees of freedom, where k is the number of known vertices (which are shared with already existing neighbours of the hexagon to be constructed).

This yields a discrete Cauchy problem with a unique solution which initial data consisting of two strips of hexagons in different directions as indicated in the figure aside.

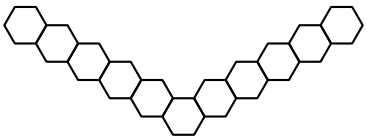

Example 2.13. Figure 2.14 shows a hexagonal mesh Σ which is circumscribed to the unit sphere and its Christoffel dual mesh Φ which assumes the shape of an Enneper's surface. This example is constructed as follows: We start with an isothermic curvature-line parametrization $x(u, v)$ of the

known smooth Enneper's surface M. Next we tile the parameter domain with non-convex hexagons — we used dilates of the hexagon with vertices $(0,0)$, $(\frac{1}{2},\frac{1}{4})$, $(1,0)$, $(1,1)$, $(\frac{1}{2},\frac{3}{4})$, $(0,1)$. Mapping the vertices of this tiling with the parametrization x yields a hexagonal mesh Φ_0 with non-planar faces inscribed to M (it looks very much like Figure 2.14, right). Each planar hexagon has a center, say (u^*, v^*), and we consider $x(u^*, v^*)$ as the center of the corresponding spatial hexagon. Next we construct the mesh Σ by parallel translating the tangent planes of M in the centers of hexagons such that they touch the unit sphere. Vertices q_i of Σ are found by intersection of planes (see Figure 2.14, left). Having constructed Σ, we find its Christoffel dual Φ by optimizing Φ_0 such that mixed areas of corresponding faces Q in Σ and P in Φ are zero, and such that corresponding edges q_iq_j and p_ip_j are parallel. This amounts to minimizing the quadratic functional

$$\lambda_{\text{par}} \sum_{\text{edges}} \|(q_i - q_j) \times (p_i - p_j)\|^2 + \lambda_{\text{mix}} \sum_{\text{faces}} \| \operatorname{area}(P, Q)\|^2.$$

This is done by a standard conjugate gradient method, and turns out not to change the shape of Φ_0 much, despite the fact that the theoretical number of degrees of freedom is larger.

2.4.2 Reciprocal parallelity in discrete minimal surfaces

In the quad mesh case, there is an interesting connection of minimal surfaces with *reciprocal-parallel meshes*. A reciprocal-parallel mesh pair is defined as meshes which are combinatorial duals of each other (there is a correspondence face–vertex, vertex–face, and edge–edge), such that corresponding edges are parallel [23]. Proposition 2.2 immediately shows that Φ is a minimal surface with respect to Σ if meshes composed from diagonals of quads in both Σ, Φ are reciprocally parallel [20]. This is illustrated in Figure 2.17. It should be mentioned that reciprocal parallelity of meshes in connection with discrete minimal surfaces also occurs in other places, for instance in [27].

For *hexagonal* meshes, we similarly can derive pairs of reciprocal-parallel meshes from a Christoffel dual pair (Σ, Φ). The geometric characterization of vanishing mixed area according to Theorem 2.7 and Figure 2.7 leads to the configuration of lines in meshes Σ and Φ, which is illustrated in Figures 2.16a and 2.16b. Obviously, the configuration of diagonals in Σ (Figure 2.16c) is

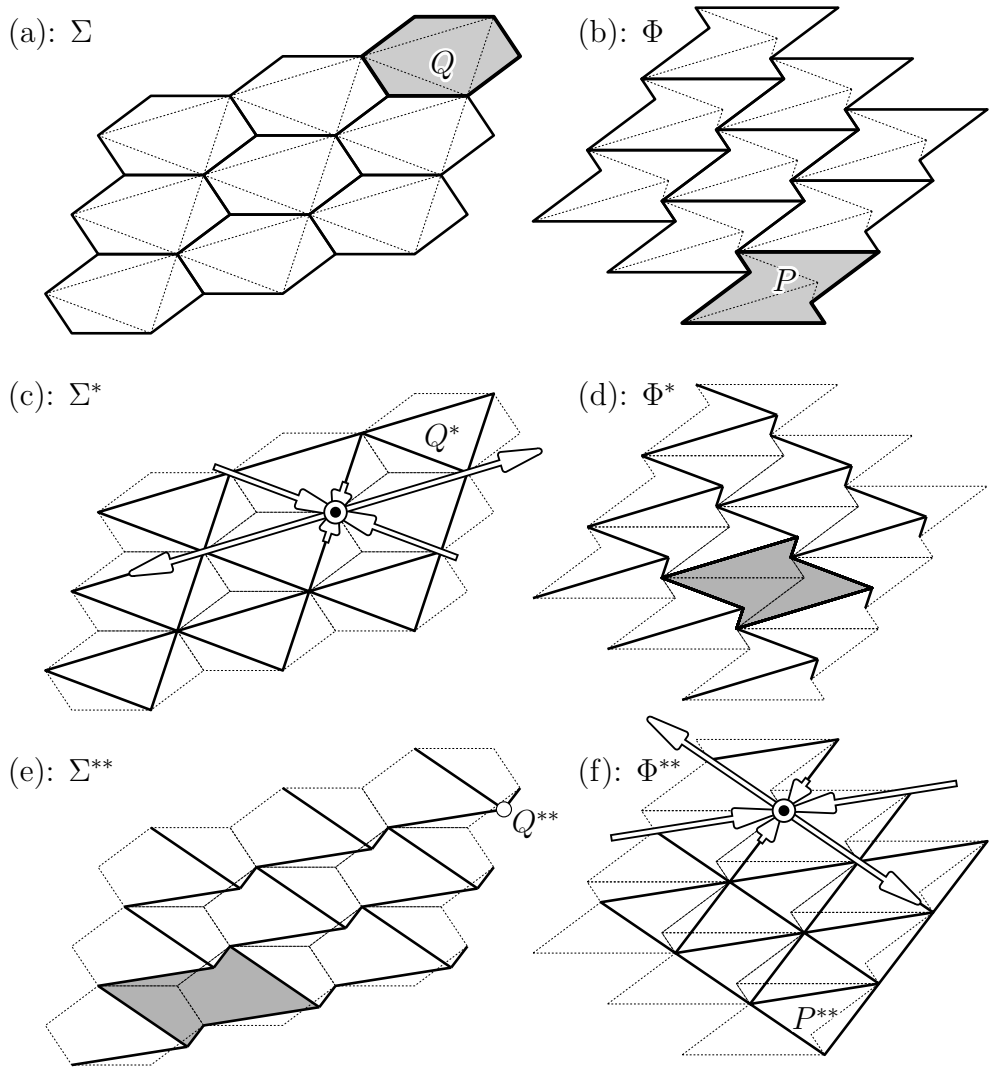

FIGURE 2.16: Reciprocal-parallel meshes Σ^*, Φ^* derived from Christoffel dual meshes Σ, Φ. The edges around a face in Φ^* serve as equilibrium forces acting in the edges adjacent to the corresponding vertex of Σ^*. (a) Hexagonal mesh Σ with face Q. (b) Hexagonal mesh Φ of the same combinatorics such that corresponding faces Q of Σ and P of Φ have vanishing mixed area. (c) Triangle mesh whose edges are derived polygons Q^* in mesh Σ. (d) Hexagonal mesh whose edges are the lines p_1p^*, p_3p^*, p_5p^* in each hexagon of Φ, where p^* is the degenerate polygon P^*. Note that Φ^* does not have planar faces. In (e) and (f), the geometric characterization of vanishing mixed area which yields diagonals and their parallels is read in reverse order compared to (a)–(d): Diagonals are taken from the non-convex hexagons in the mesh Φ.

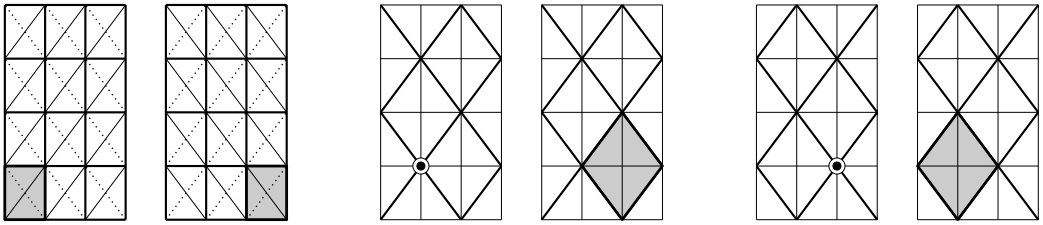

FIGURE 2.17: Reciprocal-parallel meshes derived from a quadrilateral mesh Σ and its Christoffel dual mesh Φ, which is combinatorially equivalent such that corresponding quadrilaterals P and Q have vanishing mixed area. From left: (a) Mesh Σ with face P. (b) Mesh Φ with face Q corresponding to P. (c) Quadrilateral mesh Σ^* composed from one half of diagonals of Σ. (d) Those diagonals in Φ which are parallel to the previous ones according to Proposition 2.2 constitute a mesh Φ^* reciprocal-parallel to Σ^*: vertices in Σ^* correspondence faces of Φ^*. (e) and (f) show the reciprocal-parallel mesh pair Σ^{**}, Φ^{**} composed from the diagonals omitted in (c) and (d).

reciprocally parallel to the configuration of lines in Φ, which consist of the to-be edges of degenerate derived polygons (Figure 2.16d). A different choice of diagonals in Σ would lead to a different pair of reciprocal-parallel meshes.

Obviously for each vertex of Σ^*, the cycle of edge vectors adjacent to the corresponding face of Φ^* serves as equilibrium forces acting on that vertex. Thus, Φ^* represents a collection of equilibrium forces for Σ^*. These forces (scaled) are shown by Figure 2.16c.

As the relation $\text{area}(P, Q) = 0$ is symmetric, the geometric configuration of the triangle P^* and the degenerate triangle Q^* exists also if the roles of P and Q (i.e., the roles of Σ and Φ) are exchanged: One half of the diagonals in Φ constitute a triangle mesh Φ^{**}, which possesses a reciprocal-parallel hexagonal mesh Σ^{**} associated with Σ (see Figures 2.16e and 2.16f). Figure 2.16f also shows equilibrium forces for Φ^{**} which are a scaled version of the edges of Σ^{**}.

2.5 Discrete constant mean curvature surfaces

In contrast to Section 2.3 where we studied vanishing mixed area of parallel polygons to obtain vanishing mean curvature, we are now interested in a geometric characterization of nonzero constant mean curvature. We give a

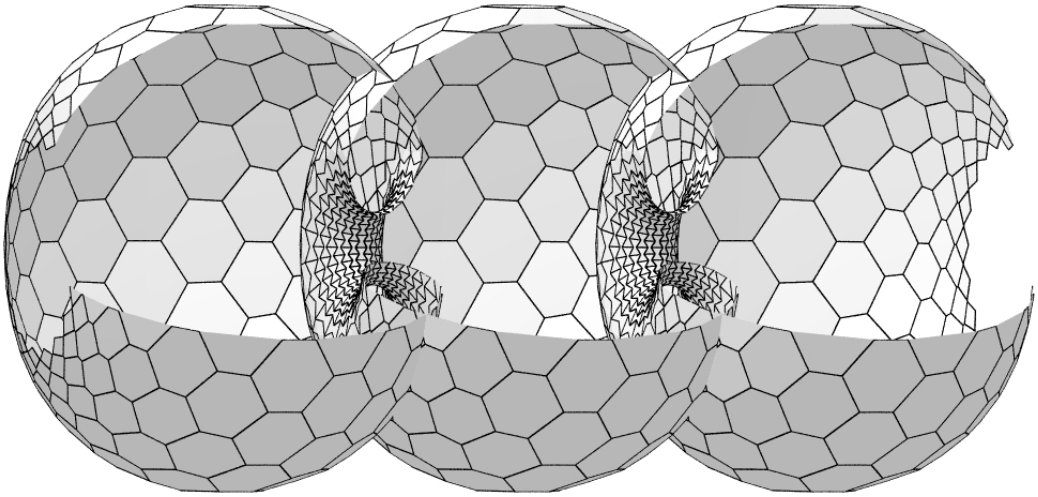

FIGURE 2.18: A discrete *nodoid* which is a surface of revolution with constant mean curvature (see Remark 2.17, Example 2.18, and Figure 2.21).

constant $c \in \mathbb{R} \setminus 0$ and discuss an incidence geometric characterization of a mesh with $H_P = c$ for all faces P of the mesh. After simple manipulations of the definition of the discrete mean curvature we get the following equivalence:

$$H_P = c \quad \Longleftrightarrow \quad \text{area}(P, P + c^{-1}Q) = 0 \qquad \text{(see [5])}.$$

Since a dilation with factor λ changes the mean curvature with factor $1/\lambda$, which is valid in the smooth setting as well as in the discrete setting, we can always prescribe $c = -1$. We choose $c = -1$ just for the sake of simplicity of further computations.

The above formula already indicates the connection between vanishing mixed area and constant mean curvature and therefore suggests the use of the derived polygons defined in § 2.2.2. We extend these polygons with one further derived polygon $\tilde{P}^* = (\tilde{p}_i^*)$ (see Figures 2.19 and 2.20) defined as

$$\tilde{p}_i^* = (p_{2i-1} + [p_{2i-2} - p_{2i}]) \cap (p_{2i+1} + [p_{2i} - p_{2i+2}]).$$

Theorem 2.14. *Let $P = (p_0, \ldots, p_{N-1})$ and $Q = (q_0, \ldots, q_{N-1})$ be two parallel polygons, where N is even, and let P^* and Q^* be a pair of derived polygons (see § 2.2.2). Then the discrete mean curvature H_P is equal to -1 if Q^* and $\tilde{P}^*$ are equal up to translation.*

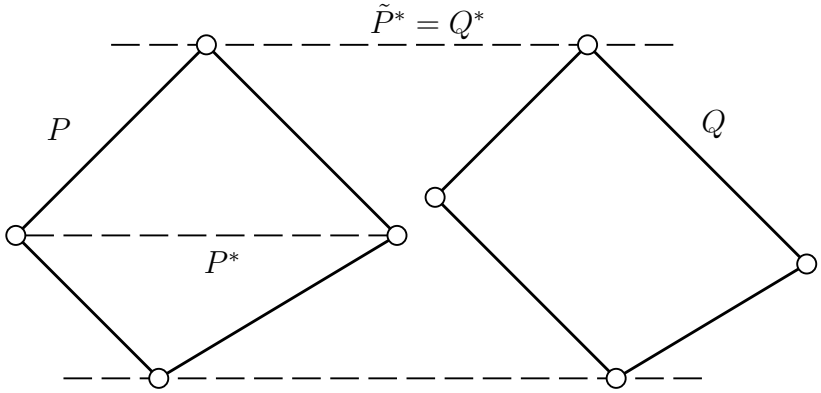

FIGURE 2.19: A pair of parallel quadrilaterals P and Q such that the mean curvature H_P equals -1 (see Theorem 2.16). The derived polygon P^* of a quadrilateral consists just of the diagonal of P. $\tilde{P}^*$ degenerates to a pair of parallel lines.

PROOF. We show that $\operatorname{area}(P,Q) = \operatorname{area}(P)$ which is equivalent to $H_P = -1$. Since the mixed area of two polygons is invariant under translations, we can assume that Q^* coincides with $\tilde{P}^*$. From the definition of $\tilde{p}_i^*$ follows that

$$\tilde{p}_i^* = p_{2i-1} + \mu_{2i-1}(p_{2i-2} - p_{2i}) \quad \text{and} \quad \tilde{p}_i^* = p_{2i+1} + \lambda_{2i+1}(p_{2i} - p_{2i+2})$$

for some λ_i and μ_i.

$$\begin{aligned}
&4\operatorname{area}(P,Q) = 4\operatorname{area}(P^*,Q^*) = 4\operatorname{area}(P^*,\tilde{P}^*)\\
&= \sum\nolimits_{i=0}^{(N-1)/2} \det(p_i^*, \tilde{p}_{i+1}^* - \tilde{p}_{i-1}^*)\\
&= \sum\nolimits_{i=0}^{(N-1)/2} \det(p_{2i}, p_{2i+1} + \mu_{2i+1}(p_{2i} - p_{2i+2})\\
&\qquad\qquad - (p_{2i-1} + \lambda_{2i-1}(p_{2i-2} - p_{2i})))\\
&= \sum\nolimits_{i=0}^{(N-1)/2} \det(p_{2i}, p_{2i+1}) + \det(p_{2i}, p_{2i+1})\\
&\qquad\qquad + \mu_{2i+1}\det(p_{2i}, -p_{2i+2}) + \lambda_{2i-1}\det(p_{2i}, -p_{2i-2})\\
&= 2\operatorname{area}(P) + \sum\nolimits_{i=0}^{(N-1)/2} \mu_{2i-1}\det(p_{2i}, p_{2i-2}) + \lambda_{2i+1}\det(p_{2i}, p_{2i+2})\\
&\overset{(*)}{=} 2\operatorname{area}(P) + \sum\nolimits_{i=0}^{(N-1)/2} \det(p_{2i}, \mu_{2i-1}(p_{2i-2} - p_{2i}))\\
&\qquad\qquad + \det(p_{2i}, p_{2i+1} - p_{2i-1} - \mu_{2i-1}(p_{2i-2} - p_{2i}))
\end{aligned}$$

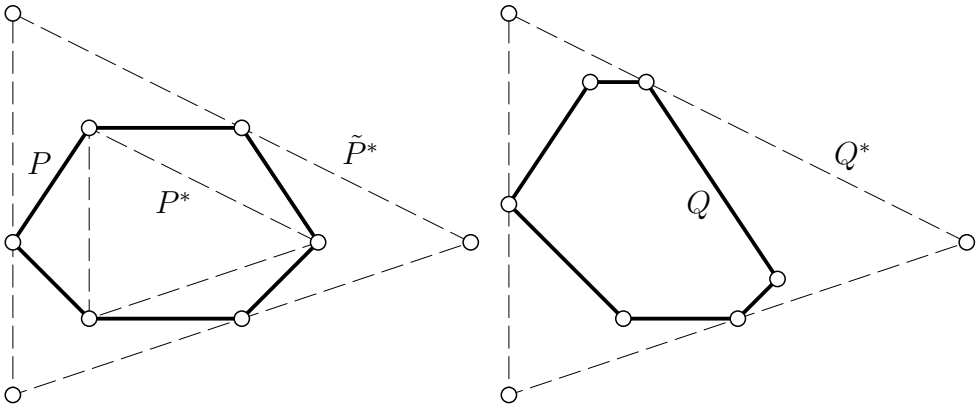

FIGURE 2.20: A pair of parallel hexagons P and Q such that the mean curvature H_P equals -1. The derived polygons $\tilde{P}^*$ and Q^* are equal up to translation.

$$= 4\,\mathrm{area}(P).$$

For the equality $(*)$ we used $\det(a,b) = \det(a, b-a)$ and the equality

$$\tilde{p}_i^* = p_{2i-1} + \mu_{2i-1}(p_{2i-2} - p_{2i}) = p_{2i+1} + \lambda_{2i+1}(p_{2i} - p_{2i+2}).$$

□

We can show by a simple numerical example that the condition in Theorem 2.14 that the two derived polygons Q^* and $\tilde{P}^*$ are equal is not sufficient for constant mean curvature. However, for quadrilaterals and hexagons the 'if' can be replaced by 'if and only if'.

Theorem 2.15. *Let $P = (p_0, \ldots, p_5)$ and $Q = (q_0, \ldots, q_5)$ be two parallel hexagons which fulfill the requirements of Definition 2.4, and let $\tilde{P}^*$ and Q^* be a pair of derived polygons (see § 2.2.2 and Figure 2.20). Then the discrete mean curvature H_P is equal to -1 if and only if Q^* and $\tilde{P}^*$ are equal up to translation.*

PROOF. The 'if' part is Theorem 2.14. Let us assume that $H_P = -1$. We have to show that the tiangles $\tilde{p}_0^*, \tilde{p}_2^*, \tilde{p}_4^*$ and q_0^*, q_2^*, q_4^* (w.l.o.g. we consider the even labeled polygons) are equal up to translation. By the definition of the derived polygons which implies that corresponding edges are parallel we have only to show e.g. $\tilde{p}_1^* - \tilde{p}_0^* = q_1^* - q_0^*$.

The construction of the derived polygons also guarantees the existence of

surface name	generating curve	mean curvature
plane	straight line orthogonal to the axis of revolution	$= 0$
cylinder	straight line parallel to the axis of revolution	$\neq 0$
sphere	circle with midpoint on the axis of revolution	$\neq 0$
catenoid	cosh	$= 0$
unduloid	undulary	$\neq 0$
nodoid	nodary	$\neq 0$

TABLE 2.1: All types of surfaces of revolution with constant mean curvature. An *undulary* is the locus of one focus of an ellipse rolling on a straight line without slipping and a *nodary* is the locus of one focus of a hyperbola (see Figure 2.21) rolling on a straight line without slipping.

values $\alpha_1, \alpha_3, \beta_1, \beta_5, \lambda_1, \lambda_3, \mu_1, \mu_5$ such that

$$\begin{aligned} q_0^* &= q_1 + \alpha_1(p_2 - p_0) = q_5 + \beta_5(p_0 - p_4) \\ q_1^* &= q_3 + \alpha_3(p_4 - p_2) = q_1 + \beta_1(p_2 - p_0) \end{aligned} \tag{2.9}$$

and

$$\begin{aligned} p_0^* &= q_5 + \mu_5(p_4 - p_0) = q_1 + \lambda_1(p_0 - p_2) \\ p_1^* &= q_1 + \mu_1(p_0 - p_2) = q_3 + \lambda_3(p_2 - p_4) \end{aligned} \tag{2.10}$$

$H_P = -1$ implies $\operatorname{area}(P, P - Q) = 0$ and therefore by Lemma 2.3

$$\sum_{i \in \{0,2,4\}} \det(p_i, (q_{i+1} - p_{i+1}) - (q_{i-1} - p_{i-1})) = 0.$$

Rewriting this equation yields

$$\begin{aligned} &\det(p_0 - p_2, q_1) + \det(p_2 - p_4, q_3) + \det(p_4 - p_0, q_5) \\ &+ \det(p_2 - p_0, p_1) + \det(p_4 - p_2, p_3) + \det(p_0 - p_4, p_5) = 0, \end{aligned}$$

and using the elementary rule $\det(a, b) = \det(a, b + \lambda a)$

$$\begin{aligned} &\det(p_0 - p_2, q_1 + \beta_1(p_2 - p_0)) + \det(p_2 - p_4, q_3 + \alpha_3(p_4 - p_2)) \\ &+ \det(p_4 - p_0, q_5 + \beta_5(p_0 - p_4)) + \det(p_2 - p_0, p_1 + \mu_1(p_0 - p_2)) \\ &+ \det(p_4 - p_2, p_3 + \lambda_3(p_2 - p_4)) + \det(p_0 - p_4, p_5 + \mu_5(p_4 - p_0)) = 0. \end{aligned}$$

Replacing with the notions of (2.9) and (2.10) yields

$$\begin{aligned}&\det(p_0-p_2,q_1^*)+\det(p_2-p_4,q_1^*)+\det(p_4-p_0,q_0^*)\\+&\det(p_2-p_0,\tilde{p}_1^*)+\det(p_4-p_2,\tilde{p}_1^*)+\det(p_0-p_4,\tilde{p}_0^*)=0,\end{aligned}$$

which implies

$$\det(p_0-p_4,(q_1^*-q_0^*)-(\tilde{p}_1^*-\tilde{p}_0^*))=0.$$

$q_1^*-q_0^*$ as well as $\tilde{p}_1^*-\tilde{p}_0^*$ are both parallel to p_0-p_2. We also assumed that p_0,p_2,p_4 is a non-degenerate triangle. Thus we conclude that

$$(q_1^*-q_0^*)-(\tilde{p}_1^*-\tilde{p}_0^*)$$

must be zero, which is what we wanted to show. □

Analogous to the case $N=6$ of Theorem 2.15 there is also the if and only if condition for the quadrilateral case $N=4$ even though the derived polygons $\tilde{P}^*$ and Q^* degenerate to pairs of parallel lines (see Figure 2.19).

Theorem 2.16. *Let $P=(p_0,\dots,p_3)$ and $Q=(q_0,\dots,q_3)$ be two parallel quadrilaterals and let $\tilde{P}^*$ and Q^* be a pair of derived polygons which degenerate to pairs of parallel polygons (see § 2.2.2 and Figure 2.19). Then the discrete mean curvature H_P is equal to -1 if and only if Q^* and $\tilde{P}^*$ are equal up to translation.*

Proof. The 'if' part is Theorem 2.14. We have to show that

$$\langle p_3-p_1,(p_0-p_2)^\perp\rangle=\langle q_3-q_1,(p_0-p_2)^\perp\rangle.$$

Analogous to the proof of Thoerem 2.15, we get

$$H_P=-1\quad\Longleftrightarrow\quad\sum_{i\in\{0,2\}}\det(p_i,(q_{i+1}-p_{i+1})-(q_{i-1}-p_{i-1}))=0$$

and therefore

$$\det(p_0-p_2,p_3-p_1-(q_3-q_1))=0,$$

which is what we wanted to show. □

Remark 2.17. *According to the Theorem of Delaunay (see e.g. [12, Theorem 3.4, p. 46]) a surface of revolution with constant mean curvature is locally one of the surfaces listed in Table 2.1.*

Example 2.18. Figures 2.18 and 2.21 show a hexagonal mesh which assumes the shape of a nodoid (see Remark 2.17). We construct this example as follows: We start with a rotational symmetric hexagonal mesh Σ covering the sphere and construct a mesh Φ parallel to Σ (i.e., same combinatorics and edgewise parallel) minimizing energies according to the following goals:

(i) Constant mean curvature $H_p = -1$ for all facets of the mesh.

(ii) Arbitrary radius of one circle of hexagons of Σ.

(iii) Fairness of the mesh.

(iv) Same rotational symmetry as Σ.

With some specific choice of the radius for the circle of hexagons (ii) the optimization prozess could result in Φ covering a sphere again. However, the choice which leads to Figure 2.18 leads to a discrete surface which after a visual inspection reminds us of a *nodoid* (see Remark 2.17). A smooth nodoid is a surface of revolution whose generating curve in a plan through the axis is a *nodary*. Nodaries are plane curves which are can be generated as locus of focus of a hyperbola rolling on a straight line without slipping. Figure 2.21 shows a nodary and indicates how close the discrete nodoid approximates the smooth one.

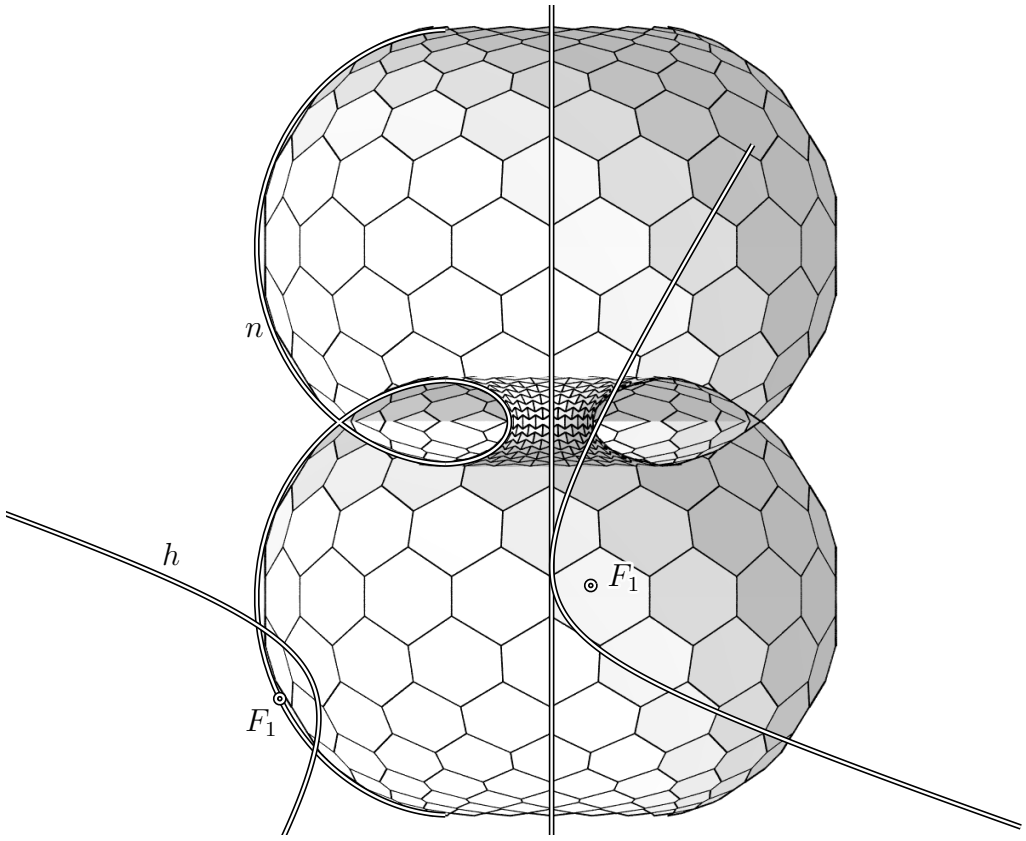

FIGURE 2.21: A discrete surface of revolution with constant mean curvature (see Remark 2.17 and Example 2.18). The surface is cut open along a plane passing through the axis. Visual inspection reveals that the considered surface is a *nodoid*. The generating curve n, which is a *nodary*, is indicated. Also the hyperbola h with its two focal points F_1 and F_2 which generates the nodary is illustrated.

Chapter 3

Conformal hexagonal meshes and minimal surfaces

In the present chapter we establish a discrete Christoffel dual construction for special hexagonal meshes, namely conformal ones. Most of this chapter can be found in [16].

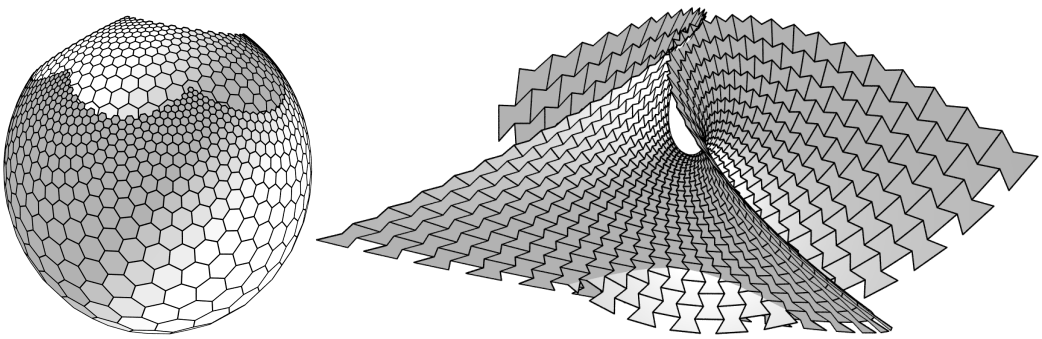

FIGURE 3.1: A discrete Enneper's surface (right) and its discrete Gauss image (see Example 3.24). This instance of the discrete Enneper's surface is a result of the discrete Christoffel dual construction stated in Definition 3.8 whereas Figures 2.14 and 2.15 are the result of an optimazation prozess minimizing the mixed area (see Example 2.13).

3.1 Multi-ratio and vertex offset meshes

For the notion of pairs of parallel meshes see the introduction of § 2.1.3 and for offset meshes and offset distances of parallel meshes we refer back to § 2.4.1

For quad meshes H. Pottmann et al. [20, 21] showed a connection between the existence of vertex and face offsets on the one hand, and circular and conical meshes on the other hand. In the present chapter the circular meshes are the more important ones. A *circular polygon* is a polygon with a circumcircle and a *quasi-circular polygon* is edge-wise parallel to a polygon with a circumcircle (see e.g. [14]). A *circular mesh* is a mesh where each face is a circular polygon and a *quasi-circular mesh* is a mesh where each face is a quasi-circular polygon.

A quadrilateral is circular if and only if its cross-ratio is real. A generalization of the cross-ratio to polygons with an even number of vertices $z_0, \dots, z_{n-1}$ is the so-called *multi-ratio* (see e.g. [3])

$$\mathrm{q}(z_0, \dots, z_{n-1}) := \frac{(z_0 - z_1)(z_2 - z_3) \cdot \ldots \cdot (z_{n-2} - z_{n-1})}{(z_1 - z_2)(z_3 - z_4) \cdot \ldots \cdot (z_{n-1} - z_0)}.$$

Obviously, the multi-ratio $\mathrm{q}(z_0, \dots, z_{n-1})$ is invariant under orientatin preserving Möbius transformations since it is invariant under translations, dilations, rotations and transformations of the form $z \mapsto 1/z$. However, a real value for the multi-ratio is invariant under anti-Möbius transformations as well (see § 1.2.1).

Lemma 3.1. *Let $(z_i) = (z_0, \dots, z_{n-1})$ with n even be a polygon in the complex plane. Further let α_i denote the angles between $z_{i-2} - z_{i-3}$ and $z_{i+1} - z_i$ and let θ_i be the internal angles between $z_{i-1} - z_i$ and $z_{i+1} - z_i$, where indices are taken modulo n. Then the following statements are equivalent.*

(i) There exists a polygon parallel to (z_i) with all vertices on a circle.

(ii) The angles α_i fulfill

$$\sum\nolimits_{i \ even} \alpha_i \in \pi\mathbb{Z}, \quad \text{or, which is equivalent,} \quad \sum\nolimits_{i \ odd} \alpha_i \in \pi\mathbb{Z}.$$

(iii) The multi-ratio $\mathrm{q}(z_0, \dots, z_{n-1})$ is real.

(iv) The interior angles θ_i have the property

$$\sum\nolimits_{i \ even} \theta_i = \sum\nolimits_{i \ odd} \theta_i = \frac{n-2}{2}\pi.$$

PROOF. (i) $\Longrightarrow$ (ii): Without loss of generality assume that (z_i) lie on a circle. For regular n-gons (w_i) (see Figure 3.2) we have $\alpha_i = 3\frac{2\pi}{n}$ for all i, which yields $\sum_{i \text{ even}} \alpha_i = 3\pi$. When changing one single vertex of (w_i) on the circle, e.g. $w_j \longmapsto \tilde{w}_j$, the directions $w_{j+1} - w_j$ and $w_j - w_{j-1}$ will change about the same angle α, which follows from the inscribed angle theorem. We get a new n-gon $(\tilde{w}_i)$ with $\tilde{w}_i = w_i$ for all i except for $i = j$. For the corresponding angles we have

$$\tilde{\alpha}_{j-1} = \alpha_{j-1} - \alpha, \ \tilde{\alpha}_j = \alpha_j - \alpha, \ \tilde{\alpha}_{j+2} = \alpha_{j+2} + \alpha \quad \text{and} \quad \tilde{\alpha}_{j+3} = \alpha_{j+3} + \alpha,$$

where all others remain unchanged. Therefore

$$\sum_{i \text{ even}} \tilde{\alpha}_i = \sum_{i \text{ even}} \alpha_i = 3\pi \in \pi\mathbb{Z}.$$

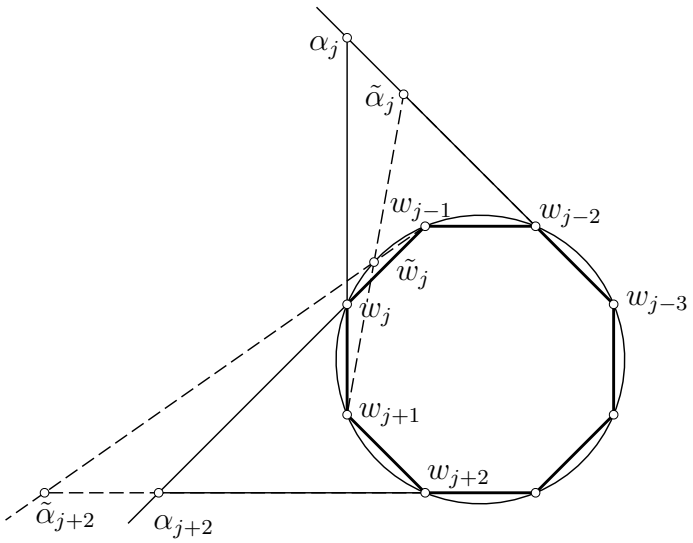

FIGURE 3.2: For a regular 8-gon we have an angle of $3\pi/4$ for all $\alpha_i = \angle(w_{i-2} - w_{i-3}, w_{i+1} - w_i)$. When changing a vertex w_j to $\tilde{w}_j$ on the circumcircle the corresponding angles α_{j-1}, α_j, α_{j+2} and α_{j+3} are replaced by $\tilde{\alpha}_{j-1} = \alpha_{j-1} - \alpha$, $\tilde{\alpha}_j = \alpha_j - \alpha$, $\tilde{\alpha}_{j+2} = \alpha_{j+2} + \alpha$ and $\tilde{\alpha}_{j+3} = \alpha_{j+3} + \alpha$, respectively.

If we change each vertex of the regular polygon (w_i) until they come to the positions of (z_i) the sum of the considered angles remains in $\pi\mathbb{Z}$.

(ii) $\Longrightarrow$ (i): Now we start with a polygon (z_i) with corresponding angles α_i such that

$$\sum_{i \text{ even}} \alpha_i \in \pi\mathbb{Z}.$$

Starting with an arbitrary vertex w_0 on a circle we construct vertices $w_1, \ldots, w_n$ on this circle with edges $w_i - w_{i-1}$ parallel to $z_i - z_{i-1}$ for all $i \in \{0, \ldots, n\}$, where indices are taken modulo n only for z_i but not yet for the points w_i (see Figure 3.3 with $w_i = z_i$). Until now we do not know whether $w_n = w_0$ or not. From "(i) $\Longrightarrow$ (ii)" we know that the polygon $(w_i)_{i=0}^{n-1}$ fulfills condition (ii). Using the assumptions we can conclude that also $w_n - w_{n-1}$ is parallel to $w_0 - w_{n-1}$ which yields $w_n = w_0$.

(i) $\Longleftrightarrow$ (iii): With $z_k - z_{k-1} = a_k \exp(i\varphi_k)$ and $\alpha_k = \varphi_{k-2} - \varphi_{k+1}$ we get

$$\begin{aligned} \mathrm{q}(z_0, \ldots, z_{n-1}) &= \prod_{k \text{ even}} \frac{(z_{k-2} - z_{k-3})}{(z_{k+1} - z_k)} = \prod_{k \text{ even}} \frac{a_{k-2} e^{i\varphi_{k-2}}}{a_{k+1} e^{i\varphi_{k+1}}} = \\ &= \prod_{k \text{ even}} \frac{a_{k-2}}{a_{k+1}} e^{i\alpha_k} = \Big(\prod_{k \text{ even}} \frac{a_{k-2}}{a_{k+1}} \Big) \exp\Big(i \sum_{j \text{ even}} \alpha_j \Big). \end{aligned}$$

This yields

$$\mathrm{q}(z_0, \ldots, z_{n-1}) \in \mathbb{R} \Longleftrightarrow \sum_{j \text{ even}} \alpha_j \in \pi\mathbb{Z}.$$

(i) $\Longleftrightarrow$ (iv): This statement without proof can be found in [14]. Our prove is analogue to '(i) $\Longleftrightarrow$ (ii)'. We start with a regular n-gon, where the angle condition of (iv) is obviously fulfilled, and move the vertices along the circumcircle. According to the inscribed angle theorem this does not change the sum of odd and even labeled agles, respectively.

Now we start with a polygon fulfilling the equation of (iv). Again, we move the vertices of a regular n-gon on its circumcircle until its edges are parallel to the given one. This is posslible since the circular polygon fulfills the angle condition even when moving the vertices. □

Corollary 3.2. *Let M be a Möbius transformation and let (z_i) be an n-gon with n even. Then (z_i) is quasi-circular if and only if $(M(z_i))$ is.*

PROOF. $\mathrm{q}(z_0,\dots,z_{n-1}) = \mathrm{q}(M(z_0),\dots,M(z_{n-1})) \in \mathbb{R}$ follows from the Möbius invariance of the multi-ratio. □

Remark 3.3. *The construction of a parallel polygon with vertices on a circle either closes up for all starting points z_0, or for none of them (see Figure 3.3). Let $(w_i)_{i=0}^{n-1}$ be an arbitrary polygon and let $(z_i)_{i=0}^{n}$ be contained in the circle $\mathcal{S}^1$ where $z_i - z_{i+1}$ is parallel to $w_i - w_{i+1}$ (indices taken modulo n only for w_i). We define*

$$\begin{aligned} \mu : \mathcal{S}^1 &\longrightarrow \mathbb{R}^2 \\ z &\longmapsto \mu(z) = [z_1 - z] \cap [z_{n-1} - z_n]. \end{aligned}$$

Then the set $\mu(\mathcal{S}^1)$ is a conic section, which is a consequence of properties of projective mappings between pencils of lines (see Figure 3.3, right).

Theorem 3.4 applies the above properties of polygons to meshes. The multi-ratios which are mentioned are computed w.r.t. an arbitrary choice of Cartesian coordinate system in each face.

Theorem 3.4. *Each of the following statements concerning a mesh $\mathcal{M}$ with planar faces implies the other five.*

(i) $\mathcal{M}$ has a vertex offset.

(ii) Every face of $\mathcal{M}$ is a quasi-circular polygon.

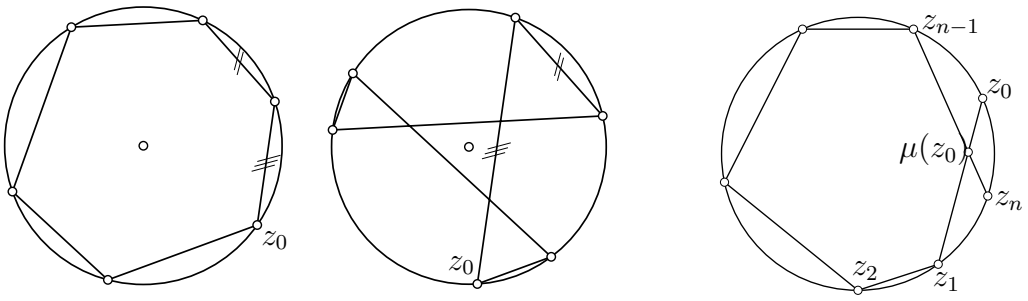

FIGURE 3.3: *Left:* The construction of a parallel polygon with vertices on a circle closes up for all starting points z_0 or for none. *Right:* The set of all points $\mu(z_0)$ which arise from the construction of Remark 3.3 are located on a conic section.

(iii) For each face, the angles α_i fulfill both,

$$\sum_{i \ even} \alpha_i \in \pi\mathbb{Z} \quad \textit{and} \quad \sum_{i \ odd} \alpha_i \in \pi\mathbb{Z},$$

respectively.

(iv) For each face, the angles α_i fulfill $\sum_{i \ odd} \alpha_i \in \pi\mathbb{Z}$.

(v) The multi-ratio of each face is real.

(vi) For each face, the interior angles θ_i have the property

$$\sum_{i \ even} \theta_i = \sum_{i \ odd} \theta_i.$$

The equivalence of statements (i) $\Leftrightarrow$ (ii) $\Leftrightarrow$ (iv) can be found in [14], and (i) $\Leftrightarrow$ (ii) for quad meshes can be found in [20]. The rest follows immediately from Lemma 3.1.

3.2 Conformal hexagons

Both conformal and curvature line parametrisations play a fundamental role in the theory of minimal surfaces. On the one hand, the Weierstrass representation converts a pair of a holomorphic and a meromorphic function (i.e., conformal parametrizations of $\mathcal{S}^2$) to a certain parametrization of a minimal surface. On the other hand, Christoffel duality converts a conformal parametrization of the sphere to an isothermic parametrization of a minimal surface and vice versa. We now aim at a discrete analogue of a continuous conformal surface, using hexagonal meshes.

Definition 3.5. *A hexagon $(z_0, \dots, z_5)$ is called* conformal *if both* $\mathrm{cr}(z_0, z_1, z_2, z_3) = -1/2$ *and* $\mathrm{cr}(z_0, z_5, z_4, z_3) = -1/2$.

The prototype of a conformal hexagon is a regular hexagon. Since Möbius transformations leave a real cross-ratio of four points invariant, we immediately see that conformality of hexagons is Möbius invariant and each hexagon which is Möbius equivalent to a regular hexagon is conformal.

For a conformal hexagon both quadrilaterals z_0, z_1, z_2, z_3 and z_0, z_5, z_4, z_3 are circular since their cross-ratios are real (see Figure 3.4). The multi-ratio of conformal hexagons is

$$\mathrm{q}(z_0, \ldots, z_5) = \frac{(z_0 - z_1)(z_2 - z_3)(z_4 - z_5)}{(z_1 - z_2)(z_3 - z_4)(z_5 - z_0)} = -\frac{1}{2}\frac{(z_3 - z_0)(z_4 - z_5)}{(z_3 - z_4)(z_5 - z_0)} = -1,$$

which implies, with Lemma 3.1, that this hexagon is quasi-circular.

Definition 3.6. *Let $f : U \subseteq \mathbb{R}^2 \longrightarrow \mathbb{R}^3$ be a smooth regular mapping. Then the hexagon*

$$\begin{aligned} f_0 &= f + \varepsilon f_x & f_3 &= f - \varepsilon f_x \\ f_1 &= f + \frac{\varepsilon}{2} f_x + \frac{\sqrt{3}}{2}\varepsilon f_y & f_4 &= f - \frac{\varepsilon}{2} f_x - \frac{\sqrt{3}}{2}\varepsilon f_y \\ f_2 &= f - \frac{\varepsilon}{2} f_x + \frac{\sqrt{3}}{2}\varepsilon f_y & f_5 &= f + \frac{\varepsilon}{2} f_x - \frac{\sqrt{3}}{2}\varepsilon f_y \end{aligned}$$

is called infinitesimal hexagon *at (x, y) where $f = f(x, y) \in \mathbb{R}^3$, $f_x = \partial f/\partial x$ and $f_y = \partial f/\partial y$.*

Note that in general infinitesimal hexagons are not planar. According to the Taylor expansion the vertices f_i of the infinitesimal hexagon differ from $f(z_i)$ in terms of order $o(\varepsilon)$, where z_i are the vertices of a regular hexagon with radius ε and centered at (x, y).

For the following we extend the cross-ratio to points of $\mathbb{R}^3$ (see e.g. [4]). Four points in $\mathbb{R}^3$ define a plane or sphere, which is identified with $\mathbb{C} \cup \infty$ via stereographic projection.

Theorem 3.7. *Consider a regular mapping $f : U \subseteq \mathbb{R}^2 \longrightarrow \mathbb{R}^3$ and the associated infinitesimal hexagon $f_0, \ldots, f_5$ for a point $(x, y) \in U$. Then*

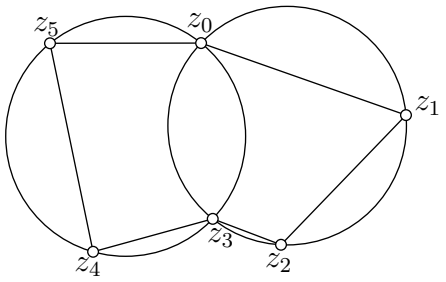

FIGURE 3.4: An arbitrary conformal hexagon (z_i) with its two circles.

$\mathrm{cr}(f_0, f_1, f_2, f_3) = -1/2 + o(\varepsilon)$ *and* $\mathrm{cr}(f_0, f_5, f_4, f_3) = -1/2 + o(\varepsilon)$ *for all* $(x, y) \in U$ *if and only if* f *is a conformal mapping.*

PROOF. Translation $x \mapsto x - f - \varepsilon f_x$ and scaling $x \mapsto 2x/\varepsilon$ transform the vertices to

$$\begin{aligned} \hat{X}_0 &= 0 & \hat{X}_3 &= -4f_x \\ \hat{X}_1 &= -f_x + \sqrt{3}f_y & \hat{X}_4 &= -3f_x - \sqrt{3}f_y \\ \hat{X}_2 &= -3f_x + \sqrt{3}f_y & \hat{X}_5 &= -f_x - \sqrt{3}f_y. \end{aligned}$$

The inversion $\tilde{X}_i = \hat{X}_i/\|\hat{X}_i\|^2$ sends $\hat{X}_0$ to ∞. As all three transformations do not change the cross-ratio up to complex conjugation we get

$$\mathrm{cr}(f_0, f_1, f_2, f_3) = \mathrm{cr}(\hat{X}_0, \hat{X}_1, \hat{X}_2, \hat{X}_3) = \mathrm{cr}(\infty, \tilde{X}_1, \tilde{X}_2, \tilde{X}_3) = \frac{\tilde{X}_3 - \tilde{X}_2}{\tilde{X}_1 - \tilde{X}_2}.$$

We start with the first cross-ratio condition

$$\mathrm{cr}(f_0, f_1, f_2, f_3) = -\frac{1}{2} + o(\varepsilon) \Longleftrightarrow \tilde{X}_3 - \tilde{X}_2 = -\frac{1}{2}(\tilde{X}_1 - \tilde{X}_2) + o(\varepsilon), \quad (3.1)$$

which is equivalent to

$$-\frac{f_x}{2C} - 3\frac{-3f_x + \sqrt{3}f_y}{A} + \frac{-f_x + \sqrt{3}f_y}{B} = o(\varepsilon),$$

where $A = \|-3f_x + \sqrt{3}f_y\|^2$, $B = \|-f_x + \sqrt{3}f_y\|^2$ and $C = \|f_x\|^2$. Collecting the coefficients of f_x and f_y we get

$$f_x \cdot \Big(\frac{-1/2}{C} + \frac{9}{A} - \frac{1}{B}\Big) + f_y \cdot \Big(\frac{-3\sqrt{3}}{A} + \frac{\sqrt{3}}{B}\Big) = o(\varepsilon),$$

which is equivalent to

$$-\frac{1}{2}AB + 9BC - AC = 0 \quad \text{and} \quad -3B + A = 0$$

because of the linear independence of $\{f_x, f_y\}$. It is easy to see that $-3B + A = 0 \Leftrightarrow \|f_x\| = \|f_y\|$ and $-\frac{1}{2}AB + 9CB - CA = 0 \Leftrightarrow 3\langle f_x, f_x\rangle^2 - 6\langle f_y, f_y\rangle\langle f_x, f_x\rangle + 12\langle f_x, f_y\rangle^2 + 3\langle f_y, f_y\rangle^2 - 8\sqrt{3}\langle f_x, f_y\rangle\langle f_y, f_y\rangle = 0$. Further, it is easy to see that Equation (3.1) is equivalent to

$$\|f_x\| = \|f_y\| \quad \text{and} \quad \Big[\langle f_x, f_y\rangle = 0 \text{ or } \langle f_x, f_y\rangle = \frac{2\sqrt{3}\langle f_y, f_y\rangle}{3}\Big]. \quad (3.2)$$

Since $\|f_y\|^2 \geq \langle f_x, f_y\rangle = 2\sqrt{3}/3\|f_y\|^2$ would impliy $1 \geq 2\sqrt{3}/3$, which is a contradiction, f_x and f_y must be orthogonal. We get

$$\mathrm{cr}(f_0, f_1, f_2, f_3) = -1/2 + o(\varepsilon) \quad \text{and} \quad \mathrm{cr}(f_0, f_5, f_4, f_3) = -1/2 + o(\varepsilon)$$

is equivalent to $\|f_x\| = \|f_y\|$ and $\langle f_x, f_y\rangle = 0$, which is further equivalent to the conformality of f. □

3.3 A dual construction for conformal hexagons

With a view towards the smooth Christoffel dual construction of Section 3.4, we introduce a dual construction for conformal hexagons.

Definition 3.8. *For a conformal hexagon (z_i), let $a_i := z_{i+1} - z_i$ be the edge vectors, where indices are taken modulo n. A hexagon (z_i^*) is called* dual *to (z_i) if*

$$\begin{aligned} z_1^* - z_0^* &= -1/(\overline{z_1 - z_0}) = -1/\overline{a_0} & z_4^* - z_3^* &= -1/(\overline{z_4 - z_3}) = -1/\overline{a_3} \\ z_2^* - z_1^* &= 2/(\overline{z_2 - z_1}) = 2/\overline{a_1} & z_5^* - z_4^* &= 2/(\overline{z_5 - z_4}) = 2/\overline{a_4} \\ z_3^* - z_2^* &= -1/(\overline{z_3 - z_2}) = -1/\overline{a_2} & z_0^* - z_5^* &= -1/(\overline{z_0 - z_5}) = -1/\overline{a_5} \end{aligned}$$

(see Figure 3.5).

Proposition 3.9. *Let (z_i) be a conformal hexagon, $a_i := z_{i+1} - z_i$ and $b := z_0 - z_3$. Then*

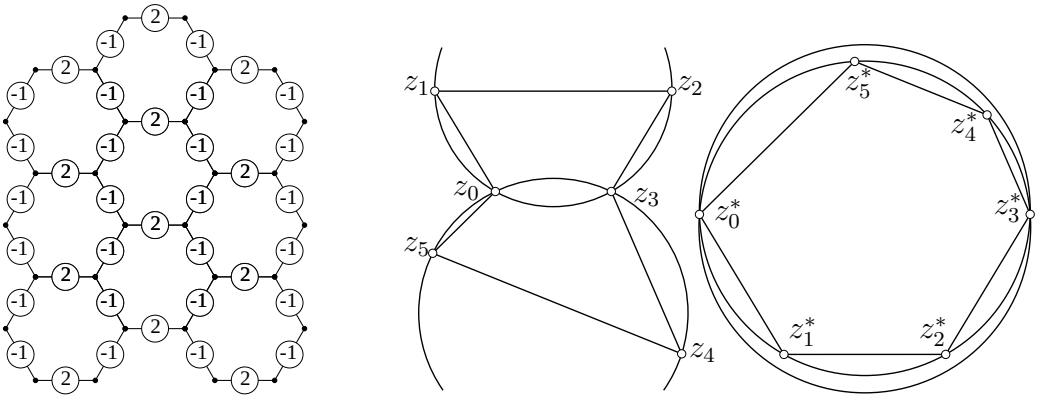

FIGURE 3.5: *Left:* Edge coefficients in the discrete dual construction (Definition 3.8). *Right:* A conformal hexagon and its dual. For each conformal hexagon $z_0, \ldots, z_5$ both quadrilaterals z_0, z_1, z_2, z_3 and z_0, z_3, z_4, z_5 are circular.

(i) $\sum_{i=0}^{5} a_i = 0, \quad a_0 + a_1 + a_2 + b = 0, \quad \dfrac{a_0 a_2}{a_1 b} = -\dfrac{1}{2}, \quad \dfrac{a_3 a_5}{a_4 b} = \dfrac{1}{2}.$

(ii) $z_0^* - z_3^* = 2/\overline{b}$ *and in particular* $z_0 - z_3$ *is parallel to* $z_0^* - z_3^*$.

(iii) The hexagon (z_i) *posesses a dual hexagon.*

(iv) The dual (z_i^*) *is a conformal hexagon, and is unique up to translation.*

(v) Non-corresponding diagonals of both quadrilaterals z_0, z_1, z_2, z_3 *and* z_0, z_5, z_4, z_3 *are transformed according to*

$$z_1^* - z_3^* = 3\frac{z_0 - z_2}{|z_0 - z_2|^2}, \qquad z_2^* - z_0^* = 3\frac{z_3 - z_1}{|z_3 - z_1|^2},$$
$$z_5^* - z_3^* = 3\frac{z_0 - z_4}{|z_0 - z_4|^2}, \qquad z_4^* - z_0^* = 3\frac{z_3 - z_5}{|z_3 - z_5|^2}.$$

In particular they are parallel:

$$z_2 - z_0 \parallel z_1^* - z_3^*, \qquad z_1 - z_3 \parallel z_0^* - z_2^*,$$
$$z_4 - z_0 \parallel z_5^* - z_3^*, \qquad z_5 - z_3 \parallel z_4^* - z_0^*.$$

(vi) Applying the duality twice yields the original hexagon, up to translation: $(z_i^{**}) = (z_i)$.

Proof. The properties of (i) follow immediately from the definition. Using the properties of (i) we get

$$z_0^* - z_3^* = \frac{1}{\overline{a_0}} - \frac{2}{\overline{a_1}} + \frac{1}{\overline{a_2}} = \frac{\overline{a_1 a_2} - 2\overline{a_0 a_2} + \overline{a_0 a_1}}{\overline{a_0 a_1 a_2}} = \frac{\overline{a_1 a_2} + \overline{a_1}\overline{b} + \overline{a_0 a_1}}{\overline{a_0 a_1 a_2}} =$$
$$= \frac{2(\overline{a_2} + \overline{b} + \overline{a_0})}{2\overline{a_0 a_2}} = \frac{-2\overline{a_1}}{\overline{a_1}\overline{b}} = \frac{2}{\overline{b}}$$

which implies (ii). We consider $1/\overline{a_3} - 2/\overline{a_4} + 1/\overline{a_5}$ which is $-2/\overline{b}$ analog to the proof of (ii). This yields

$$-1/\overline{a_0} + 2/\overline{a_1} - 1/\overline{a_2} - 1/\overline{a_3} + 2/\overline{a_4} - 1/\overline{a_5} = -2/\overline{b} + 2/\overline{b} = 0,$$

and therefore (iii). The cross-ratios of the involved quadrilaterals are

$$\operatorname{cr}(z_0^*, z_1^*, z_2^*, z_3^*) = \frac{(z_0^* - z_1^*)(z_2^* - z_3^*)}{(z_1^* - z_2^*)(z_3^* - z_0^*)} = \frac{\frac{1}{\overline{a_0}}\frac{1}{\overline{a_2}}}{-\frac{2}{\overline{a_1}}\left(-\frac{2}{\overline{b}}\right)} = -\frac{1}{2}$$

and

$$\operatorname{cr}(z_0^*, z_5^*, z_4^*, z_3^*) = -\frac{1}{2},$$

which implies (iv).

The proof of (v) can be found in in A.I. Bobenko and Yu.B. Suris [7, Corollary 31].

$$\begin{aligned}
\operatorname{cr}(z_0, \dots, z_3) = -\frac{1}{2} &\iff \frac{z_0 - z_1}{z_1 - z_2} = -\frac{1}{2}\frac{z_3 - z_0}{z_2 - z_3} \\
&\iff \frac{z_0 - z_2 + z_2 - z_1}{z_1 - z_2} = -\frac{1}{2}\frac{z_3 - z_2 + z_2 - z_0}{z_2 - z_3} \\
&\iff 2\frac{z_0 - z_2}{z_1 - z_2} - 2 = -\frac{z_2 - z_0}{z_2 - z_3} + 1 \\
&\iff \frac{2}{z_1 - z_2} - \frac{1}{z_2 - z_3} = \frac{3}{z_0 - z_2}.
\end{aligned}$$

Taking the complex conjugate of the last equation yields

$$z_1^* - z_3^* = z_1^* - z_2^* + z_2^* - z_3^* = \frac{2}{\overline{(z_1 - z_2)}} - \frac{1}{\overline{(z_2 - z_3)}} = \frac{3(z_0 - z_2)}{|z_0 - z_2|^2}.$$

All other cases in (v) can be shown analogously.

Applying the dual operator * twice yields

$$z_{i+1}^{**} - z_i^{**} = -\frac{1}{\overline{(z_{i+1}^* - z_i^*)}} = -\frac{1}{\overline{\left(-\frac{1}{\overline{(z_{i+1} - z_i)}}\right)}} = z_{i+1} - z_i$$

or

$$z_{i+1}^{**} - z_i^{**} = \frac{2}{\overline{(z_{i+1}^* - z_i^*)}} = \frac{2}{\overline{\left(\frac{2}{\overline{(z_{i+1} - z_i)}}\right)}} = z_{i+1} - z_i,$$

which implies (vi).

□

3.4 Christoffel dual construction

The following theorem by E.B. Christoffel [9] characterizes isothermic surfaces via a dual construction. An *isothermic* parametrization is a conformal

cuvature line parametrization. It is known that all minimal surfaces can be expressed in isothermic parameters. For the unit sphere $\mathcal{S}^2$, every conformal parametrization is isothermic.

Theorem 3.10 (Christoffel)**.** *Let f be an isothermic parametrisation. Then the* Christoffel dual *f^*, defined by the formulas*

$$f_x^* = \frac{f_x}{\|f_x\|^2} \quad \text{and} \quad f_y^* = -\frac{f_y}{\|f_y\|^2}$$

exists and is isothermic again. The dual f^* is a minimal surface if and only if f is a sphere.

The next two propositions state properties of the smooth Christoffel dual construction.

Proposition 3.11. *Let $f : U \subseteq \mathbb{R}^2 \longrightarrow \mathbb{R}^3$ be an isothermic parametrisation, let f^* be its dual, and consider the ball $B_r(x, y)$ with radius r centered at (x, y). Then*

$$\lim_{r\to 0} \frac{\mathcal{A}(f(B_r(x,y)))}{\mathcal{A}(f^*(B_r(x,y)))} = \|f_x(x,y)\|^2 \|f_y(x,y)\|^2,$$

where $\mathcal{A}$ is the surface area.

Proposition 3.12. *Let $f : U \subseteq \mathbb{R}^2 \longrightarrow \mathbb{R}^3$ be an isothermic parametrisation, $\varepsilon > 0$ and $r = \varepsilon/\sqrt{\pi}$. Further let $\varphi : U' \longrightarrow U$ with $\varphi(x, y) = (\varepsilon x, \varepsilon y)$*

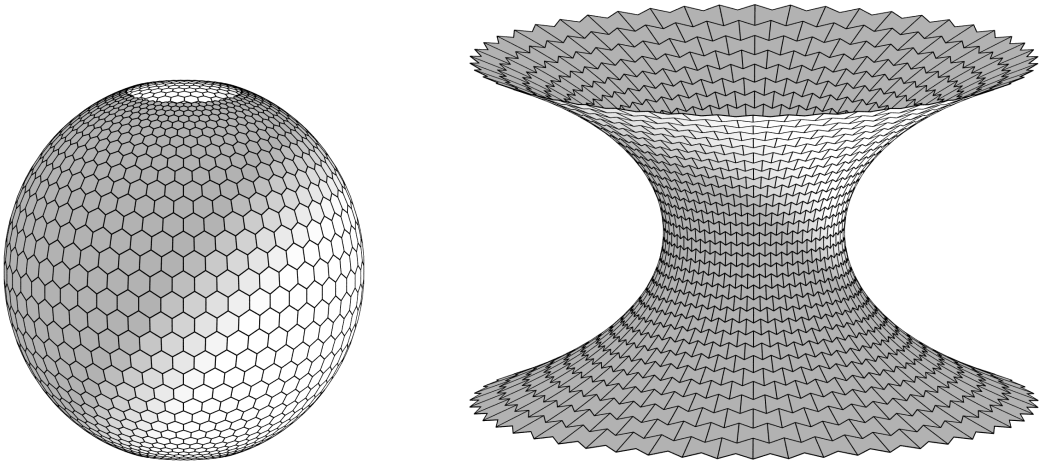

FIGURE 3.6: A discrete catenoid and its discrete Gauss image (see Example 3.25).

be a parameter transformation, $f_\varepsilon := f \circ \varphi$ the transformed function and f_ε^* its dual. Then

$$\lim_{\varepsilon \to 0} \mathcal{A}(f_\varepsilon(B_r(x,y)))\mathcal{A}(f_\varepsilon^*(B_r(x,y))) = 1. \tag{3.3}$$

We consider the dual construction of discrete isothermic surfaces as quad meshes [4, 2]. The dual $z_0^*, \dots, z_3^*$ of a conformal square with vertices $z_0, \dots, z_3$ is defined via

$$z_{i+1}^* - z_i^* = (-1)^i / \overline{(z_{i+1} - z_i)}.$$

For a square P with edge length l and its dual P^*, which then has edge length $1/l$, we obtain $\mathcal{A}(P) = l^2$, $\mathcal{A}(P^*) = 1/l^2$ and therefore

$$\frac{\mathcal{A}(P)}{\mathcal{A}(P^*)} = l^4 \quad \text{and} \quad \mathcal{A}(P)\mathcal{A}(P^*) = 1,$$

which are discrete analogues of Propositions 3.11 and 3.12.

Computing the area of hexagons is more involved than the rectangle case. For a conformal hexagon (z_i) and its dual (z_i^*) we have

$$z_{i+1}^* - z_i^* = -1/(\overline{z_{i+1} - z_i})$$

for $i \in \{0, 2, 3, 5\}$ and

$$z_{i+1}^* - z_i^* = 2/(\overline{z_{i+1} - z_i})$$

for $i \in \{1, 4\}$. Multiplying each vertex z_i with $r \in \mathbb{R} \setminus 0$ we get the hexagon $(w_i) := (rz_i)$ and its dual (w_i^*) with

$$w_{i+1} - w_i = r(z_{i+1} - z_i) \quad \text{and} w_{i+1}^* - w_i^* = -r^{-1}/(\overline{z_{i+1} - z_i})$$

for $i \in \{0, 2, 3, 5\}$ and

$$w_{i+1}^* - w_i^* = 2r^{-1}/(\overline{z_{i+1} - z_i})$$

for $i \in \{1, 4\}$. Consequently

$$w_{i+1}^* - w_i^* = r^{-1}(z_{i+1}^* - z_i^*).$$

The areas of (z_i) and (z_i^*), are denoted by $\mathcal{A}(z_i) = p$ and $\mathcal{A}(z_i^*) = q$ respectively. Then

$$\mathcal{A}(w_i) = r^2\mathcal{A}(z_i) = r^2 p \quad \text{and} \quad \mathcal{A}(w_i^*) = \mathcal{A}\big(\frac{1}{r} z_i^*\big) = \frac{1}{r^2} q.$$

This yields disretizations of Propositions 3.11 and 3.12, namely

$$\frac{\mathcal{A}(v_i)}{\mathcal{A}(v_i^*)} = \frac{r^2 p}{\frac{1}{r^2} q} = r^2 r^2 \frac{p}{q} \quad \text{and} \quad \mathcal{A}(v_i)\mathcal{A}(v_i^*) = pq. \tag{3.4}$$

The fact that r does not occur in (3.4) means that $\mathcal{A}(v_i)\mathcal{A}(v_i^*)$ does not depend on the discrete parametrisation.

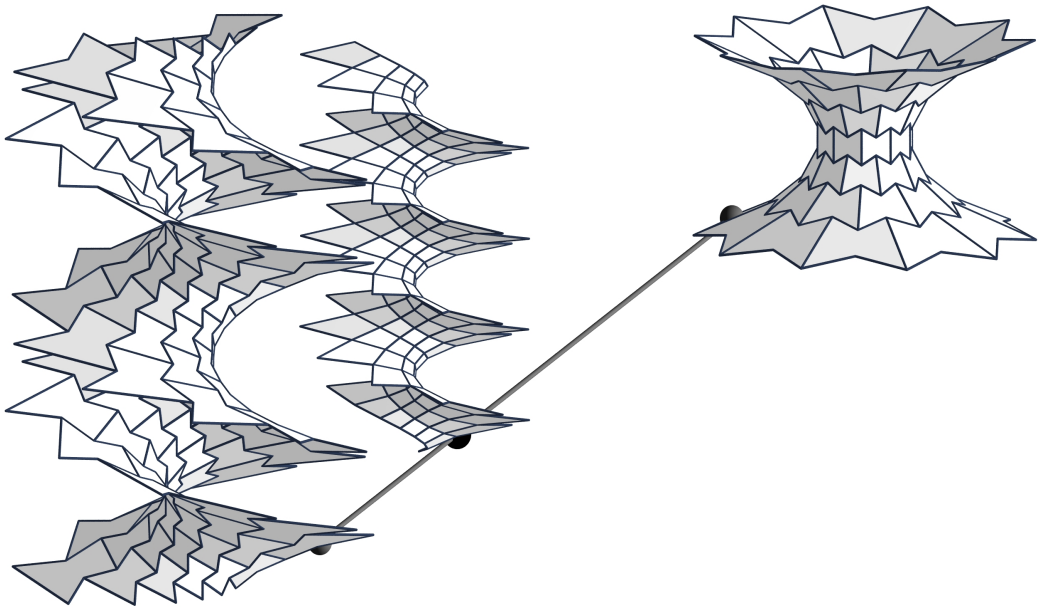

FIGURE 3.7: Linear combinations of parallel meshes, where one is a discrete catenoid and the second is a discrete helical surface are members of the corresponding associated family of minimal surfaces. Special combinations can lead to quad meshes (see Figure 3.21 on page 74). The case illustrated here is in fact a discrete helicoid, which means that it discretizes a surface generated by the helical motion of a straight line which orthogonally intersects the helical axis (see Example 3.30).

3.5 Discrete conformal and discrete minimal surfaces

Definition 3.13. *A* discrete (hexagonal) conformal surface *is a mesh with regular hexagonal combinatorics where each hexagon is conformal in the sense of Definition 3.5.*

This definition is motivated by the following statements:

(i) The definition of planar discrete conformal surfaces (Definition 3.13) is Möbius invariant (see Section 3.2).

(ii) According to Theorem 3.7, the limit of cross-ratios of the two quadrilaterals of the infinitesimal hexagon both equal $-1/2$ if and only if the considered mapping is conformal.

(iii) The discrete dual construction fulfils the property $(z_i^{**}) = (z_i)$, which is analogous to the smooth dual construction (see Proposition 3.9 (vi)).

(iv) The discrete dual construction always closes for conformal hexagons and transforms a discrete conformal surface into another one (see Proposition 3.9).

(v) The discrete dual construction of Definition 3.8 fulfils discrete analogues of properties of the smooth dual construction (see Propositions 3.11 and 3.12 and Equations (3.4)).

Consequently, a discrete conformal surface can be seen as a discrete analogue of a smooth conformal parametrized surface.

Remark 3.14. *(i) Since each face of a conformal mesh has multi-ratio* -1*, it posesses the vertex offset property (see Theorem 3.4).*

(ii) All vertices of a circular hexagonal mesh are always contained in a sphere or in a plane. We can say that a circular hexagonal surface is a discrete analogue of a surface with umbilic points only.

The next definition is motivated by Theorem 3.10.

Definition 3.15. *A* discrete (hexagonal) minimal surface *is the dual of a conformal mesh covering the unit sphere.*

Here the word "covering" can be understood as "inscribed", "edge-wise tangent", i.e., circumscribed or "face-wise tangent", i.e., circumscribed. Later we show that a certain notion of discrete mean curvature vanishes for all such minimal surfaces.

Remark 3.16. *A more general definition of conformal hexagonal meshes can be derived from the dual construction for quad meshes in [7]. Instead of taking cross-ratios $-1/2$ in Definition 3.5, we take fractions $-\alpha_n/\beta_m$ where m and n identify the row and the column of the position of the quadrilateral. This can be interpreted as a discrete reparametrization of the standard conformal mesh. The dual construction then must be modified in the following way:*

$$\begin{aligned} z_1^* - z_0^* &= -\beta_m/(\overline{z_1 - z_0}) & \qquad z_4^* - z_3^* &= -\beta_m/(\overline{z_4 - z_3}) \\ z_2^* - z_1^* &= \alpha_n/(\overline{z_2 - z_1}) & \qquad z_5^* - z_4^* &= \alpha_n/(\overline{z_5 - z_4}) \\ z_3^* - z_2^* &= -\beta_m/(\overline{z_3 - z_2}) & \qquad z_0^* - z_5^* &= -\beta_m/(\overline{z_0 - z_5}). \end{aligned}$$

After this change Proposition 3.9 is still valid.

3.6 A construction of planar conformal meshes

This section describes an explicit construction of a conformal hexagonal mesh, which we are going to use later.

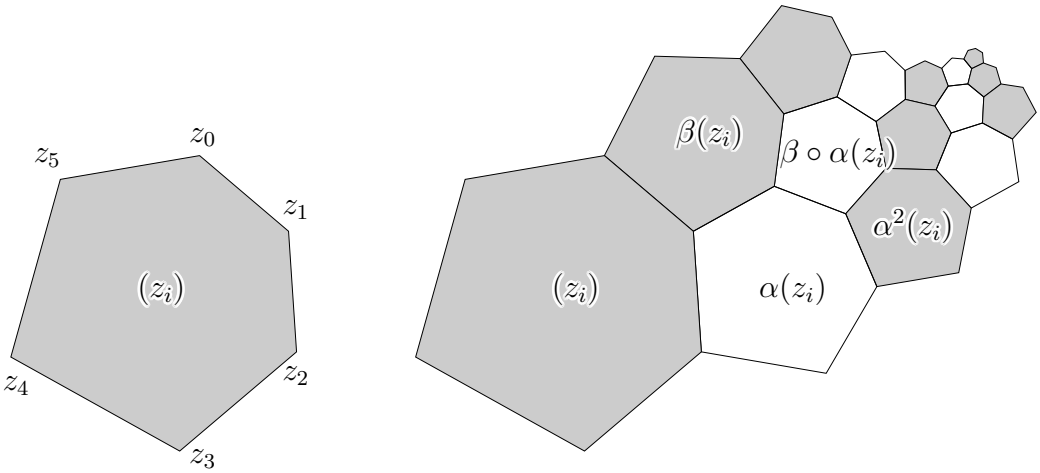

FIGURE 3.8: *Left:* An arbitrary conformal hexagon (z_i). *Right:* A planar conformal mesh $\beta^k \circ \alpha^l(z_i) = \alpha^l \circ \beta^k(z_i)$ (see Proposition 3.17).

Proposition 3.17. *Let (z_i) be a conformal hexagon and let α and β be two similarities, which map (z_4, z_5) to (z_2, z_1) and (z_3, z_4) to (z_1, z_0), respectively. Then α and β commute, i.e.,*

$$\alpha \circ \beta = \beta \circ \alpha \quad \textit{and} \quad \beta^k \circ \alpha^l(z_i) = \alpha^l \circ \beta^k(z_i)$$

is a conformal mesh, with no gaps, where $(k, l) \in \mathbb{Z}^2$ (Figure 3.8).

Proof. There exist $\varphi, \psi \in \mathbb{R}$ and $v, w \in \mathbb{C}$ such that

$$\alpha(z) = re^{i\varphi}z + v \quad \text{and} \quad \beta(z) = se^{i\psi}z + w.$$

We obtain

$$\begin{aligned} \alpha(z_5) &= re^{i\varphi}z_5 + v = z_1 & \beta(z_4) &= se^{i\psi}z_4 + w = z_0 \\ \alpha(z_4) &= re^{i\varphi}z_4 + v = z_2 & \beta(z_3) &= se^{i\psi}z_3 + w = z_1, \end{aligned}$$

which implies

$$re^{i\varphi}(z_5 - z_4) = z_1 - z_2 \quad \text{and} se^{i\psi}(z_4 - z_3) = z_0 - z_1.$$

It follows that

$$\frac{r}{s}e^{i(\varphi-\psi)}\frac{z_4 - z_5}{z_3 - z_4} = \frac{z_1 - z_2}{z_0 - z_1} \quad \Longleftrightarrow \quad \frac{r}{s}e^{i(\varphi-\psi)}\frac{z_5 - z_0}{z_0 - z_3} = -\frac{z_2 - z_3}{z_3 - z_0},$$

because of the cross-ratio condition of conformal hexagons. Further,

$$se^{i\psi}z_2 + w - \underbrace{(se^{i\psi}z_3 + w)}_{=z_1} = re^{i\varphi}z_0 + v - \underbrace{(re^{i\varphi}z_5 + v)}_{=z_1},$$

which implies $\beta(z_2) = \alpha(z_0)$. Since

$$\beta^{-1}(z) = s^{-1}e^{-i\psi}z - s^{-1}e^{-i\psi}w, \alpha^{-1}(z) = r^{-1}e^{-i\varphi}z - r^{-1}e^{-i\varphi}v$$

and

$$\alpha^{-1}(z_2) = \beta^{-1}(z_0)$$

we have

$$r^{-1}e^{-i\varphi}z_2 - r^{-1}e^{-i\varphi}v = s^{-1}e^{-i\psi}z_0 - s^{-1}e^{-i\psi}w$$

and

$$re^{i\varphi}z_0 + v = se^{i\psi}z_2 + w.$$

We multiply the last two equations and get

$$z_0z_2 - z_0v + v\alpha^{-1}(z_2) = z_0z_2 - wz_2 + w\beta^{-1}(z_0) \iff v = w\frac{(z_4 - z_2)}{(z_4 - z_0)}.$$

We want to show that $\beta \circ \alpha = \alpha \circ \beta$. Therefore we compute

$$\alpha \circ \beta(z) = rse^{i(\varphi+\psi)}z + re^{i\psi}w + v$$

and

$$\beta \circ \alpha(z) = rse^{i(\varphi+\psi)}z + se^{i\varphi}v + w.$$

Consequently,

$$\alpha \circ \beta = \beta \circ \alpha \iff (re^{i\varphi} - 1)w = (se^{i\psi} - 1)v. \tag{3.5}$$

Replacing v by $w(z_4 - z_2)/(z_4 - z_0)$, the last equation is further equivalent to

$$(re^{i\varphi} - 1) = (se^{i\psi} - 1)\frac{(z_4 - z_2)}{(z_4 - z_0)} \iff \beta(z_2) = \alpha(z_0),$$

which we have already shown to be true. □

To obtain circular conformal meshes we have to start with a circular conformal hexagon and then apply Proposition 3.17.

A similarity which is no translation is decomposable into a dilation and a rotation. The center of rotation of α and β is $v/(1 - re^{i\varphi})$ and $w/(1 - se^{i\psi})$, respectively. From equation (3.5) we obtain that both centers must be the same if and only if $\alpha \circ \beta = \beta \circ \alpha$. In $\mathbb{R}^2$ we take the 3×3 matrices

$$A = \left(\begin{array}{c|c} 1 & \mathbf{0} \\ \hline \begin{matrix}\operatorname{Re} v \\ \operatorname{Im} v\end{matrix} & rD_\varphi \end{array}\right) \quad \text{and} \quad B = \left(\begin{array}{c|c} 1 & \mathbf{0} \\ \hline \begin{matrix}\operatorname{Re} w \\ \operatorname{Im} w\end{matrix} & sD_\psi \end{array}\right)$$

for α and β, where D_ω is the 2×2 rotation matrix by an angle of ω. Since A and B commute, i.e., $AB = BA$, $\alpha^l \circ \beta^k$ can be written in the form $\exp(l \log A + k \log B)$.

3.6.1 Discrete holomorphic functions

Now, we consider a mesh $\mathcal{M}$ with arbitrary combinatorics stored in the graph $\mathcal{G}$. The *double* $\mathcal{D}$ of $\mathcal{G}$ is a quad graph defined such that the new vertices $V(\mathcal{D})$ are the old ones $V(\mathcal{G})$ combined with the vertices of the dual graph $V(\mathcal{G}^*)$ (see e.g. [6] and Figure 3.9). A quadrilateral of $\mathcal{D}$ consists of the two vertices incident with an edge of $\mathcal{G}$ and the two vertices incident with the corresponding edge of $\mathcal{G}^*$. A function f is *discrete holomorphic with (possibly complex) weights* ν if for each quadrilateral (z_0, w_0, z_1, w_1) of the double graph $\mathcal{D}$ the equation

$$\frac{f(w_1) - f(w_0)}{f(z_1) - f(z_0)} = i\nu(z_0, z_1) = -\frac{1}{i\nu(w_0, w_1)} \tag{3.6}$$

holds. A *discrete Laplacian operator with weights* ν then acts on a complex-valued function via

$$(\Delta f)(z) = \sum_{w \in \mathrm{star}(z)} \nu(w, z)(f(w) - f(z)),$$

where $\mathrm{star}(z)$ consists of all vertices which are connected with z by an edge of $\mathcal{G}$. Further, f is called *discrete harmonic* if

$$(\Delta f)(z) = 0$$

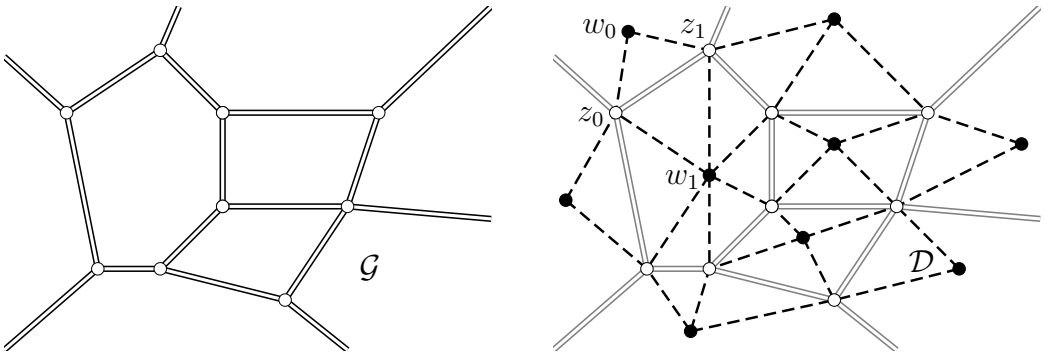

FIGURE 3.9: *Left:* A graph $\mathcal{G}$ with arbitrary combinatorics. *Right:* The double $\mathcal{D}$ (dashed lines) of $\mathcal{G}$ (see § 3.6.1). The vertices of $V(\mathcal{D})$ are the vertices $V(\mathcal{G})$ (white points) and the vertices of the dual graph $V(\mathcal{G}^*)$ (black points). The double $\mathcal{D}$ is a quad-graph where each quadrilateral (z_0, w_0, z_1, w_1) consists of two vertices (z_0, z_1) of $V(\mathcal{G})$ and the two vertices (w_0, w_1) of $V(\mathcal{G}^*)$ corresponding to the two adjacent faces incident with (z_o, z_1).

for all verticies z of the graph.

We consider complex functions defined an a graph $\mathcal{G}$ with values coming from the embedding in $\mathbb{C}$.

Proposition 3.18. *The vertex coordinates of the mesh $\mathcal{M}$ with double graph combinatorics derived from a conformal hexagonal mesh generated with Proposition 3.17 are function values of a discrete holomorphic function defined on a regular hexagonal graph.*

PROOF. We consider points w_i generated with the same similarities as the mesh $\mathcal{M}$, starting with one arbitrary point. These new points are the function values of the vertices of the dual mesh $\mathcal{M}^*$. Here, the word 'dual' does not mean the Christoffel dual of the mesh $\mathcal{M}$ but the combinatorial dual of $\mathcal{M}$ being seen as a graph. Since the new mesh with vertices

$$V(\mathcal{M}) \cup V(\mathcal{M}^*)$$

and double graph combinatorics is generated via similarities, the ratio $(z_1 - z_0)/(w_1 - w_0)$ is constant for each quadrilateral. Therefore there exists a "nice" weight function ν that fulfills (3.6) and which is constant at the edges (z_0, z_1) and (w_0, w_1) of the mesh. □

Corollary 3.19. *The vertex coordinates of the conformal hexagonal mesh $\mathcal{M}$ generated with Proposition 3.17 and its dual mesh $\mathcal{M}^*$ are function values of a discrete harmonic function defined on a regular hexagonal graph.*

PROOF. This follows immediately from Proposition 3.18 and [6, Theorem 7.3], which says that a discrete holomorphic function f, defined on the double graph $\mathcal{D}$ of an arbitrary graph $\mathcal{G}$, restricted to $\mathcal{G}$ or $\mathcal{G}^*$ is discrete harmonic. □

Corollary 3.20. *Let (z_i) be a hexagon which is Möbius equivalent to a regular one. Then, the conformal hexagonal mesh $\mathcal{M}$ generated with Proposition 3.17 is discrete harmonic with constant weights.*

PROOF. Let (z_i) be a hexagon of the mesh $\mathcal{M}$ (see Figure 3.10). Then, without loss of generality we have to show that the sum of the vectors of the edges emanating from z_2 is the zero vector. If (z_i) is a regular hexagon, then

the proposition is obvious. For the non-regular case let us assume further without loss of generality that

$$\alpha(z) = re^{i\varphi}z$$

which means that the center of rotation is 0. Therefore we have to show that

$$(z_1 - z_2) + (z_3 - z_2) + (re^{i\varphi}z_3 - z_2) = 0.$$

$$\begin{aligned} re^{i\varphi}z_3 - z_2 = re^{i\varphi}(z_3 - z_4) = -\frac{1}{2}re^{i\varphi}\frac{(z_2 - z_3)(z_4 - z_1)}{(z_1 - z_2)} = \\ = -\frac{1}{2}\frac{(z_2 - z_3)(z_4 - z_1)}{(z_5 - z_4)} = \frac{(z_1 - z_2)(z_3 - z_4)}{(z_5 - z_4)}. \end{aligned}$$

To finish the proof we must show that

$$p := (z_1 - z_2)(z_5 - z_4) + (z_3 - z_2)(z_5 - z_4) + (z_1 - z_2)(z_3 - z_4)$$

is zero. The cross-ratio conditions of four successive vertices of (z_i) are equivalent to $\mathrm{crp}(k) = 0$ for all $k \in \{0, \ldots, 5\}$, where

$$\mathrm{crp}(k) := (z_k - z_{k+1})(z_{k+2} - z_{k+3}) + \frac{1}{2}(z_{k+1} - z_{k+2})(z_{k+3} - z_k).$$

A computer analysis with *Mathematica* of the system of algebraic equations

$$\begin{cases} \mathrm{crp}(0) = 0 \\ \quad\vdots \\ \mathrm{crp}(5) = 0 \\ \quad p = 0 \end{cases}$$

in the unknowns $z_1, \ldots, z_5$ leads to the following equation which can be verified by hand by a careful computation:

$$\begin{aligned} p^2 = \frac{4}{3}\mathrm{crp}(0)\mathrm{crp}(2) - \frac{8}{3}\mathrm{crp}(1)\mathrm{crp}(2) + \frac{4}{3}\mathrm{crp}(1)\mathrm{crp}(3) \\ - \frac{2}{3}\mathrm{crp}(0)p + \frac{4}{3}\mathrm{crp}(1)p + 2\mathrm{crp}(2)p - \frac{4}{3}\mathrm{crp}(3)p + \frac{2}{3}\mathrm{crp}(4)p = 0. \end{aligned}$$

Therefore, $p = 0$. That is what we wanted to show. □

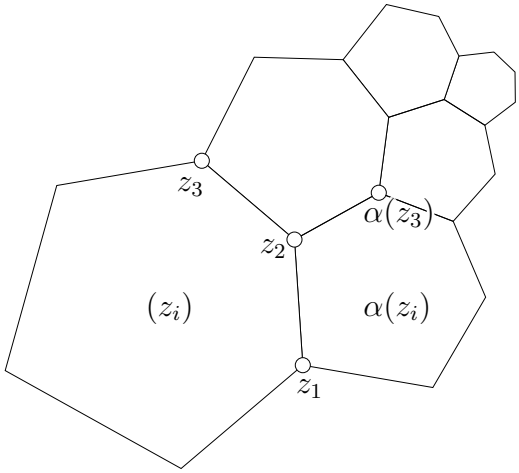

FIGURE 3.10: Illustration to the proof of Corollary 3.20. This mesh is harmonic with constant weights if the vectors $z_1 - z_2$, $z_3 - z_2$, and $\alpha(z_3) - z_2$ sum up to 0. Because of the construction with similarities it is sufficient to verify this property for one single vertex only.

3.7 Polygons with vanishing mixed area and discrete minimal surfaces

In this section we discuss the connection between discrete minimal surfaces defined in [5] and those of Definition 3.15.

In smooth differential geometry a minimal surface can be defined as a surface with vanishing mean curvature in each point. A discrete minimal surface in this setting is a mesh where the discrete mean curvature H_P (see Subsection 2.1.3) is zero for all faces P of the mesh. Incidence geometric properties of the polygons with vanishing mixed area were studied in Section 2.3 and [17]. A result of [5] is that two parallel quadrilaterals have vanishing mean curvature if and only if their non-corresponding diagonals are parallel (see Figure 2.2).

According to Proposition 3.9, (v) the non-corresponding diagonals of the quadrilaterals of a conformal hexagon and its dual are parallel. This yields

Proposition 3.21. *A discrete minimal surface in the sense of Definition 3.15 has vanishing discrete mean curvature and therefore is a discrete minimal surface in the sense of [5].*

Remark 3.22. *A pair of meshes $\mathcal{M}$ and $\mathcal{M}'$ is called* reciprocal parallel, *if their combinatorics are dual (correspondences are vertex-face, face-vertex and edge-edge) and corresponding edges are parallel. The connection between the existence of a reciprocal parallel mesh and infinitesimal flexibility was studied in [27].*

Proposition 3.9, (v) says that non-corresponding diagonals of conformal hexagons of the quadrilaterals with cross-ratio equal to $-1/2$ are parallel.

From a discrete conformal surface and its dual we can derive two pairs of reciprocal parallel quad *meshes by choosing the edges*

$$z_2 - z_0 \parallel z_3^* - z_1^* \quad \textit{and} \quad z_4 - z_0 \parallel z_3^* - z_5^*$$

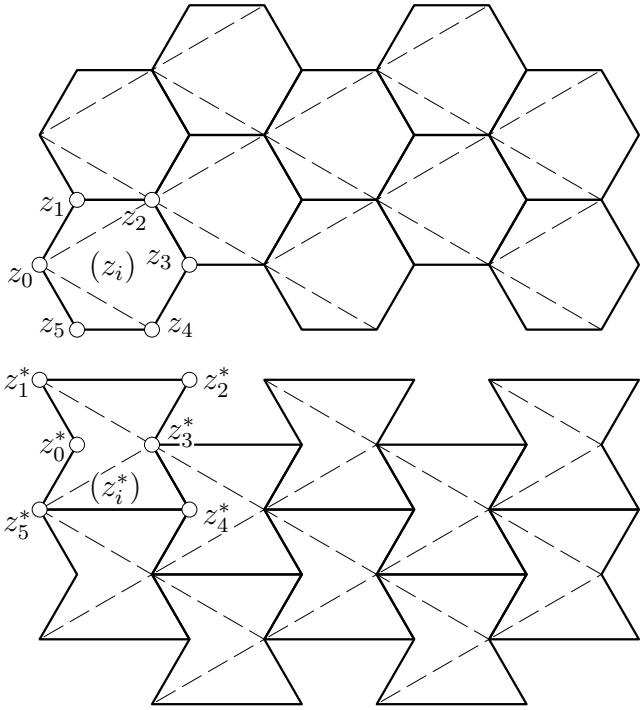

FIGURE 3.11: A pair of dual hexagonal meshes $\mathcal{M}$ and $\mathcal{M}^*$. The mesh $\mathcal{M}$ on the upper side consists of hexagons (z_i) where the union of the vertices z_0, z_2, z_4 form a quad mesh $\overline{\mathcal{M}}$ (dashed). The dual hexagonal mesh $\mathcal{M}^*$ consists of hexagons (z_i^*), where the union of the vertices z_1^*, z_3^*, z_5^* form a quad mesh $\overline{\mathcal{M}}^*$. According to Remark 3.22 and Proposition 3.9, (v), $\overline{\mathcal{M}}$ and $\overline{\mathcal{M}}^*$ are reciprocal parallel.

for the first pair and

$$z_1 - z_3 \parallel z_0^* - z_2^* \quad \textit{and} \quad z_5 - z_3 \parallel z_0^* - z_4^*$$

for the second pair (see Figure 3.11).

3.8 Examples of discrete minimal surfaces

As a preparation to the construction of examples, we have to discuss the relation between Christoffel duality and Weierstrass representation. We start with an arbitrary *conformal map* which is a holomorphic function $g : U \subset \mathbb{C} \longrightarrow \mathbb{C}$ where $g'(z_0) \neq 0$ for all $z_0 \in U$. This is a conformal parametrisation of a part of the plane. With the stereographic projection

$$\Phi(z) := \frac{1}{(|z^2| + 1)}(2z, |z|^2 - 1)$$

we get

$$n := \Phi \circ g$$

as a conformal parametrisation of the sphere. By applying the Christoffel duality (Theorem 3.10) to n we get an isothermic parametrisation f^* of a minimal surface with

$$f_x^* = \frac{n_x}{\|n_x\|^2} \quad \text{and} \quad f_y^* = -\frac{n_y}{\|n_y\|^2}. \tag{3.7}$$

On the other hand we get minimal surfaces f with the same Gauss image as f^* via the Weierstrass representation (see e.g. [11]):

Theorem 3.23 (Weierstrass representation)**.** *For a holomorphic function h and a meromorphic function g (with some restrictions) the map*

$$f = \operatorname{Re} \int h \cdot \left(\frac{1}{2}(\frac{1}{g} - g), -\frac{1}{2i}(\frac{1}{g} + g), 1 \right) \tag{3.8}$$

is a parametrisation of a minimal surface. $\Phi \circ g$ is the Gauss image of f.

As any holomorphic function $f(x + iy)$ satisfies

$$\operatorname{Re}(f') = \frac{\partial}{\partial x} \operatorname{Re} f,$$

Equations (3.7) and (3.8) produce the same result if and only if $n = \Phi \circ g$ satisfies the condition that $n_x/\|n_x\|^2$ equals the integrand in (3.8).

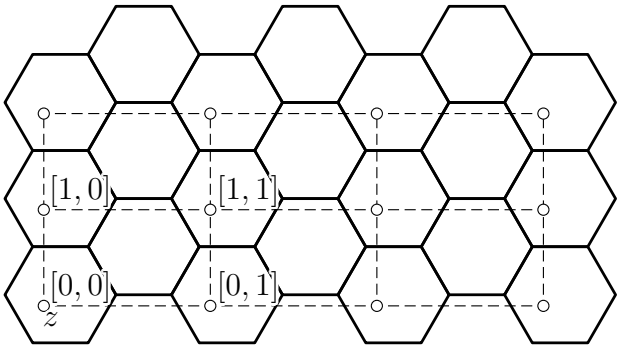

FIGURE 3.12: The derived quad mesh (dashed) $[m, n] := \alpha^{m-n} \circ \beta^{2n}(z)$ with $(m, n) \in \mathbb{Z}^2$ represents a discrete parametrization of the conformal hexagonal mesh generated with two similarities α and β following Proposition 3.17. We chose z arbitrarily.

3.8.1 Examples

For our examples, we start with a circular hexagonal conformal mesh in $\mathbb{C}$ and apply the discrete Christoffel duality to the stereographic projection of the mesh.

Let α and β be two similarities which generate a conformal hexagonal mesh as explained in Section 3.6 and choose $z \in \mathbb{C}$ such that $\alpha(z) \neq z \neq \beta(z)$. We call a mesh $\alpha^{m-n} \circ \beta^{2n}(z)$ with $(m, n) \in \mathbb{Z}^2$ a *derived quad mesh* (Figure 3.12). The derived quad mesh represents a discrete parametrization assigned to the conformal hexagonal surface. We basically distinguish three cases:

(i) Both α and β are translations.

(ii) α is a rotation and β is a dilation with the same fixed point.

(iii) Both, α and β are similarities with the same fixed point but different from a pure translation, rotation, or dilation.

For $(m, n) \in \mathbb{Z}^2$ and after an appropriate change of parameters, the derived quad mesh is of the form $m + in$ in (i), $e^{a(m+in)}$ in (ii), and $e^{(a+ib)(m+in)}$ in (iii), where $a, b \in \mathbb{R}$, $a, b \neq 0$. Therefore the meshes discretize the meppings $z \mapsto z$, $z \mapsto e^{az}$, and $z \mapsto e^{(a+ib)z}$, respectively.

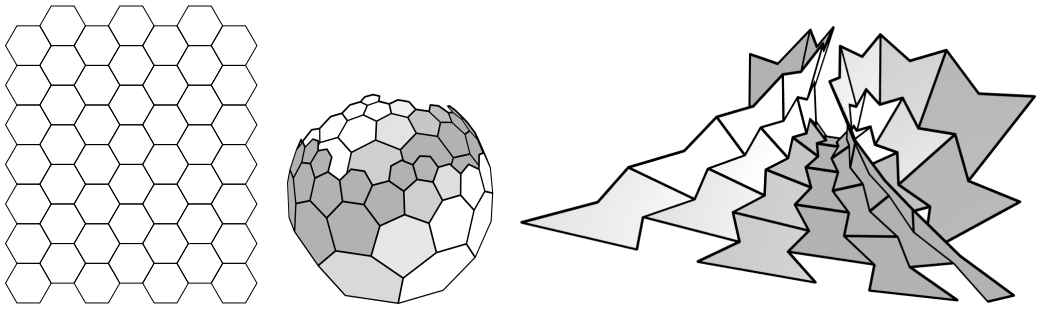

FIGURE 3.13: *Left:* Circular conformal mesh which discretizes $z \mapsto z$. *Center:* Discrete Gauss image, which is the stereographic projection of the circular conformal mesh. *Right:* Discrete minimal surface generated as the discrete Christoffel dual of the Gauss image. According to Example 3.24 the hexagonal mesh is a discrete Enneper's surface.

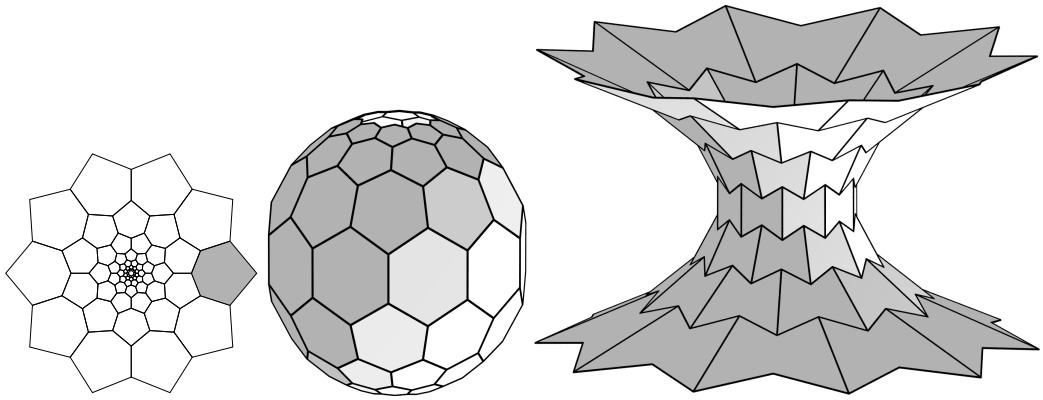

FIGURE 3.14: *Left:* Circular conformal mesh which discretizes $z \longmapsto e^{\lambda z}$ $(\lambda > 0)$ (a symmetric hexagon, which is Möbius equivalent to a regular one is marked). *Center:* Discrete Gauss image, which is the stereographic projection of the circular conformal mesh. *Right:* Discrete minimal surface generated as the discrete Christoffel dual of the Gauss image. Referring to Example 3.25 the hexagonal mesh is a discrete catenoid.

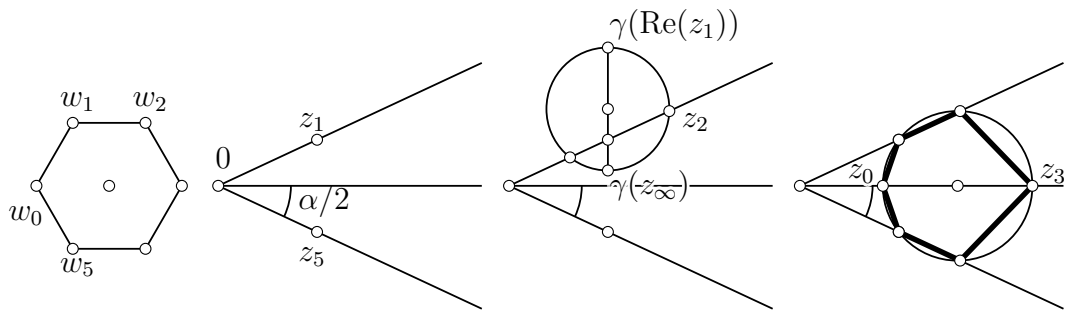

FIGURE 3.15: The construction of a symmetric hexagon which is Möbius equivalent to a regular hexagon. Here the angle α and the point z_1 are given. The construction is described in Remark 3.26.

Example 3.24 (Discrete Enneper's surface)**.** Letting $g(z) = z$ and $h(z) = z$ yields

$$n(x+iy) = \frac{1}{x^2+y^2+1}(2x, 2y, x^2+y^2-1),$$

and it is easy to verify that $n_x/\|n_x\|^2$ is equal to the real part of the integrand of (3.8). This is exactly the case of Enneper's surface (see Figures 3.1 and 3.13). We see that Christoffel duality of the regular hexagonal mesh generates a discrete Enneper's suface.

Example 3.25 (Discrete catenoid)**.** We start with a symmetric hexagon which is Möbius equivalent to a regular hexagon but not itself regular (see Figure 3.14, left and Remark 3.26) and apply Proposition 3.17 to get a circular conformal mesh with rotational symmetry. This mesh discretizes the holomorphic function

$$g(z) = e^{\lambda z}$$

with an appropriate choice of $\lambda > 0$. We compute $n(z) = (\Phi \circ g)(z) = \Phi(e^{\lambda z})$ and see that $n_x/\|n_x\|^2$ equals the real part of the integrand of (3.8) for $h(z) = 1/\lambda = \text{const}$. The resulting minimal surface is the catenoid (see also § 3.8.2). We see that Christoffel duality of a hexagonal mesh with rotational symmetries as described generates a discrete catenoid (see Figures 3.6 and 3.14).

Remark 3.26 (Symmetric conformal hexagons)**.** *There are several ways to construct a symmetric hexagon (z_i), which is Möbius equivalent to a regular*

hexagon. We consider a very simple construction where z_1 and α, which is the angle between $z_1 - z_2$ and $z_5 - z_4$, are given.

The following construction is demonstrated in Figure 3.15. Without loss of generality we choose the hexagon to be symmetric with respect to the real axis of the complex plane. Then $z_5 = \overline{z_1}$.

We consider the Möbius transformation γ_1 which maps z_5, 0, z_1 onto w_5, w_0, w_1, where (w_i) is a regular hexagon. Likewise, γ_2 maps w_5, w_0, w_1 onto w_5, w_2, w_1. The Möbius transformation $\gamma = \gamma_1^{-1} \circ \gamma_2 \circ \gamma_1$ maps an arbitrary choice of z_0 onto a point z_2 so that z_5, z_0, z_1, z_2 and w_5, w_0, w_1, w_2 are Möbius equivalent. Because of the symmetry we have to choose z_0 on the real axis. $\gamma(\mathbb{R})$ is a circle. Therefore z_2 is one point of the intersection of this circle with the line $\mathbb{R}z_1$.

To construct this circle we consider the image under γ of the two special points $\operatorname{Re}(z_1)$ and the point at infinity z_∞ of the complex plane. Because of the cross-ratio condition we get

$$\gamma(\operatorname{Re}(z_1)) = \operatorname{Re}(z_1) + i3\operatorname{Im}(z_1) \quad \textit{and} \quad \gamma(z_\infty) = \operatorname{Re}(z_1) + i\frac{1}{3}\operatorname{Im}(z_1).$$

Because of the symmetry of the Möbius transformation γ with respect to the line joining z_1 and z_5, the above constructed points $\gamma(\operatorname{Re}(z_1))$ and $\gamma(z_\infty)$ form a diameter of the circle. The hexagon (z_i) lies on a circle which completes the construction.

We got now a symmetric hexagon which is also shown in Figure 3.14 left.

3.8.2 Discrete hyperbolic cosine

In this subsection we discuss discretizations of the smooth hyperbolic cosine which provides us with a motivation for the naming of the discrete catenoid of Example 3.25. First, we consider four properties of this smooth trigonometric curve, the first and second also appears in physics:

(i) The *catenary* is the solution to the problem of describing the curve of an ideal chain hanging in the gravitational field. This leads to the second order ODE (see e.g. [28, III. § 11])

$$x'' = c\sqrt{1 + (x')^2}, \tag{3.9}$$

with a constant c, which includes the gravitational acceleration and material specifications. The solution to the ODE (3.9) is the catenary

$$x(y) = \frac{1}{c}\cosh(cy + d_1) + d_2$$

with $d_1, d_2 \in \mathbb{R}$.

(ii) The catenoid is the only nontrivial surface of revolution which is a minimal surface (see e.g. [10]). The meridian of this surface, possibly after a change of the parameter, is of the form

$$c\cosh(y/c)$$

for some nonzero real number c, when rotating round the y-axis. Therefore, the graph of the cosh function appears as the Christoffel dual of the meridian curve $\Phi \circ exp(x)$ of the unit sphere, where Φ is the stereographic projection.

(iii) We have the following connection between the length of the catenary and its area under the graph:

Theorem 3.27. *A curve $(x(y), y)$ in $\mathbb{R}^2$ describes a possibly stretched hyperbolic cosine if and only if for all $y_1, y_2 \in \mathbb{R}$ the equation*

$$A = cl$$

holds, where c is a real number, A is the area under the graph and l is the length of the graph, both between the points y_1 and y_2.

For the proof see [8].

(iv) Let $x(y) = \cosh(y)$ be the radius function of the parallel circuits of a surface of revolution. Then $n(y) = (-\tanh(y), 1/\cosh(y))$ is its Gauss image and $x(y)$ and $n(y)$ fulfills

$$(\log x(y))' = (\log n(y))'.$$

This property is used in [5, Example 1] to define discrete catenoids.

We now turn to the discrete setting and consider polygons $(p_i)_{i\in\{0,\dots,N\}}$ with $p_i = (p_i^1, p_i^2) \in \mathbb{R}^2$ and segment lengths $l_i = \|p_{i+1} - p_i\|$. There are straight forward disrcetizations of the above smooth properties of cosh, which can serve as a definition:

(i) The discretization of the catenary is a polygon which fulfills the second order difference equation

$$\Delta\Delta p_i^1 = c(l_i + l_{i+1}). \tag{3.10}$$

This equation implies a position of equilibrium.

(ii) We consider a planar conformal quadmesh, which is rotational symmetric (see Figure 3.16), project it stereographic to the unit sphere and compute the Christoffel dual according to [4]. The dualized meridian polygons can be seen as a discrete cosh (see also [5, Example 1]).

(iii) A discrete cosh is a polygon which fulfills

$$A_i = cl_i$$

for all $i \in \{0, \dots, N\}$, where A_i is the area between the line segment $p_{i+1}p_i$ and the y-axis.

(iv) The discrete curvature theory of [5] leads to a construction of a discrete catenoid which is described there ([5, Example 1]) and which fulfills the difference equation

$$\Delta \log p_i^1 = \Delta \log n_i^1,$$

where (n_i) represents the corresponding meridian polygon on the unit sphere.

Unfortunately, as can be seen from numerical examples, the definitions of the discrete versions of the hyperbolic cosine of (i), (ii), and (iii) are not equivalent. However, we can combine the three cases. We substitute the length l_i in (i) by l_i from (iii). Note that the constants are possibly different and therefore they do not cancel. We get

$$\Delta\Delta p_i^1 = c(A_i + A_{i+1}) \tag{3.11}$$

with some constant c. Now we have the following

Theorem 3.28. *The discrete hyperbolic cosine of (ii) constructed via the discrete Christoffel duality for the quad mesh setting fulfills Equation* (3.11).

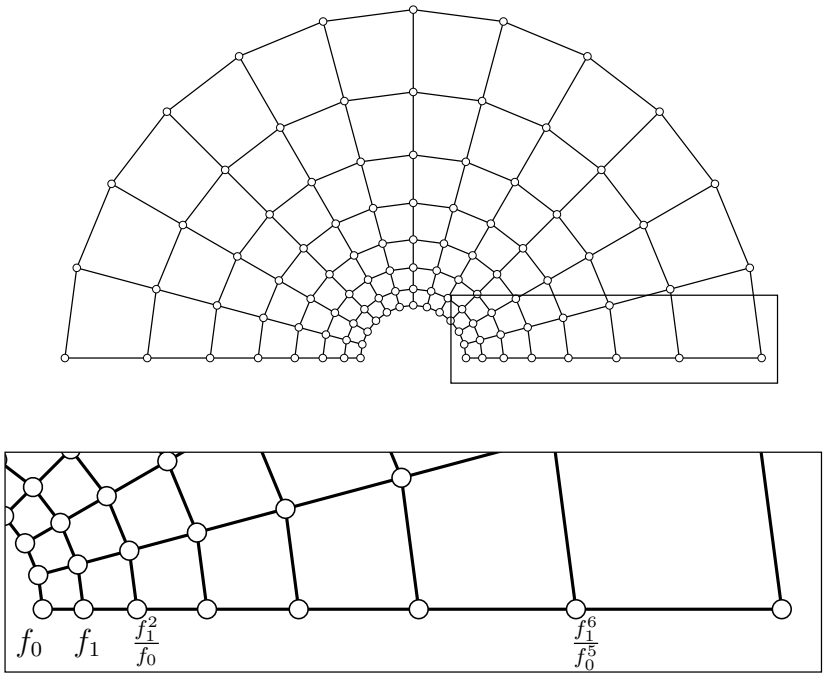

FIGURE 3.16: A planar conformal quad mesh discretizing e^z. The zoom illustrates the sequence (3.12) generated with the similarity $x \mapsto xf_1/f_0$.

PROOF. We consider the planar conformal mesh discretizing e^z and constructed via similarities (see Figure 3.16 and [4]). W.l.o.g. one discrete parameter line $(f_i)_{i\in\{0,\dots,N\}}$ lies in the x-axis and therefore we denote by f_i the x value of this point. Then we have $0 < f_0 < f_1$ and

$$f_i = f_{i-1}\frac{f_1}{f_0}, \quad \text{which implies} \quad f_i = \frac{f_1^i}{f_0^{i-1}}. \tag{3.12}$$

The stereographic projection to the unit circle in the xy-plane, which has the form

$$\Phi(x) = \frac{1}{x^2+1}\begin{pmatrix} 2x \\ x^2-1 \end{pmatrix},$$

leads to points $\phi_i = \Phi(f_i)$. Now we compute the discrete Christoffel dual (p_i) of (ϕ_i) with the initial value $p_0 = (r, 0)$ (see also Figure 3.17). Then,

$$p_i = p_{i-1} + \frac{\Delta\phi_{i-1}}{\|\Delta\phi_{i-1}\|^2} \tag{3.13}$$

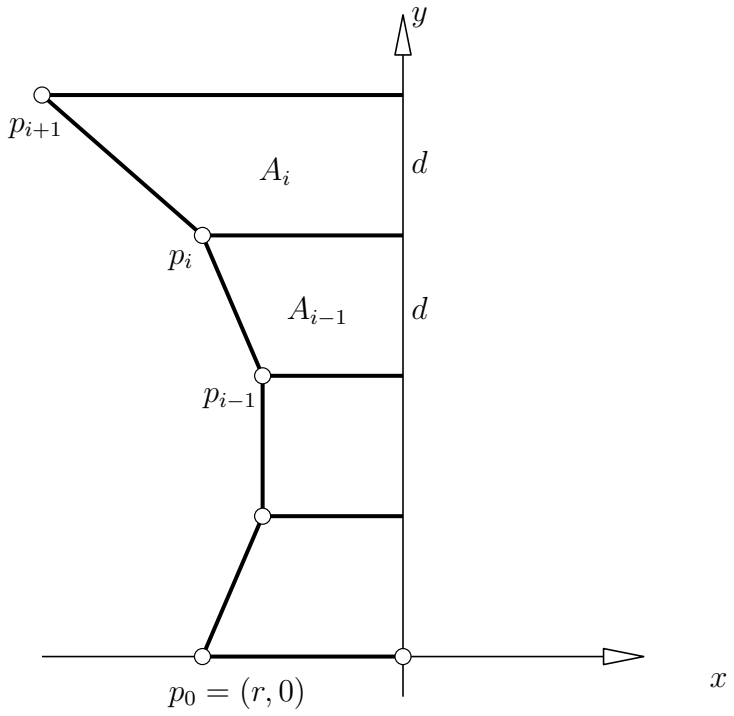

FIGURE 3.17: The Christoffel dual polygon of a meridian polygon of the unit sphere which on the other hand is the stereographic projection of the planar quad mesh illustrated in Figure 3.16.

for all $i \in \{1, \dots, N\}$. We set $a := f_{i-1}$ and $b := f_i$ and compute

$$\begin{aligned}\Delta\phi_{i-1} &= \phi_i - \phi_{i-1} = \Phi(b) - \Phi(a)\\ &= \frac{1}{b^2+1}\begin{pmatrix}2b\\ b^2-1\end{pmatrix} - \frac{1}{a^2+1}\begin{pmatrix}2a\\ a^2-1\end{pmatrix}\\ &= -\frac{2(a-b)}{(a^2+1)(b^2+1)}\begin{pmatrix}1-ab\\ a+b\end{pmatrix}\end{aligned}$$

and its norm

$$\|\Delta\phi_{i-1}\|^2 = \frac{4(a-b)^2}{(a^2+1)(b^2+1)},$$

and get

$$\Delta p_{i-1} = -\frac{1}{2(a-b)}\begin{pmatrix}1-ab\\ a+b\end{pmatrix}.$$

An interesting fact is that the y component d of Δp_{i-1} is independent of i because inserting f_{i-1+j} for a and f_{i+j} for b yields

$$d = \frac{f_{i+j} + f_{i-1+j}}{2(f_{i+j} - f_{i-1+j})} = \frac{f_1^{i+j}/f_0^{i-1+j} + f_1^{i-1+j}/f_0^{i-2+j}}{2(f_1^{i+j}/f_0^{i-1+j} - f_1^{i-1+j}/f_0^{i-2+j})} =$$
$$= \frac{f_i + f_{i-1}}{2(f_i - f_{i-1})} = \frac{a+b}{2(b-a)}.$$

Further we compute the second differences

$$\Delta\Delta p_i = -\Delta p_{i-1} + \Delta p_i = \frac{1}{2(a-b)} \begin{pmatrix} 1-ab \\ a+b \end{pmatrix} - \frac{1}{2(b-\frac{b^2}{a})} \begin{pmatrix} 1-b\frac{b^2}{a} \\ b+\frac{b^2}{a} \end{pmatrix}$$
$$= \begin{pmatrix} (b^2+1)/2b \\ 0 \end{pmatrix}.$$

We recall that A_i denots the area between the line segment $p_{i+1}p_i$ and the y-axis and d is the y component of this segment. Therefore

$$A_{i-1} = \frac{p_{i-1}^1 + p_i^1}{2} d \quad \text{and} \quad A_i = \frac{p_i^1 + p_{i+1}^1}{2} d.$$

We choose the initial value $p_0 = (r, 0)$ in such a way that

$$p_{i-1}^1 = -\frac{b + a^2 b}{2(a-b)^2}.$$

Then, $p_i^1 = p_{i-1}^1 + \Delta p_{i-1}^1$ and $p_{i+1}^1 = p_i^1 + \Delta p_i^1$. It turns out that p_i^1 is equal to p_{i-1}^1 with a replaced by b and b replaced by b^2/a. And analogous for p_{i+1} with a replaced by b^2/a and b replaced by b^3/a^2. This mean that the choice of that special r is independent of i. Therefore

$$p_i^1 = -\frac{a + ab^2}{2(a-b)^2} \quad \text{and} \quad p_{i+1}^1 = -\frac{a^2 + b^4}{2b(a-b)^2}$$

and further

$$A_{i-1} + A_i = \frac{(a+b)^3(1+b^2)}{8b(a-b)^3}.$$

Now we can compute the factor c of Equation (3.11)

$$c = \frac{\Delta\Delta p_i^1}{(A_i + A_{i+1})} = \frac{4(a-b)^3}{(a+b)^3},$$

which is independent of transformations of the form a replacing by b^i/a^{i-1} and b replacing by b^{i+1}/a^i. Therefore c is independent of i. □

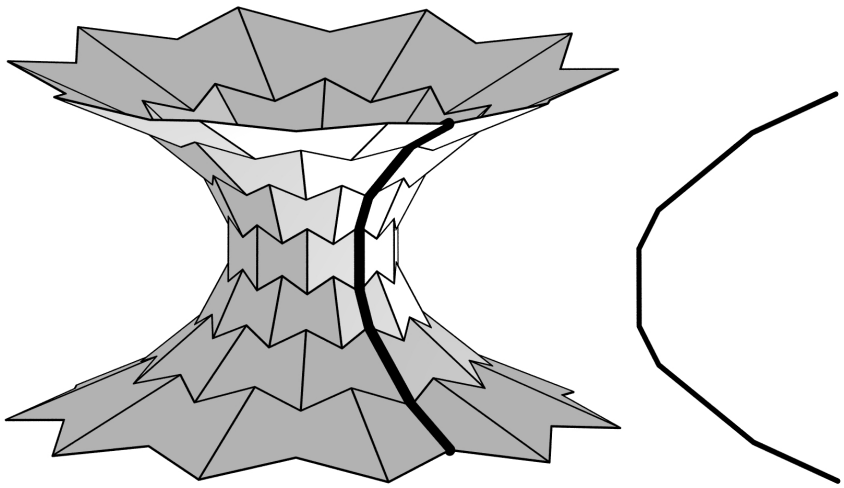

FIGURE 3.18: Hexagonal mesh as discrete catenoid. The meridian polygon, which is indicated can be seen as a discrete cosh.

The last theorem is a result for the discrete cosh function appearing as the Christoffel dual of a meridian polygon in the setting of quad meshes. However, since we want to give a motivation for the hexagonal case (see Exapmle 3.25) with the appropriate duality construction (see Definition 3.8), additional considerations are necessary. Our goal is to interpret the polygonal line indicated in Figure 3.18 as discrete hyperbolic cosine. Because of the coefficients appearing in Definition 3.8 and Proposition 3.9 the dual construction of (3.13) must be modified as follows:

$$p_i = \begin{cases} p_{i-1} + 2\dfrac{\Delta\phi_{i-1}}{\|\Delta\phi_{i-1}\|^2} & \text{for } i \text{ even,} \\ p_{i-1} + 3\dfrac{\Delta\phi_{i-1}}{\|\Delta\phi_{i-1}\|^2} & \text{for } i \text{ odd.} \end{cases}$$

Also the sequence (3.12) changes into $0 < f_0 < f_2$ and

$$f_i = \begin{cases} f_{i-2}\dfrac{f_2}{f_0} & \text{for } i \text{ even,} \\ \lambda f_{i+1} + (1-\lambda) f_{i-1} & \text{for } i \text{ odd.} \end{cases}$$

with some $\lambda \in (0,1)$. With this changed notions Theorem 3.28 modifies to the conjecture

The discrete hyperbolic cosine constructed via the discrete Christoffel duality in the hexagonal setting fulfills

$$\Delta\Delta p_i^1 = \begin{cases} c_1 A_i + c_2 A_{i+1} & \text{for } i \text{ even}, \\ c_2 A_i + c_1 A_{i+1} & \text{for } i \text{ odd}, \end{cases}$$

where c_1 and c_2 are independent from i.

The proof of this conjecture appears to be much more complex than the proof of Theorem 3.28, such that we can only provide verifications for a list of examples with the help of a computer. The following program was written in *Mathematica*. Note that in the list of examples all etries of the form `r[i] - r[0]` are all zero, which is expected and which supports the conjecture.

```
f[i_/;EvenQ[i]] := f[i - 2]*f[2]/f[0]
f[i_/;OddQ[i]] := la*f[i + 1] + (1 - la)*f[i - 1]
st[x_] := 1/(x^2 + 1)*{2*x, x^2 - 1}
s[i_] := st[f[i]]
p[0] := {r, 0}
p[i_/;EvenQ[i]] :=
   p[i - 1] + 2*(s[i] - s[i - 1])/Norm[s[i] - s[i - 1]]^2
p[i_/;OddQ[i]] :=
   p[i - 1] + 3*(s[i] - s[i - 1])/Norm[s[i] - s[i - 1]]^2
p1[i_] := p[i + 2][[1]] - 2*p[i + 1][[1]] + p[i][[1]]
d[i_] := p[i + 1][[2]] - p[i][[2]]
A[i_] := (p[i + 1][[1]] + p[i][[1]])/2*d[i]
AA[i_/;EvenQ[i]] := c*A[i + 1] + A[i]
AA[i_/;OddQ[i]] := A[i + 1] + c*A[i]
gl[i_] := (p1[i]/AA[i])/(p1[i + 1]/AA[i + 1])

For[i = 0, i < 5, i++,
  {
  f[0] = Random[Integer, {1, 1000}],
  f[2] = f[0] + Random[Integer, {1, 100}],
  la = 1/Random[Integer, {2, 100}],
  Lc = Flatten[Solve[{gl[0] == 1, gl[1] == 1}, c, r]],
  ggl[i_] = gl[i] /. Lc,
  Lr = Flatten[Solve[ggl[j] == 1, r]],
  rrr = r /. Lr,
  For[j = 0, j < 4, j++,
```

```
   {
    ii = Random[Integer, {0, 100}],
    Lr = Flatten[Solve[ggl[ii] == 1, r]],
    rr = r /. Lr,
    Print["f[0]=", f[0], "  f[2]=", f[2], "  la=", la, "  r[", ii,
     "]-r[0]=", rr - rrr]
    }]
  }]
```

```
f[0]=111  f[2]=116  la=1/99  r[46]-r[0]=0
f[0]=111  f[2]=116  la=1/99  r[63]-r[0]=0
f[0]=111  f[2]=116  la=1/99  r[45]-r[0]=0
f[0]=111  f[2]=116  la=1/99  r[35]-r[0]=0
f[0]=467  f[2]=567  la=1/78  r[70]-r[0]=0
f[0]=467  f[2]=567  la=1/78   r[8]-r[0]=0
f[0]=467  f[2]=567  la=1/78  r[48]-r[0]=0
f[0]=467  f[2]=567  la=1/78  r[13]-r[0]=0
f[0]=666  f[2]=711  la=1/32  r[30]-r[0]=0
f[0]=666  f[2]=711  la=1/32  r[84]-r[0]=0
f[0]=666  f[2]=711  la=1/32  r[58]-r[0]=0
f[0]=666  f[2]=711  la=1/32  r[69]-r[0]=0
f[0]=26   f[2]=80   la=1/94  r[36]-r[0]=0
f[0]=26   f[2]=80   la=1/94  r[89]-r[0]=0
f[0]=26   f[2]=80   la=1/94  r[76]-r[0]=0
f[0]=26   f[2]=80   la=1/94  r[56]-r[0]=0
f[0]=109  f[2]=137  la=1/17  r[21]-r[0]=0
f[0]=109  f[2]=137  la=1/17  r[51]-r[0]=0
f[0]=109  f[2]=137  la=1/17  r[16]-r[0]=0
f[0]=109  f[2]=137  la=1/17  r[89]-r[0]=0
```

Example 3.29 (Helical surface)**.** We start with an arbitrary hexagon, which is not regular, but Möbius equivalent to a regular hexagon. We apply Proposition 3.17 to get a mesh which discretizes the function

$$g(z) = e^{az},$$

where $a \in \mathbb{C} \setminus 0$ (see Figure 3.19, left). With $h(z) = 1/a$ it is easy to verify that $n_x/\|n_x\|^2$ equals the real part of the integrand of (3.8). For $a \in \mathbb{R}$ we obtain the catenoid (see Example 3.25) and for $a \in i\mathbb{R}$ we obtain the helicoid and especially for $a = i$ the helicoid with the parametrization

$$f(x, y) = (\sin(x)\sinh(y), \cos(x)\sinh(y), x).$$

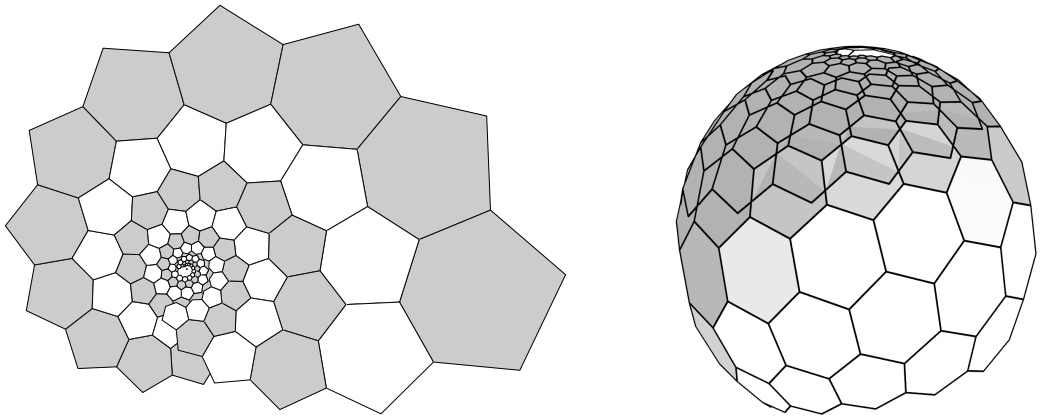

FIGURE 3.19: *Left:* Circular conformal mesh $\mathcal{M}$ which discretizes $z \mapsto e^{az}$ ($a \in \mathbb{C} \setminus (\mathbb{R} \cup i\mathbb{R})$). According to Proposition 3.17 we start with an arbitrary hexagon which is Möbius equivalent to a regular hexagon and apply similarities. Here the mesh $\mathcal{M}$ overlaps itself (multi-valued function). *Right:* Stereographic projection of the mesh $\mathcal{M}$.

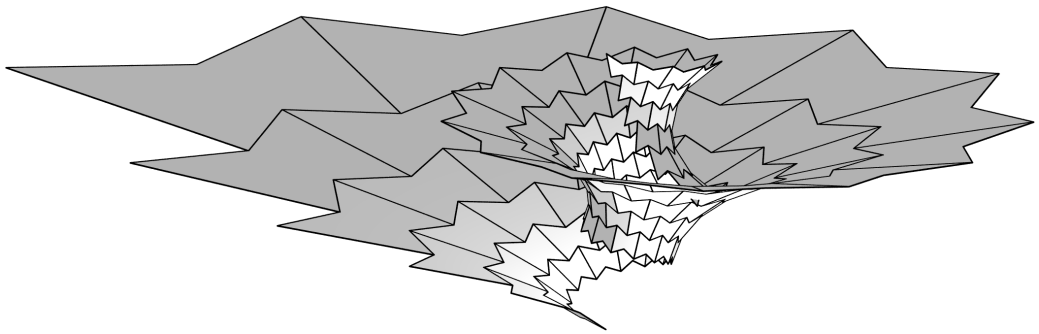

FIGURE 3.20: A discrete minimal surface which discretizes the smooth helical surface given by (3.14). The corresponding Gauss image is shown by Figure 3.19, right.

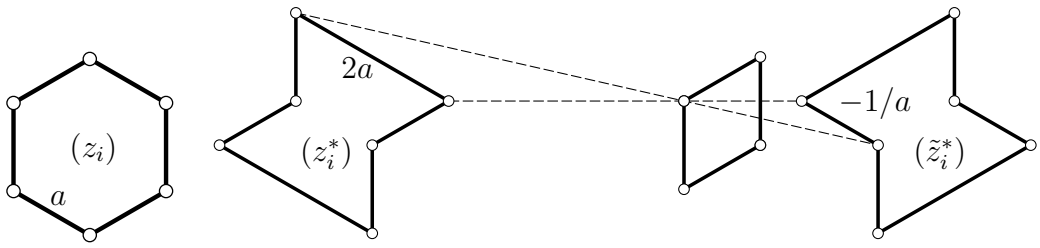

FIGURE 3.21: Each hexagon (z_i), which is Möbius equivalent to a regular one (left) can be dualized in three different ways, by interchanging the coefficients 2 and -1 in the discrete dual construction (Definition 3.8). Two of them, (z_i^*) and $(\tilde{z}_i^*)$ are illustrated here. The linear combination $1/3z_i^* + 2/3\tilde{z}_i^*$ yields a quadrilateral.

For $a = a_1 + ia_2$ $(a_1, a_2 \neq 0)$ we get the surface

$$f(u,v) = D_{\omega u} \cdot D_{\alpha v} \begin{pmatrix} (-a_1^2 + a_2^2)/(a\overline{a})^2 \cosh v \\ 2a_1 a_2/(a\overline{a})^2 \sinh v \\ 0 \end{pmatrix} + \begin{pmatrix} 0 \\ 0 \\ u/(a\overline{a}) \end{pmatrix}, \qquad (3.14)$$

where D_t is the rotation matrix for rotation around the z-axis by an angle of t, $\omega = a\overline{a}/(2a_1a_2)$ and $\alpha = (a_2^2 - a_1^2)/(2a_1a_2)$. We see that this is a helical surface too.

The Christoffel dual of the considered hexagonal mesh generates a discrete minimal surface illustrated in Figure 3.20.

Example 3.30 (Associated family, helicoid)**.** The spherical hexagonal mesh of Example 3.25 can be dualized in yet another way. We interchange the coefficients 2 and -1 in the discrete dual construction and get a helical surface. The edges of all faces of this mesh are parallel to the corresponding edges of the catenoid given in Example 3.25. Linear combinations of these two discrete surfaces give all members of the associated family of this minimal surface. A special combination yields a quad mesh which discretizes the helicoid (see Figures 3.8.2 and 3.21).

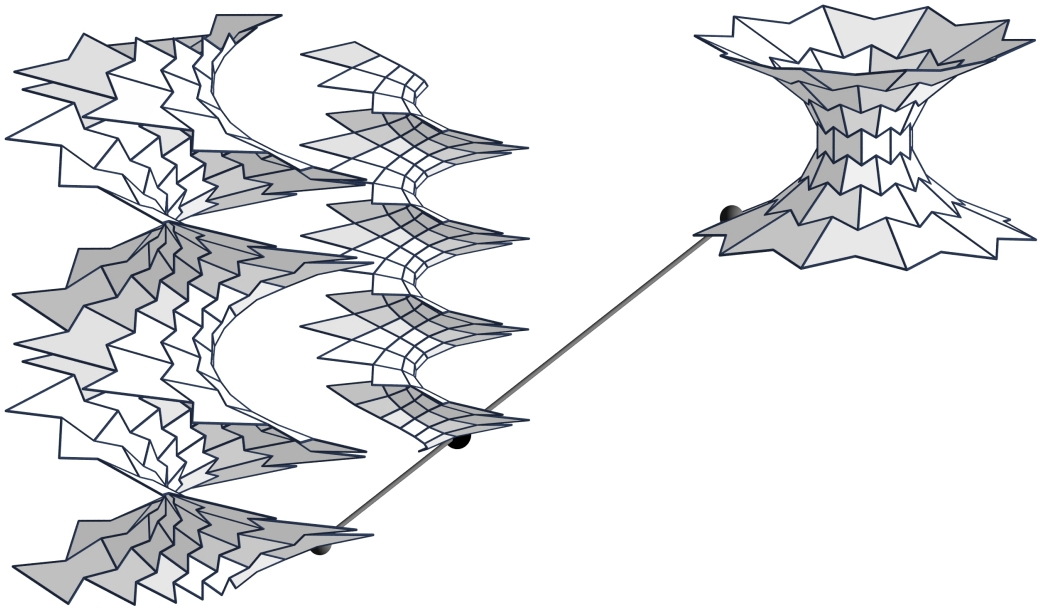

FIGURE 3.22: Linear combinations of parallel meshes, where one is a discrete catenoid and the second is a discrete helical surface are members of the corresponding associated family of minimal surfaces. Special combinations can lead to quad meshes (see Figure 3.21 on page 74). The case illustrated here is in fact a discrete helicoid, which means that it discretizes a surface generated by the helical motion of a straight line which orthogonally intersects the helical axis (see Example 3.30).

Bibliography

[1] W. Blaschke. *Vorlesungen über Differentialgeometrie und geometrische Grundlagen von Einsteins Relativitätstheorie. Band III. Differentialgeometrie der Kreise und Kugeln.* Verlag von Julius Springer, Berlin, 1929.

[2] A. I. Bobenko, T. Hoffmann, and B. Springborn. Minimal surfaces from circle patterns: Geometry from combinatorics. *Ann. of Math.*, 164:231–264, 2006.

[3] A. I. Bobenko, T. Hoffmann, and Yu. B. Suris. Hexagonal circle patterns and integrable systems: patterns with the multi-ratio property and Lax equations on the regular triangular lattice. *Int. Math. Res. Not.*, 2002(3):111–164, 2002.

[4] A. I. Bobenko and U. Pinkall. Discrete isothermic surfaces. *J. Reine Angew. Math.*, 475:187–208, 1996.

[5] A. I. Bobenko, H. Pottmann, and J. Wallner. A curvature theory for discrete surfaces based on mesh parallelity. *Math. Annalen*, 2010. to appear.

[6] A. I. Bobenko and Yu. B. Suris. *Discrete differential geometry: Integrable Structure.* Number 98 in Graduate Studies in Math. American Math. Soc., 2008.

[7] A. I. Bobenko and Yu. B. Suris. Discrete Koenigs nets and discrete isothermic surfaces. *Int. Math. Res. Not.*, pages 1976–2012, 2009.

[8] F. Chorlton. Some geometrical properties of the catenary. *The Mathematical Gazette*, 83(496):121–123, 1999.

[9] E. B. Christoffel. Ueber einige allgemeine Eigenschaften der Minimumsflächen. *J. Reine Angew. Math.*, 67:218–228, 1867.

[10] M. P. do Carmo. *Differential geometry of curves and surfaces*. Prentice-Hall Inc., Englewood Cliffs, N.J., 1976.

[11] J.-H. Eschenburg and J. Jost. *Differentialgeometrie und Minimalflächen*. Springer-Verlag, Berlin, 2007.

[12] K. Kenmotsu. *Surfaces with constant mean curvature*, volume 221 of *Translations of Mathematical Monographs*. American Mathematical Society, Providence, RI, 2003.

[13] E. Kreyszig. *Differential geometry*. Dover Publications Inc., New York, 1991. Reprint of the 1963 edition.

[14] Y. Liu and W. Wang. On vertex offsets of polyhedral surfaces. In *Proc. of Advances in Architectural Geometry*, pages 61–64. TU Wien, 2008.

[15] S. Montiel and A. Ros. *Curves and surfaces*, volume 69 of *Graduate Studies in Mathematics*. American Mathematical Society, Providence, RI, 2005.

[16] Ch. Müller. Conformal hexagonal meshes. Geometry Preprint 2009/03, TU Graz, April 2009.

[17] Ch. Müller and J. Wallner. Oriented mixed area and discrete minimal surfaces. *Discrete Comput. Geom.*, 43:303–320, 2010.

[18] J. C. C. Nitsche. *Vorlesungen über Minimalflächen*. Springer-Verlag, Berlin, 1975. Die Grundlehren der mathematischen Wissenschaften, Band 199.

[19] U. Pinkall and K. Polthier. Computing discrete minimal surfaces and their conjugates. *Experiment. Math.*, 2:15–36, 1993.

[20] H. Pottmann, Y. Liu, J. Wallner, A. I. Bobenko, and W. Wang. Geometry of multi-layer freeform structures for architecture. *ACM Trans. Graphics*, 26(3):#65,1–11, 2007.

[21] H. Pottmann and J. Wallner. The focal geometry of circular and conical meshes. *Adv. Comp. Math*, 29:249–268, 2008.

[22] W. Rudin. *Real and complex analysis*. McGraw-Hill Book Co., New York, third edition, 1987.

[23] R. Sauer. *Differenzengeometrie*. Springer-Verlag, Berlin, 1970.

[24] R. Schneider. *Convex bodies: the Brunn-Minkowski theory*. Cambridge Univ. Press, 1993.

[25] M. Spivak. *A comprehensive introduction to differential geometry. Vol. IV*. Publish or Perish Inc., Houston, Texas, third edition, 1999.

[26] B. Springborn, P. Schröder, and U. Pinkall. Conformal equivalence of triangle meshes. *ACM Transactions on Graphics*, 27(3):#77,1–11, 2008.

[27] J. Wallner and H. Pottmann. Infinitesimally flexible meshes and discrete minimal surfaces. *Monatshefte Math.*, 153:347–365, 2008.

[28] W. Walter. *Gewöhnliche Differentialgleichungen*. Springer-Verlag, Berlin, seventh edition, 2000.